



CERN-PH-EP-2015-060

Submitted to: JHEP

Analysis of events with b -jets and a pair of leptons of the same charge in pp collisions at $\sqrt{s} = 8$ TeV with the ATLAS detector

The ATLAS Collaboration

Abstract

An analysis is presented of events containing jets including at least one b -tagged jet, sizeable missing transverse momentum, and at least two leptons including a pair of the same electric charge, with the scalar sum of the jet and lepton transverse momenta being large. A data sample with an integrated luminosity of 20.3 fb^{-1} of pp collisions at $\sqrt{s} = 8$ TeV recorded by the ATLAS detector at the Large Hadron Collider is used. Standard Model processes rarely produce these final states, but there are several models of physics beyond the Standard Model that predict an enhanced rate of production of such events; the ones considered here are production of vector-like quarks, enhanced four-top-quark production, pair production of chiral b' -quarks, and production of two positively charged top quarks. Eleven signal regions are defined; subsets of these regions are combined when searching for each class of models. In the three signal regions primarily sensitive to positively charged top quark pair production, the data yield is consistent with the background expectation. There are more data events than expected from background in the set of eight signal regions defined for searching for vector-like quarks and chiral b' -quarks, but the significance of the discrepancy is less than two standard deviations. The discrepancy reaches 2.5 standard deviations in the set of five signal regions defined for searching for four-top-quark production. The results are used to set 95% CL limits on various models.

Analysis of events with b -jets and a pair of leptons of the same charge in pp collisions at $\sqrt{s} = 8$ TeV with the ATLAS detector

The ATLAS Collaboration

ABSTRACT: An analysis is presented of events containing jets including at least one b -tagged jet, sizeable missing transverse momentum, and at least two leptons including a pair of the same electric charge, with the scalar sum of the jet and lepton transverse momenta being large. A data sample with an integrated luminosity of 20.3 fb^{-1} of pp collisions at $\sqrt{s} = 8$ TeV recorded by the ATLAS detector at the Large Hadron Collider is used. Standard Model processes rarely produce these final states, but there are several models of physics beyond the Standard Model that predict an enhanced rate of production of such events; the ones considered here are production of vector-like quarks, enhanced four-top-quark production, pair production of chiral b' -quarks, and production of two positively charged top quarks. Eleven signal regions are defined; subsets of these regions are combined when searching for each class of models. In the three signal regions primarily sensitive to positively charged top quark pair production, the data yield is consistent with the background expectation. There are more data events than expected from background in the set of eight signal regions defined for searching for vector-like quarks and chiral b' -quarks, but the significance of the discrepancy is less than two standard deviations. The discrepancy reaches 2.5 standard deviations in the set of five signal regions defined for searching for four-top-quark production. The results are used to set 95% CL limits on various models.

Contents

1	Introduction	1
2	Data and Monte Carlo simulations	5
3	Event selection	6
4	Background estimation	10
5	Selection optimization	13
6	Systematic uncertainties	15
7	Results	17
8	Checks of the background estimate	29
9	Features of events in signal regions with most significant excesses	29
10	Conclusion	30

1 Introduction

The Standard Model (SM) has been repeatedly confirmed experimentally. Nonetheless there is a need for physics beyond the SM (BSM) at about the TeV scale, with additional features that explain the baryon asymmetry of the universe, specify the nature of dark matter, and provide a mechanism to naturally stabilize the Higgs boson mass at its observed value of approximately 125 GeV [1, 2]. This paper reports on a search for BSM physics resulting in pairs of isolated high-transverse-momentum (high- p_T) leptons¹ with the same electric charge, hereafter denoted as same-sign leptons, (or three or more leptons of any charge) missing transverse momentum, and b -jets. This is a promising search channel since the SM yields of such events are small, and several types of BSM physics may contribute.

Among the models that predict enhanced same-sign lepton production are those that postulate the existence of vector-like quarks, an enhancement of the four-top-quark production cross section, the existence of a fourth generation of chiral quarks, or production of two positively charged top quarks. A common data sample is used to search for each of these signatures, but separate final selection criteria are defined based on the characteristics of each signal model.

¹Only electrons and muons are considered in the search. Tau leptons are not explicitly reconstructed, but electrons and muons from τ decay may enter the selected samples.

Mass (model)	B			T		
	Wt	Zb	Hb	Wb	Zt	Ht
0.50 TeV (singlet)	42	31	27	50	17	33
0.50 TeV (doublet)	100	0	0	0	34	66
0.55 TeV (singlet)	43	30	27	49	18	32
0.55 TeV (doublet)	100	0	0	0	37	63
0.60 TeV (singlet)	44	29	26	49	19	31
0.60 TeV (doublet)	100	0	0	0	38	62
0.65 TeV (singlet)	45	29	26	49	20	30
0.65 TeV (doublet)	100	0	0	0	40	60

Table 1: B and T quark branching fractions (in percent), assuming the singlet and (T, B) doublet models of ref. [25]. In the doublet case it is assumed that the mixing of the T quark with the Standard Model bottom quark is much smaller than the mixing of the B quark with the top quark.

Several extensions to the SM that regulate the Higgs boson mass in a natural way require the existence of vector-like quarks (VLQ) [3–21], where ‘vector-like’ means that the left- and right-handed components transform identically under the $SU(2)_L$ weak isospin gauge symmetry. Since quarks with this structure do not require a Yukawa coupling to the Higgs field to attain mass, their existence would not enhance the Higgs boson production cross section, and thus the motivation persists for a direct search [22]. There are several possible varieties of VLQ; those having the same electric charge as the SM b - and t -quarks are called B and T . In addition the exotic charge states $T_{5/3}$ and $B_{-4/3}$ may occur, where the subscripts indicate the electric charge. Vector-like quarks may exist as isospin singlets, doublets, or triplets. Arguments based on naturalness suggest that VLQ may not interact strongly with light SM quarks [23, 24]. Thus it is assumed for this analysis that VLQ decay predominantly to third-generation SM quarks. For the B and T quarks, charged- and neutral-current decays may both occur ($B \rightarrow Wt, Zb$, or Hb ; $T \rightarrow Wb, Zt$, or Ht), providing many paths for same-sign lepton production for events with $B\bar{B}$ or $T\bar{T}$ pairs.

The branching fractions to each allowed final state are model-dependent, and the ones occurring in models where the B and T exist as singlets or as a (T, B) doublet [25] are used as a reference. These branching fractions vary with the B or T mass, and values for some masses are given in table 1. Since the pair production of heavy quarks is mediated by the strong interaction, the cross section is identical for vector-like quarks and b' quarks (described below) of a given mass. The next-to-next-to-leading-order (NNLO) cross sections from TOP++ v2.0 [26, 27] are used in this paper. The $T_{5/3}$ quark must decay to W^+t , and therefore both single and pair production of this quark can result in same-sign lepton pairs, and both sources are considered.

Same-sign lepton pairs may also arise from the production of four top quarks ($t\bar{t}t\bar{t}$). The SM rate for this production is small (≈ 1 fb [28, 29]), but there are several BSM physics

models that can enhance the rate, such as top compositeness models [30–32] or Randall-Sundrum models with SM fields in the bulk [33]. These can generically be described in terms of a four-fermion contact interaction with coupling strength C_{4t}/Λ^2 , where C_{4t} is the coupling constant and Λ is the scale of the BSM physics [32]. The Lagrangian for this interaction is

$$\mathcal{L}_{4t} = \frac{C_{4t}}{\Lambda^2} (\bar{t}_R \gamma^\mu t_R) (\bar{t}_R \gamma_\mu t_R) \quad (1.1)$$

where t_R is the right handed top spinor and the γ_μ are the Dirac matrices. Two specific models are also considered. The first is sgluon pair production, where sgluons are colour-adjoint scalars that appear in several extensions to the SM [34–39]. If the sgluon mass is above the top quark pair-production threshold, the dominant decay is to $t\bar{t}$, resulting in four top quarks in the final state² ($t\bar{t}t\bar{t}$). The cross sections considered in this paper are rescaled to the next-to-leading order (NLO) prediction of Ref. [41]. The second model is one with two universal extra dimensions under the real projective plane geometry (2UED/RPP) [42]. The compactification of the extra dimensions leads to discretization of the momenta along their directions. The model is parameterized by the radii R_4 and R_5 of the extra dimensions or, equivalently, by $m_{\text{KK}} = 1/R_4$ and $\xi = R_4/R_5$. This model predicts the pair production of tier³ (1,1) Kaluza–Klein excitations of the photon ($A_\mu^{(1,1)}$) with mass approximately $\sqrt{2}m_{\text{KK}}$ that decay to $t\bar{t}$ with a branching fraction assumed to be 100%. The model also predicts a four-top-quark signal from tiers (2,0) and (0,2). Cosmological observations constrain m_{KK} in this model to lie approximately between 600 GeV and 1200 GeV [43].

A fourth generation of SM-like quarks includes a charge $-1/3$ quark, called the b' [44–47]. Under the assumption that the b' -quark decays predominantly to Wt , b' pair production results in four W bosons in the final state. If two W bosons with the same electric charge decay leptonically, there will be a same-sign lepton pair in the final state. If the b' -quark can also decay to Wq , where q is a light (u or c) quark, some b' pairs would also result in same-sign lepton pairs or trileptons (provided that at least one b' -quark decays to Wt), and therefore the possibility of such decays is explored as well. The existence of additional chiral quark generations greatly enhances the Higgs boson production cross section, so if the new boson observed at the LHC is a manifestation of a minimal Higgs sector, additional quark generations are ruled out [48–53]. However, a more complex Higgs sector, as in some Two-Higgs-Doublet models [54], allows a fourth generation of chiral quarks.

Production of two positively charged top quarks via $uu \rightarrow tt$ can also result in an excess of same-sign lepton pairs. This process may be mediated via s - or t -channel exchange of a heavy particle [55, 56]. In the t -channel exchange case, the process must include a vertex with a flavour-changing neutral current (FCNC). The neutral particle that is exchanged may be a vector, Z -like, particle or a scalar, Higgs-like, particle. Past searches for a new Z' boson have already put strong constraints on this possibility, thus only the scalar case is considered, with the following generic model Lagrangian [57]:

$$\mathcal{L}_{\text{FCNC}} = \kappa_{utH} \bar{t} H u + \kappa_{ctH} \bar{t} H c + \text{h.c.} \quad (1.2)$$

²The decays predominantly to $t\bar{t}$ is model-dependent, as discussed in ref. [40].

³A tier of the Kaluza–Klein towers is labelled by two integers, corresponding to the two extra dimensions.

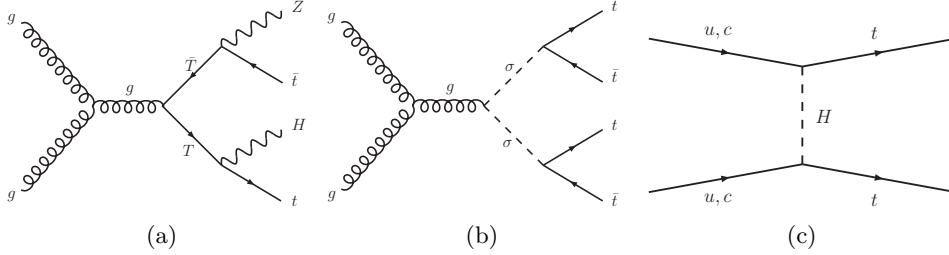


Figure 1: Leading-order diagrams for (a) vector-like top quark pair production, (b) sgluon pair production, and (c) same-sign top quark pair production through a BSM flavour-changing Higgs coupling.

where H is a Higgs-like particle with mass m_H and κ_{utH} and κ_{ctH} denote the flavour-changing couplings of H to up-type quarks. Two scenarios are tested, one corresponding to a possible FCNC coupling of the newly discovered Higgs boson ($m_H = 125$ GeV) and the other to a second scalar boson with a mass in the range $[250, 750]$ GeV. If the mass of the mediating particle is much greater than the electroweak symmetry breaking scale, an effective four-fermion contact interaction can describe the process, thus extending the search to non-scalar particles. The corresponding Lagrangian contains separate operators for the different initial-state chiralities [58]:

$$\begin{aligned} \mathcal{L}_{tt} = & \frac{1}{2} \frac{C_{LL}}{\Lambda^2} (\bar{u}_L \gamma^\mu t_L) (\bar{u}_L \gamma_\mu t_L) + \frac{1}{2} \frac{C_{RR}}{\Lambda^2} (\bar{u}_R \gamma^\mu t_R) (\bar{u}_R \gamma_\mu t_R) \\ & - \frac{1}{2} \frac{C_{LR}}{\Lambda^2} (\bar{u}_L \gamma^\mu t_L) (\bar{u}_R \gamma_\mu t_R) - \frac{1}{2} \frac{C'_{LR}}{\Lambda^2} (\bar{u}_{La} \gamma^\mu t_{Lb}) (\bar{u}_{Rb} \gamma_\mu t_{Ra}) + \text{h.c.} \end{aligned} \quad (1.3)$$

where C_{LL} , $C_{LR}^{(\prime)}$ and C_{RR} are the coefficients of effective operators corresponding to each chirality configuration and Λ is the scale of the BSM physics. The C_{LR} and C'_{LR} terms lead to kinematically equivalent events, hence only one term is considered in this paper.

Leading-order Feynman diagrams for the production in pp collisions of some of the signals searched for in this analysis are presented in figure 1.

Previous searches by the ATLAS collaboration [58] using an integrated luminosity of 1.04 fb^{-1} of pp collisions at a centre-of-mass energy $\sqrt{s} = 7$ TeV and the CMS collaboration [59], using an integrated luminosity of 19.5 fb^{-1} of pp collisions at $\sqrt{s} = 8$ TeV, did not observe a significant excess of same-sign dilepton production. The ATLAS result was used to set a lower limit of 450 GeV on the mass of a heavy down-type quark, under the assumption that the branching ratio to Wt is 100%, while the CMS result set upper limits on the four-top-quark production cross section of 49 fb ,⁴ on the sum of the tt and $t\bar{t}$ production cross sections of 720 fb , and on the tt production cross section of 370 fb . The CMS collaboration used the same-sign lepton signature to search for $T_{5/3}$ quarks [60], ruling out such quarks with mass below 0.80 TeV, and as part of a broader search for vector-like T quarks [61], ruling out such quarks with mass less than 0.69 TeV. A more recent search by

⁴Unless stated otherwise, all limits reported are at the 95% confidence level (CL).

the ATLAS collaboration [62] using an integrated luminosity of 20.3 fb^{-1} of pp collisions at $\sqrt{s} = 8 \text{ TeV}$ with similar final states to those reported here was interpreted in the context of supersymmetric models. The present analysis improves upon the $\sqrt{s} = 7 \text{ TeV}$ ATLAS analysis by using a larger data set recorded at a higher centre-of-mass energy, having a higher signal acceptance, and expanding the range of BSM models considered.

2 Data and Monte Carlo simulations

The data were recorded by the ATLAS detector [63] in LHC pp collisions at $\sqrt{s} = 8 \text{ TeV}$ between April and December 2012, corresponding to an integrated luminosity of 20.3 fb^{-1} . The ATLAS detector consists of an inner tracking system surrounded by a superconducting solenoid that provides a 2 T magnetic field, electromagnetic (EM) and hadronic calorimeters, and a muon spectrometer. The inner detector provides tracking information from pixel and silicon microstrip detectors within pseudorapidity⁵ $|\eta| < 2.5$, and from a transition radiation tracker that covers $|\eta| < 2.0$. The EM sampling calorimeter uses lead as absorber and liquid argon (LAr) as the active medium, and is divided into a barrel region that covers $|\eta| < 1.475$ and endcap regions that cover $1.375 < |\eta| < 3.2$. The hadronic calorimeter consists of either LAr or scintillator tile as the active medium, and either steel, copper, or tungsten as the absorber, and covers $|\eta| < 4.9$. The muon spectrometer covers $|\eta| < 2.7$, and uses multiple layers of high-precision tracking chambers to measure the deflection of muons as they traverse a toroidal field of approximately 0.5 (1.0) T in the central (endcap) regions of the detector. A three-level trigger system selects events to be recorded for offline analysis.

Signal and the background sources that contain prompt same-sign leptons or trileptons are modelled using Monte Carlo (MC) simulations. The remaining background sources are determined from the data, as described in section 4. B and T pair production is modelled using the PROTOS v2.2 [25] generator using the MSTW2008LO [64] parton distribution functions (PDFs), with PYTHIA v6.4 [65] used to model extra gluon emission and hadronization. $T_{5/3}$ production (both single and pair) is modelled with MADGRAPH v5.1 [66] using the CTEQ6L1 [67] PDFs, with PYTHIA v8.1 [68] used for hadronization. Production of four top quarks is modelled under four scenarios: *i*) Standard Model, *ii*) contact interaction, *iii*) sgluon pair, and *iv*) 2UED/RPP. The sgluon case is generated with PYTHIA v6.4 using the CTEQ6L1 PDFs; the other three models are generated with MADGRAPH using the MSTW2008LO PDFs followed by PYTHIA v8.1; in the case of 2UED/RPP the BRIDGE generator [69] is used to decay the pair-produced excitations from MADGRAPH to $t\bar{t}$. The simulated 2UED/RPP samples correspond to the tier (1,1) for the symmetric ($R_4 = R_5$) case, with m_{KK} ranging from 600 to 1200 GeV. Constraints on the asymmetric ($R_4 > R_5$)

⁵ATLAS uses a right-handed coordinate system with its origin at the nominal interaction point (IP) in the centre of the detector and the z -axis coinciding with the axis of the beam pipe. The x -axis points from the IP to the centre of the LHC ring, and the y -axis points upward. Cylindrical coordinates (r, ϕ) are used in the transverse plane, ϕ being the azimuthal angle around the beam pipe. The pseudorapidity is defined in terms of the polar angle θ as $\eta = -\ln \tan(\theta/2)$. For the purpose of the fiducial selection, this is calculated relative to the geometric centre of the detector; otherwise, it is relative to the reconstructed primary vertex of each event.

case are derived by an extrapolation that uses kinematical considerations [70]. These considerations also permit the extrapolation to signals arising from tiers (2,0) and (0,2) from the generated tier (1,1) signal. Pair production of b' events is modelled with the PYTHIA v8.1 generator for b' masses ranging from 400 to 1000 GeV, using the MSTW2008LO PDFs. Production of two positively charged top quarks via a contact interaction is also modelled using PROTOS [71] and PYTHIA v6.4, with three different chirality configurations of the contact interaction operator; production via the FCNC exchange of a Higgs-like particle is modelled with MADGRAPH with PYTHIA v8.1 used for showering and hadronization. The MSTW2008LO PDFs are used in simulating both types of tt production.

The background contributions from $t\bar{t}W$ and $t\bar{t}Z$ (abbreviated as $t\bar{t}W/Z$ hereafter) and $t\bar{t}W^+W^-$ are modelled with MADGRAPH followed by PYTHIA v6.4, while WZ and ZZ plus jet production and $W^\pm W^\pm jj$ production are modelled using SHERPA v1.4 [72]. Background from the production of three vector bosons is modelled using MADGRAPH and PYTHIA v6.4, and backgrounds from $t\bar{t}H$, WH and ZH production are modelled using PYTHIA v8.1. The CTEQ6L1 PDFs are used for the $t\bar{t}W/Z$, three-vector-boson, WH and ZH samples, the CT10 [73] PDFs are used for the WZ , ZZ , $W^\pm W^\pm jj$ and $t\bar{t}H$ samples, and the MSTW2008LO PDFs are used for the $t\bar{t}W^+W^-$ sample. In most cases (excluding background contributions that are negligibly small) the cross sections are scaled to match next-to-leading-order calculations.

A variable number of additional pp interactions are overlaid on simulated events to model the effect of multiple collisions during a single bunch crossing, and also the effect of the detector response to collisions from bunch crossings before or after the one containing the hard interaction. Events are then weighted to reproduce the distribution of the number of collisions per bunch crossing observed in data. The detector response is modelled using either a GEANT4 [74, 75] simulation of the entire detector or a GEANT4 simulation of the inner tracker and of the muon spectrometer combined with a fast simulation of shower development in the calorimeter [76]. Some samples are generated with both types of simulation, to allow direct comparison between the two, and agreement was found within the systematic uncertainty assigned to the efficiency estimate. In all cases the simulated events were reconstructed using the same algorithms that were applied to the collision data.

3 Event selection

The final states considered in this search require the presence of two leptons with the same electric charge in the event (events with additional leptons beyond the same-sign pair are also accepted). In addition, two or more jets are required, at least one of which is consistent with origination from a b -quark, and sizeable missing transverse momentum E_T^{miss} is also required, indicating the presence of neutrinos coming from W boson decays. The criteria used for each of these objects are given below.

Each event is required to pass either an electron trigger (where the chosen triggers require either an isolated electron with $p_T > 24$ GeV or an electron with $p_T > 60$ GeV with no isolation requirement) or a muon trigger (where the triggers chosen require either an isolated muon with $p_T > 24$ GeV or a muon with $p_T > 36$ GeV with no isolation require-

ment). The trigger efficiency for electrons is $\approx 95\%$ while for muons it is $\approx 75\%$, resulting in trigger efficiencies that range from $\approx 95\%$ for events with two muons to $> 99\%$ for events with two electrons. In addition, events are required to have at least one reconstructed vertex, which must be formed from at least five tracks with $p_T > 0.4$ GeV. If multiple vertices are reconstructed, the vertex with the largest sum of the squared transverse momenta of its associated tracks is taken as the primary vertex. Since the events used in this analysis tend to have vertices with many associated tracks, the correct vertex is selected in more than 99% of the events.

Electrons are identified by requiring a track to match an electromagnetic calorimeter energy cluster, subject to several criteria on the shape of the shower and the consistency between the shower and track. The selection requirements are varied with the η and p_T of the electron candidate to optimize the signal efficiency and background rejection [77]. The track is required to be within 2 mm in z of the reconstructed primary vertex of the event. A hit in the innermost layer of the inner detector is required to reject photon conversions. Energy clusters in the calorimeter associated with an electron are required to have transverse energy $E_T > 25$ GeV and $|\eta| < 2.47$, with the barrel/endcap transition region $1.37 < |\eta| < 1.52$ excluded. The candidate is required to be isolated from additional tracks within a cone of variable $\Delta R \equiv \sqrt{(\Delta\eta)^2 + (\Delta\phi)^2} = 10 \text{ GeV}/p_T$ [78], such that the sum of the transverse momenta of the tracks within that cone must be less than 5% of the electron p_T . In addition, electrons are required to be separated from any jet by at least $\Delta R = 0.4$.

Muons [79] are identified from hits in the muon system matched to a central track, where the track must be within 2 mm in z of the primary vertex, and are required to have an impact parameter in the transverse plane that differs from the beam position by less than three impact parameter standard deviations. Requirements are placed on the number of hits in various layers of the muon system, and on the maximum number of layers where hits are missing. Muon pairs that are consistent with the passage of a cosmic ray are discarded. Muons are subject to the same track-based isolation requirement as electrons. Muons are also required to be separated from any jet by $\Delta R = 0.04 + 10 \text{ GeV}/p_T$, and to have $p_T > 25$ GeV and $|\eta| < 2.5$. Events with a muon within $\Delta\phi \times \Delta\theta = 0.005 \times 0.005$ of any electron are rejected. At least one of the selected leptons is required to match a lepton identified by the trigger.

Jets are reconstructed from energy clusters in the calorimeter using an anti- k_t algorithm [80–82] with radius parameter 0.4. If one or more jets are within $\Delta R = 0.2$ of an electron, the jet closest to the electron is discarded (i.e. the cluster of energy in the calorimeter is treated as an electron rather than a jet). To suppress jets that do not originate from the primary vertex in the event, the jet vertex fraction (JVF) is defined by considering all tracks with $p_T > 0.5$ GeV within the jet, and finding the fraction of the summed p_T from tracks that originate from the primary vertex. Jets with $p_T < 50$ GeV and $|\eta| < 2.4$ that are matched to at least one track are required to have JVF greater than 0.5. All jets are required to have p_T greater than 25 GeV (after energy calibration [83]) and $|\eta|$ less than 2.5.

A multivariate algorithm [84] is used to test if each jet is consistent with having arisen

from a b -quark, based on the properties of the tracks associated with the jet. A requirement is placed on the output of the discriminant such that $\approx 70\%$ of b -quark jets and $\approx 1\%$ of light-quark or gluon jets pass in inclusive simulated $t\bar{t}$ events. All jets that meet this criterion are called ‘ b -tagged’ jets.

The missing transverse momentum is calculated as the negative of the vector E_T sum from all calorimeter energy clusters, with jet and electron energy calibrations applied to clusters associated with those objects, and corrected for the energy carried away by identified muons. Energy scale corrections applied to electrons and jets are also propagated to E_T^{miss} . Events are required to have $E_T^{\text{miss}} > 40$ GeV.

If the same-sign leptons are both electrons, their invariant mass m_{ee} is required to be greater than 15 GeV and to satisfy $|m_{ee} - m_Z (= 91 \text{ GeV})| > 10$ GeV. These requirements reject events from known resonances decaying to an electron–positron pair where the charge of either the electron or positron is misidentified. Finally, the scalar sum of all jet and lepton transverse momenta (H_T), is required to be greater than 400 GeV, since the signals considered here produce a high number of particles with high transverse momenta. These preselection criteria are applied to all searches; some of them are tightened when optimizing the selection for each signal model (see section 5). Figure 2 shows the distributions of H_T and E_T^{miss} after applying this selection (except for the requirements on H_T and E_T^{miss} themselves).

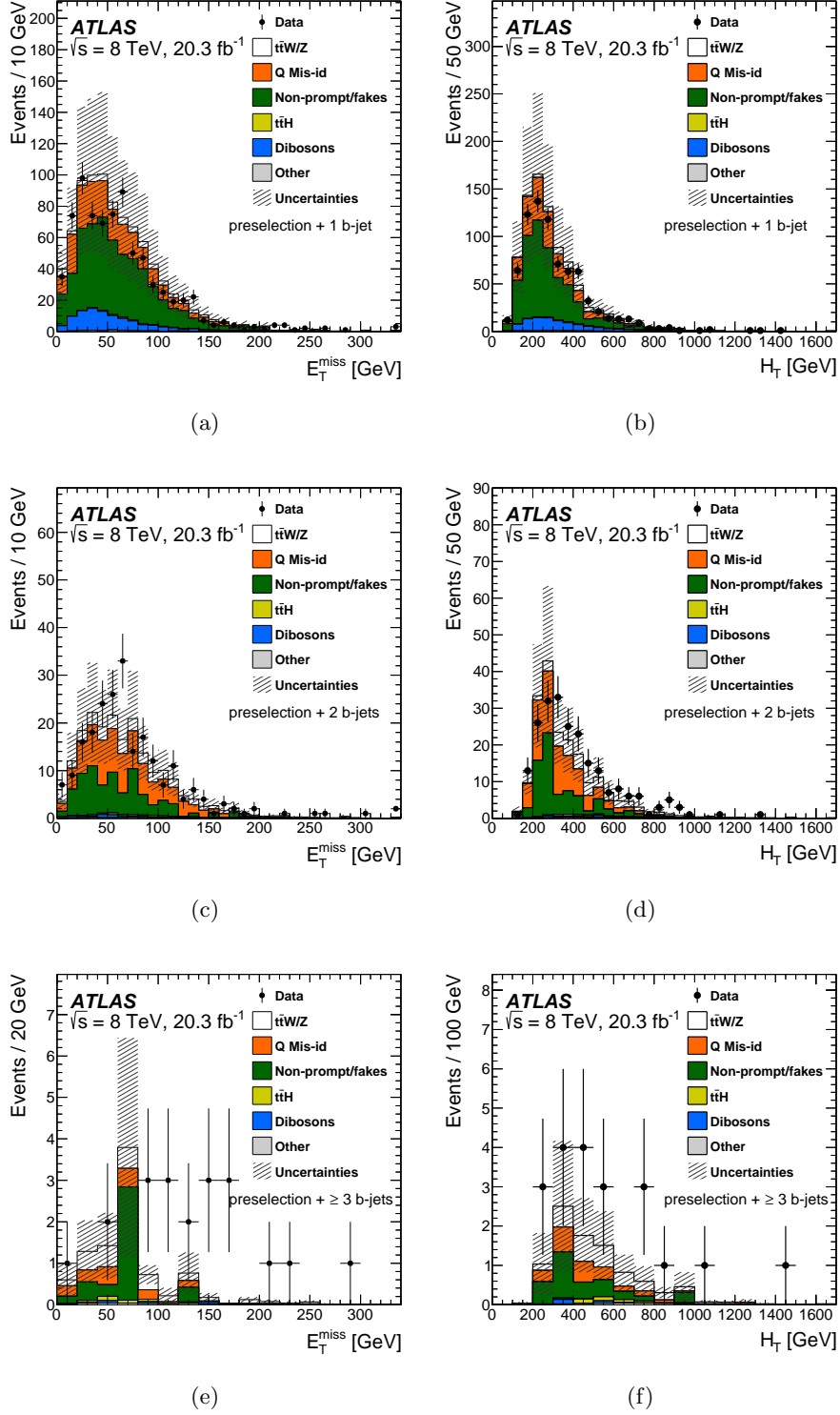


Figure 2: Distributions of the missing transverse momentum E_T^{miss} and scalar sum of jet and lepton transverse momenta H_T after applying the preselection criteria, for events with one, two, or more than two b -tagged jets. The points with error bars are the data, the stacked histograms show the expectation from background, and the shaded band is the total uncertainty on the background expectation.

4 Background estimation

Background arises from two distinct sources: SM processes that result in same-sign lepton pairs, and instrumental backgrounds where objects are misidentified or misreconstructed such that events appear to have the required set of leptons. The former category includes production of $W^\pm W^\pm jj$, $t\bar{t}W/Z$, $t\bar{t}W^+W^-$, $t\bar{t}H$, WH , ZH , tWZ , tH , WZ and ZZ with a heavy-flavour jet, or three vector bosons. In addition, the four-top-quark production predicted in the SM is included as a background to all searches for other signals, though its contribution is small due to the small cross section. All of these processes have small cross sections, and their expected yields are computed using simulation. Known differences between the lepton selection and b -tag efficiencies between the MC simulation and data control samples are taken into account when computing the expected yields.

Instrumental backgrounds have contributions from two categories: *i*) events where one or more jets are misidentified as leptons, or which contain non-prompt leptons, and *ii*) events that contain two leptons of opposite charge, where one of the charges is mismeasured. The ‘matrix method’ is used to estimate the contribution from events with misidentified (fake or non-prompt) leptons. In this method, the default (‘tight’) lepton identification criteria (section 3) are relaxed to form a ‘loose’ sample. Lepton isolation requirements are not imposed, and therefore the loose sample contains a larger fraction of fake/non-prompt leptons than the tight sample. The fraction of real leptons (meaning prompt leptons from the decay of a W , Z , or H boson) passing the loose criteria that also pass the tight criteria is referred to as r . Similarly, the fraction of fake/non-prompt leptons passing the loose cuts that also pass the tight cuts is referred to as f . Using measured values of r and f , one can construct a matrix that relates the observed yields of dilepton events in the categories loose–loose, loose–tight, and tight–tight to the real–real, real–fake, and fake–fake yields. An analogous procedure is applied to three lepton events starting with categories for all possible combinations of three loose or tight leptons, resulting in an estimate of the number of events with one or more misidentified leptons in the selected sample ($N_{\text{fake}}^{\text{tt}}$).

Single-lepton events are used to measure r and f . The criteria used to select these events are different for electrons and muons due to the differences in the sources of fake/non-prompt leptons for each flavour. For electrons, r is measured using events with $E_{\text{T}}^{\text{miss}} > 150$ GeV, where the dominant contribution is from $W \rightarrow e\nu$, and f is measured using events with the transverse mass of the $E_{\text{T}}^{\text{miss}}$ and electron⁶ $m_{\text{T}}(W) < 20$ GeV and $E_{\text{T}}^{\text{miss}} + m_{\text{T}}(W) < 60$ GeV, where the dominant contribution is from multijet production where one or more jets is misidentified as an electron. For muons, r is measured using events with $m_{\text{T}}(W) > 100$ GeV, a sample dominated by $W \rightarrow \mu\nu$, and f is measured using events where the impact parameter of the muon with respect to the primary vertex is more than five standard deviations from zero, consistent with muons arising from heavy-flavour hadron decays. The small contribution of real leptons to the control samples used to measure f is estimated from simulation, and this contribution is subtracted from the sample. The

⁶The transverse mass of a lepton and $E_{\text{T}}^{\text{miss}}$ is defined as $m_{\text{T}}(W) \equiv \sqrt{2p_{\text{T}\ell}E_{\text{T}}^{\text{miss}}(1 - \cos \Delta\phi)}$ where $p_{\text{T}\ell}$ is the lepton p_{T} and $\Delta\phi$ is the azimuthal angle between the lepton and the direction of the missing transverse momentum vector.

values of r and f are parameterized with respect to properties of the leptons (e.g. $|\eta|$ and p_T) and of the event (e.g. the number of b -tagged jets). Typical values are $r = 0.90$ and $f = 0.20 - 0.40$ for electrons, and $r = 0.95 - 1.00$ and $f = 0.12 - 0.30$ for muons.

The triggers used for low- p_T leptons require isolation; since the tight and loose lepton criteria differ in their isolation requirements, fake/non-prompt leptons in events where only the low- p_T triggers fired are more isolated, on average, than those from an unbiased trigger, meaning that f for these leptons is substantially higher. Therefore, r and f are measured separately for samples collected with the different triggers, and the appropriate values are applied based on the lepton triggers that fired in each event. A further complication may arise due to the small number of events in the loose sample, which can lead to a calculated value of $N_{\text{fake}}^{\text{tt}}$ that is negative or very close to zero. In the case of negative values $N_{\text{fake}}^{\text{tt}}$ is set to zero when computing limits. To properly estimate the statistical uncertainty on the fake/non-prompt lepton contribution given the small number of events, a Poisson likelihood for the estimate from the matrix method is used, and the standard deviation of the probability density function (p.d.f.) from this likelihood is used to set the uncertainty. In cases where the prediction from the matrix method is less than or near zero, the standard deviation is computed relative to zero rather than to the mean of the p.d.f.

Charge misidentification ('Q mis-Id') is negligible for muons due to the small probability for muons to radiate photons, the long lever arm to the muon system and the fact that the charge is measured in both the inner detector and the muon spectrometer. For electrons, the rate of charge misidentification is calculated from a sample of $Z \rightarrow ee$ events, selected with no requirement placed on the charge of the two electron tracks. It is assumed that the rate at which the charge of an electron is misidentified varies with the $|\eta|$ and p_T of each electron but is uncorrelated between the two electrons in each event. Further assuming that the sample consists entirely of opposite-sign electron pairs, the number of measured same-sign events N_{ss}^{ij} where one electron is in the i^{th} ($|\eta|, p_T$) bin and the other in the j^{th} bin is expected to be

$$N_{\text{ss}}^{ij} \approx N^{ij}(\varepsilon_i + \varepsilon_j) \quad (4.1)$$

where N^{ij} is the total number of events in the i - j $|\eta|$ - p_T bin, and ε is the rate of charge mismeasurement. The value of ε in each $|\eta|$ - p_T bin is then extracted by maximizing the Poisson likelihood for the observed number of same-sign pairs in each $|\eta|$ - p_T bin to be consistent with the expectation from equation 4.1. One limitation of this estimate is that electrons from Z decay only rarely have large p_T , rendering the uncertainty on the charge misidentification rate for high- p_T electrons large. To reduce this uncertainty, the rate of charge misidentification is estimated using simulated $t\bar{t}$ events as a function of the electron p_T . This rate is scaled to match the rate observed in data for the p_T range covered by the Z events, and the rate for electrons with larger p_T is extrapolated according to the scaled prediction from simulation. Closure tests comparing the number of events in the same-sign Z peak to the expectation based on the opposite-sign Z peak and the charge mismeasurement rates were performed in data and simulation and show good agreement.

To determine the number of events expected from charge mismeasurement in the signal region, a sample is selected using the same criteria as for the analysis selection, except that an opposite-sign rather than same-sign ee or $e\mu$ pair is required. The measured ε values are then applied to each electron in this sample to determine the expected number of mismeasured same-sign events in the analysis sample. One source of charge mismeasurement is from ‘trident’ electrons, where the electron emits a hard photon that subsequently produces an electron–positron pair, resulting in three tracks with small spatial separation. If the wrong track is matched to the EM cluster, the charge may be incorrect. However, such electrons would also appear to be isolated far less frequently than electrons that do not emit hard radiation. Therefore the value of r for trident electrons is lower than for electrons that have a correctly measured charge, meaning that they also contribute to the fake/non-prompt electron estimate from the matrix method. To avoid double-counting events with trident electrons in the background estimate, the charge mismeasurement rate is measured in a data sample where the non-prompt/fake contribution, estimated using the matrix method, has been removed.

Simulation was used to estimate the sources of events in the signal regions that have fake/non-prompt leptons and/or electrons with mismeasured charge, and it is found that $t\bar{t}$ events provide the dominant contribution.

The background estimates are validated using samples where one or more of the preselection criteria are vetoed so that the samples are statistically independent and the expected yield from signal events is small. One such validation region, called the ‘low H_T+1b ’ region, is defined by applying the preselection criteria, except that the requirement on H_T is modified to $100 \text{ GeV} < H_T < 400 \text{ GeV}$. This validation region is particularly useful because the background composition is similar to that of the preselection (including the fact that $t\bar{t}$ events are the dominant source of the fake/non-prompt lepton and charge mismeasurement background contributions). The predicted and observed yields in this validation region are given in tables 2 and 3. Events with three leptons are considered explicitly in table 3 since the fake/non-prompt lepton background contribution from trilepton events is not negligible, and it is important to check that this component of the background is well understood. The ‘other bkg.’ category includes WWW , WWZ , WH , ZH , $t\bar{t}WW$, SM four-top-quark, and single-top-quark production. Similar agreement between the data yield and background expectation is observed in validation regions where no requirement on b -tagged jets is imposed, and where E_T^{miss} is required to be less than 40 GeV or H_T is required to be in the range 100–400 GeV.

Sample	ee	$e\mu$	$\mu\mu$
Q mis-Id	$136 \pm 2 \pm 41$	$118 \pm 1 \pm 35$	—
Fake/Non-prompt	$153 \pm 11 \pm 107$	$225 \pm 11 \pm 158$	$29 \pm 3 \pm 20$
$t\bar{t}W/Z$	$4.57 \pm 0.19 \pm 1.88$	$14.2 \pm 0.3 \pm 5.8$	$8.43 \pm 0.27 \pm 3.56$
$t\bar{t}H$	$0.39 \pm 0.04 \pm 0.04$	$1.31 \pm 0.08 \pm 0.13$	$0.76 \pm 0.06 \pm 0.07$
Dibosons	$5.57 \pm 0.45 \pm 1.08$	$15.9 \pm 0.8 \pm 2.9$	$9.00 \pm 0.58 \pm 1.79$
Other bkg.	$0.32 \pm 0.11 \pm 0.11$	$0.75 \pm 0.20 \pm 0.20$	$0.27 \pm 0.06 \pm 0.06$
Total bkg.	$299 \pm 11 \pm 115$	$375 \pm 11 \pm 162$	$47 \pm 3 \pm 20$
Data	271	307	52

Table 2: Observed and expected numbers of events in the low- H_T+1b validation region for the same-sign dilepton channels. The first uncertainty is statistical and the second is systematic (systematic uncertainties are described in section 6).

Sample	eee	$ee\mu$
Fake/Non-prompt	$8.0 \pm 2.3 \pm 5.6$	$13.2 \pm 2.4 \pm 9.2$
$t\bar{t}W/Z$	$1.20 \pm 0.09 \pm 0.46$	$2.55 \pm 0.13 \pm 0.87$
$t\bar{t}H$	$0.07 \pm 0.02 \pm 0.01$	$0.28 \pm 0.03 \pm 0.03$
Dibosons	$5.78 \pm 0.51 \pm 1.14$	$6.78 \pm 0.57 \pm 1.33$
Other bkg.	$0.04 \pm 0.02 \pm 0.02$	$0.11 \pm 0.02 \pm 0.02$
Total bkg.	$15.1 \pm 2.4 \pm 5.7$	$22.9 \pm 2.5 \pm 9.4$
Data	15	18

Sample	$e\mu\mu$	$\mu\mu\mu$
Fake/Non-prompt	$17.9 \pm 2.8 \pm 12.5$	$1.34 \pm 0.55 \pm 0.94$
$t\bar{t}W/Z$	$3.38 \pm 0.16 \pm 1.15$	$2.70 \pm 0.14 \pm 1.00$
$t\bar{t}H$	$0.32 \pm 0.03 \pm 0.03$	$0.14 \pm 0.02 \pm 0.01$
Dibosons	$8.42 \pm 0.57 \pm 1.78$	$9.23 \pm 0.65 \pm 1.82$
Other bkg.	$0.12 \pm 0.02 \pm 0.02$	$0.15 \pm 0.03 \pm 0.03$
Total bkg.	$30.1 \pm 2.8 \pm 12.7$	$13.6 \pm 0.9 \pm 2.4$
Data	36	14

Table 3: Observed and expected numbers of events in the low- H_T+1b validation region for the trilepton channels. The first uncertainty is statistical and the second is systematic (systematic uncertainties are described in section 6).

5 Selection optimization

The selection is defined to optimize the expected limit on signals. Since many BSM physics models (each of them dependent on mass and/or coupling parameters) could result in anomalous production of the sort sought in this analysis, defining a selection that is sensitive

to all of them is a challenge. As a first step toward a solution, the same-sign top signal is considered separately from the others, as it has unique characteristics: contributions are expected dominantly from positively charged lepton pairs⁷, and the jet multiplicity tends to be lower. The selection for same-sign top events is optimized with respect to H_T , E_T^{miss} , and the number of b -tagged jets N_b , with contributions from the ee , $e\mu$, and $\mu\mu$ channels considered separately.

The remaining signals share a similar final-state topology, but the distribution of events differs between them in several variables. Therefore several event categories are defined, based on features of the events such as H_T , E_T^{miss} , and N_b , as shown in table 4. Splitting the sample in this manner provides good overall efficiency for signal events, while allowing events that are least likely to arise from background (i.e. events with large values of H_T , E_T^{miss} , or N_b) to be treated separately in the analysis, thereby enhancing the sensitivity to BSM physics. The boundaries between categories in H_T and E_T^{miss} were chosen to optimize the sensitivity to four-top-quark signals; these values are close to optimal for the other signals considered as well.

All of the categories are considered when searching for vector-like quarks or chiral b' -quarks, while only the categories that require at least two b -tagged jets are considered when searching for the production of four top quarks. One consequence of defining several signal categories is that the data-driven background estimates are subject to large statistical fluctuations. To mitigate this, all lepton flavours are summed within each category. The signal regions are defined based on the expected yields of signal and background, taking into account statistical and systematic effects, without considering the distribution of data.

⁷Production of $\bar{u}u \rightarrow \bar{t}t$ is also possible through these processes but the production cross section in pp collisions for this process is two orders of magnitude lower than that for $uu \rightarrow tt$. Therefore, considering only the tt final state reduces the background by a factor of two while having only a small impact on the signal.

Definition		Name	
$e^\pm e^\pm + e^\pm \mu^\pm + \mu^\pm \mu^\pm + eee + ee\mu + e\mu\mu + \mu\mu\mu, N_j \geq 2$			
$400 < H_T < 700$ GeV	$N_b = 1$	SRVLQ0	
	$N_b = 2$	SRVLQ1	
	$N_b \geq 3$	SRVLQ2	
$H_T \geq 700$ GeV	$N_b = 1$	$40 < E_T^{\text{miss}} < 100$ GeV	SRVLQ3
		$E_T^{\text{miss}} \geq 100$ GeV	SRVLQ4
	$N_b = 2$	$40 < E_T^{\text{miss}} < 100$ GeV	SRVLQ5
		$E_T^{\text{miss}} \geq 100$ GeV	SRVLQ6
	$N_b \geq 3$	$E_T^{\text{miss}} > 40$ GeV	SRVLQ7
	$e^+e^+, e^+\mu^+, \mu^+\mu^+, N_j \in [2, 4], \Delta\phi_{\ell\ell} > 2.5$		
$H_T > 450$ GeV	$N_b \geq 1$	$E_T^{\text{miss}} > 40$ GeV	SRttee, SRtte μ , SRtt $\mu\mu$

Table 4: Definitions of the different signal regions. N_j is the number of jets that pass the selection requirements, and $\Delta\phi_{\ell\ell}$ is the separation in ϕ between the leptons. In regions SRVLQ0–SRVLQ7, contributions from all lepton flavours are summed.

6 Systematic uncertainties

Tables 5 and 6 show the sources of systematic uncertainties that contribute more than 1% uncertainty on the expected background or signal yield for the four-top/ b' /VLQ selection. These uncertainties have similar impact on the expected yields for the other signal models. For the yields derived from simulation, the largest source of uncertainty is the cross-section calculation. For the $t\bar{t}W/Z$ background, this is based on variations in the PDFs, variations of the renormalization and factorization mass scales (varied up and down by a factor of four from the nominal value of 172.5 GeV) [85], and variations in the parameters controlling the initial-state radiation model, resulting in a 43% uncertainty. For other background contributions, varying the renormalization and factorization scales results in uncertainties of 30% for WZ and ZZ production, 25% for $W^\pm W^\pm jj$ production, +38%/–26% for $t\bar{t}W^+W^-$ production, and 10% for $t\bar{t}H, tH, WH, ZH, tWZ, WWW$ and ZWW production. These uncertainties, applied to the event yields shown in tables 8 and 9, result in the overall cross section uncertainties reported in table 5. The uncertainty on the integrated luminosity is 2.8% [86]. This uncertainty applies only to the backgrounds estimated from simulation, not to the data-driven estimates of the fake/non-prompt lepton and electron charge mismeasurement backgrounds, so the overall contribution of the luminosity uncertainty shown in table 5 is less than 2.8%. The largest detector-specific uncertainties arise from the jet energy scale [83], the b -tagging efficiency [84], and the lepton identification efficiency [77, 79].

Systematic uncertainties on the background contributions estimated from data are evaluated separately. Six effects are considered when assigning the systematic uncertainty on the predicted yield of events from electron charge mismeasurement: *i*) the statistical uncertainty on the probability for an electron to have its charge mismeasured, *ii*) the

Source	VLQ signal region number							
	0	1	2	3	4	5	6	7
Cross section	± 8.0	± 13.6	± 15.1	± 11.1	± 12.1	± 16.8	± 25.2	± 23.8
Jet energy scale	+1.7 -1.6	+1.2 -1.8	+1.4 -1.7	+1.8 -2.1	+2.6 -4.2	+3.8 -1.5	+8.5 -4.8	+7.3 -2.9
b -tagging efficiency	± 1.0	± 2.6	+5.7 -5.5	+1.9 -2.0	+1.6 -1.7	+3.8 -3.7	+5.1 -5.0	+8.3 -8.2
Lepton ID efficiency	± 1.3	± 1.6	± 1.6	+2.1 -2.0	+2.1 -2.0	+2.2 -2.1	+2.8 -2.2	± 2.5
Jet energy resolution	± 0.5	± 0.2	± 3.1	± 1.9	± 0.3	± 0.9	± 0.8	± 3.4
Luminosity	± 0.9	± 1.1	± 1.3	± 1.4	± 1.5	± 1.5	± 2.1	± 1.9
Fake/non-prompt leptons	± 33	± 18	± 25	± 23	± 26	± 16	± 1.5	± 3.8
Charge misID	+5.9 -5.7	+9.3 -9.1	+5.4 -5.1	+7.4 -6.7	+5.0 -4.6	+8.7 -8.1	+9.0 -8.5	+11.0 -10.1

Table 5: The largest systematic uncertainties (in %) on the total background yield for the four-top/ b' /VLQ selection.

Source	VLQ signal region number							
	0	1	2	3	4	5	6	7
Jet energy scale	+11.3 -9.0	+11.5 -6.3	+28.0 -17.3	+3.7 -2.1	+5.4 -2.4	+3.9 -2.0	+4.5 -6.5	+6.6 -3.0
b -tagging efficiency	+2.5 -3.0	+6.3 -6.1	+16.4 -15.9	+3.1 -3.7	+3.4 -4.0	+7.4 -7.2	+7.6 -7.4	+12.1 -11.9
Lepton ID efficiency	± 2.9	± 2.9	± 2.8	± 2.9	+3.2 -3.1	± 2.9	+3.2 -3.1	+3.0 -2.9
Jet energy resolution	± 0.8	± 2.5	± 3.9	± 0.3	± 0.7	± 0.7	± 1.0	± 0.1
Luminosity	± 2.8	± 2.8	± 2.8	± 2.8	± 2.8	± 2.8	± 2.8	± 2.8

Table 6: The largest systematic uncertainties (in %) on the yield of a representative signal (600 GeV vector-like B pair production) for the four-top/ b' /VLQ selection.

statistical uncertainty on the p_T -dependent scale factor, *iii*) the difference observed in simulated Z boson events between the true charge mismeasurement rate and the rate obtained by applying the same method as is used for the data, *iv*) the difference in the p_T -dependent scale factor when measured using different $t\bar{t}$ simulated samples, *v*) the variation in the result observed when the width of the Z peak region is varied, and *vi*) the statistical uncertainty on the correction for the overlap in the measurement of charge misidentification and fake-electron background estimates. The magnitudes of these effects depend on the event characteristics, so the uncertainty on the background from electron charge misidentification varies from 23 to 40% in the signal and control regions, as presented in Tables 2 and 7-9. The expected yield of fake/non-prompt leptons is subject to uncertainties in the real and fake/non-prompt lepton efficiencies that arise from *i*) variations in the values of r and f when different control regions are used to measure them, *ii*) the small number of events in

those control regions, and *iii*) the MC model used to subtract the real lepton contribution from the fake/non-prompt lepton control region. When assessing effect *i*, the following alternative control regions are used: for electrons, the alternative fake/non-prompt control region requires one loose electron and $E_T^{\text{miss}} < 20$ GeV, while for muons, the alternative control region requires one loose muon, $m_T(W) < 20$ GeV and $E_T^{\text{miss}} + m_T(W) < 60$ GeV. In both cases the expected contribution from real leptons in the control region is subtracted using simulation. The alternative control regions for *r* are formed by increasing the requirement on E_T^{miss} from > 150 GeV to > 175 GeV for electrons and by increasing the requirement on $m_T(W)$ from > 100 GeV to > 110 GeV for muons. Effects *i*)–*iii*) sum to a 70% uncertainty on the predicted yield of fake/non-prompt leptons.

7 Results

The observed yields for each signal selection are given in tables 7–9 and figure 3. The CL_s method [87, 88] is used to assess the consistency between the observed yields and each potential BSM physics signal, where the log-likelihood ratio L_R is used as the test statistic. For each model, L_R is defined as

$$L_R = -2 \log \frac{L_{s+b}}{L_b} \quad (7.1)$$

where L_{s+b} (L_b) is the Poisson likelihood to observe the data under the signal-plus-background (background-only) hypothesis. Pseudo-experiments are generated under each hypothesis, taking into account statistical fluctuations of the total predictions according to Poisson statistics, as well as Gaussian fluctuations in the signal and background expectations describing the effect of systematic uncertainties. The quantities CL_{s+b} and

	SRttee	SRtte μ	SRtt $\mu\mu$
$t\bar{t}W/Z$	$0.58 \pm 0.06 \pm 0.25$	$1.20 \pm 0.09 \pm 0.53$	$0.64 \pm 0.07 \pm 0.28$
$t\bar{t}H$	$0.05 \pm 0.02 \pm 0.01$	$0.12 \pm 0.02 \pm 0.02$	$0.03 \pm 0.01 \pm 0.01$
Dibosons	$0.27 \pm 0.14 \pm 0.07$	$0.38 \pm 0.09 \pm 0.10$	$0.19 \pm 0.12 \pm 0.04$
Fake/Non-prompt	$0.87 \pm 0.79 \pm 0.61$	$2.92 \pm 1.27 \pm 2.04$	$0.34 \pm 0.29 \pm 0.24$
Q mis-Id	$2.66 \pm 0.25 \begin{smallmatrix} +1.04 \\ -0.96 \end{smallmatrix}$	$2.79 \pm 0.26 \begin{smallmatrix} +0.96 \\ -0.92 \end{smallmatrix}$	—
Other bkg.	$0.01 \pm 0.08 \pm 0.00$	$0.05 \pm 0.08 \pm 0.01$	$0.12 \pm 0.11 \pm 0.03$
Total bkg.	$4.5 \pm 0.8 \begin{smallmatrix} +1.3 \\ -1.2 \end{smallmatrix}$	$7.5 \pm 1.3 \pm 2.5$	$1.3 \pm 0.3 \pm 0.4$
Data	6	5	2
<i>p</i> -value	0.38	0.84	0.45

Table 7: Observed and expected numbers of events with statistical (first) and systematic (second) uncertainties for the positively charged top pair signal selection. The *p*-values for agreement between the observed yield and the expected background in each signal region are reported.

	SRVLQ0	SRVLQ1/SR4t0	SRVLQ2/SR4t1
$t\bar{t}W/Z$	$16.2 \pm 0.3 \pm 7.0$	$12.6 \pm 0.3 \pm 5.4$	$1.24 \pm 0.09 \pm 0.53$
$t\bar{t}H$	$2.5 \pm 0.1 \pm 0.3$	$1.8 \pm 0.1 \pm 0.2$	$0.26 \pm 0.03 \pm 0.05$
Dibosons	$11.2 \pm 0.6 \pm 2.8$	$0.95 \pm 0.19 \pm 0.25$	$0.07 \pm 0.12 \pm 0.05$
Fake/Non-prompt	$42.1 \pm 5.4 \pm 24.6$	$8.61 \pm 2.34 \pm 5.02$	$1.17 \pm 0.82 \pm 0.68$
Q mis-Id	$20.8 \pm 0.7 \pm 5.2$	$15.1 \pm 0.6 \pm 3.5$	$0.74 \pm 0.11 \pm 0.18$
Other bkg.	$1.76 \pm 0.13 \pm 0.17$	$0.75 \pm 0.04 \pm 0.10$	$0.10 \pm 0.08 \pm 0.03$
Total bkg.	$94.5 \pm 5.4 \pm 24.9$	$40.0 \pm 2.4 \pm 7.3$	$3.6 \pm 0.9 \pm 0.8$
Data	107	54	6
p -value	0.36	0.12	0.24

	SRVLQ3	SRVLQ4
$t\bar{t}W/Z$	$2.07 \pm 0.10 \pm 0.89$	$3.14 \pm 0.13 \pm 1.35$
$t\bar{t}H$	$0.40 \pm 0.04 \pm 0.07$	$0.57 \pm 0.05 \pm 0.07$
Dibosons	$2.36 \pm 0.29 \pm 0.61$	$2.03 \pm 0.25 \pm 0.49$
Fake/Non-prompt	$3.09 \pm 1.29 \pm 1.80$	$4.24 \pm 1.59 \pm 2.47$
Q mis-Id	$1.72 \pm 0.22 \pm 0.63$	$1.45 \pm 0.17 \pm 0.52$
Other bkg.	$0.22 \pm 0.08 \pm 0.03$	$0.41 \pm 0.10 \pm 0.06$
Total bkg.	$9.87 \pm 1.35 \pm 2.10$	$11.9 \pm 1.6 \pm 2.8$
Data	7	10
p -value	0.83	0.71

Table 8: Observed and expected numbers of events with statistical (first) and systematic (second) uncertainties for five of the signal regions defined for VLQ, chiral b' -quark and four-top-quark production searches. The p -values for agreement between the observed yield and the expected background in each signal region are reported.

CL_b are defined as the fractions of signal plus background and background-only pseudo-experiments with L_R larger than the observed value. Signal cross sections for which $CL_s = CL_{s+b}/CL_b < 0.05$ are deemed excluded at the 95% CL. Expected limits assuming the absence of signal are also computed; these are the basis for assessing the intrinsic sensitivity of the analysis.

In the signal regions defined for searching for positively charged top quark pair production, the observed yields agree well with the expectation from background. The resulting limits on the cross section for this process are shown in table 10 in both the contact interaction and Higgs-like FCNC models. For the special case of the 125 GeV Higgs boson, the limit on the cross section leads to a limit of $\text{BR}(t \rightarrow uH) < 0.01$. The results can also be expressed as limits on the parameters defined in equations 1.2 and 1.3: for each chirality, the upper limit on C as a function of Λ is shown in figure 4; the same figure also shows the limits on κ_{utH} and κ_{ctH} in the Higgs-like FCNC model.

In contrast to the same-sign top signal regions, some of the signal regions defined for

	SRVLQ5/SR4t2	SRVLQ6/SR4t3	SRVLQ7/SR4t4
$t\bar{t}W/Z$	$1.87 \pm 0.09 \pm 0.80$	$2.46 \pm 0.11 \pm 1.06$	$0.57 \pm 0.05 \pm 0.25$
$t\bar{t}H$	$0.31 \pm 0.04 \pm 0.05$	$0.44 \pm 0.04 \pm 0.06$	$0.08 \pm 0.02 \pm 0.02$
Dibosons	$0.33 \pm 0.14 \pm 0.10$	$0.04 \pm 0.12 \pm 0.03$	$0.00 \pm 0.12 \pm 0.00$
Fake/Non-prompt	$1.03 \pm 0.97 \pm 0.60$	$0.00 \pm 1.02 \pm 0.28$	$0.04 \pm 0.83 \pm 0.24$
Q mis-Id	$1.17 \pm 0.16 \pm 0.38$	$1.09 \pm 0.14 \pm 0.34$	$0.30 \pm 0.09 \pm 0.10$
Other bkg.	$0.16 \pm 0.08 \pm 0.02$	$0.23 \pm 0.08 \pm 0.05$	$0.14 \pm 0.08 \pm 0.08$
Total bkg.	$4.9 \pm 1.0 \pm 1.0$	$4.3 \pm 1.1 \pm 1.1$	$1.1 \pm 0.9 \pm 0.4$
Data	6	12	6
p -value	0.46	0.029	0.036

Table 9: Observed and expected numbers of events with statistical (first) and systematic (second) uncertainties for three of the signal regions defined for VLQ, chiral b' -quark and four-top-quark production searches. The p -values for agreement between the observed yield and the expected background in each signal region are reported.

Model	$\sigma(pp \rightarrow tt)$ [fb]		Coupling const.
	Exp.	Obs.	Observed
Contact interaction model			$ C /\Lambda^2$ [TeV $^{-2}$]
Left-left	64	62	0.053
Left-right	53	51	0.137
Right-right	40	38	0.042
Higgs-like FCNC model			κ_{utH} or κ_{ctH}
$uu \rightarrow tt$ ($m_H = 125$ GeV)	37	35	0.16
$uu \rightarrow tt$ ($m_H = 250$ GeV)	21	20	0.17
$uu \rightarrow tt$ ($m_H = 500$ GeV)	12	11	0.20
$uu \rightarrow tt$ ($m_H = 750$ GeV)	9.3	8.4	0.24
$cc \rightarrow tt$ ($m_H = 250$ GeV)	71	69	0.81
$cc \rightarrow tt$ ($m_H = 500$ GeV)	37	35	1.02
$cc \rightarrow tt$ ($m_H = 750$ GeV)	28	27	1.29

Table 10: Observed and expected 95% CL upper limits on the cross section for same-sign top-quark production, and on the coupling constants.

VLQ, b' -quark, and four-top-quark production exhibit an excess over expected background. The excess is largest in the subset of the signal regions used for the four-top-quark search, where at least two b -tagged jets are required. While it is still of interest to limit the set of models consistent with the data as described above, it is also important in this case to assess the consistency of the data with the background-only hypothesis. This is done by computing $p \equiv 1 - CL_b$. The resulting p -values depend on the signal model and the signal regions considered, as shown in figures 5a and 5b. For signals where all eight signal

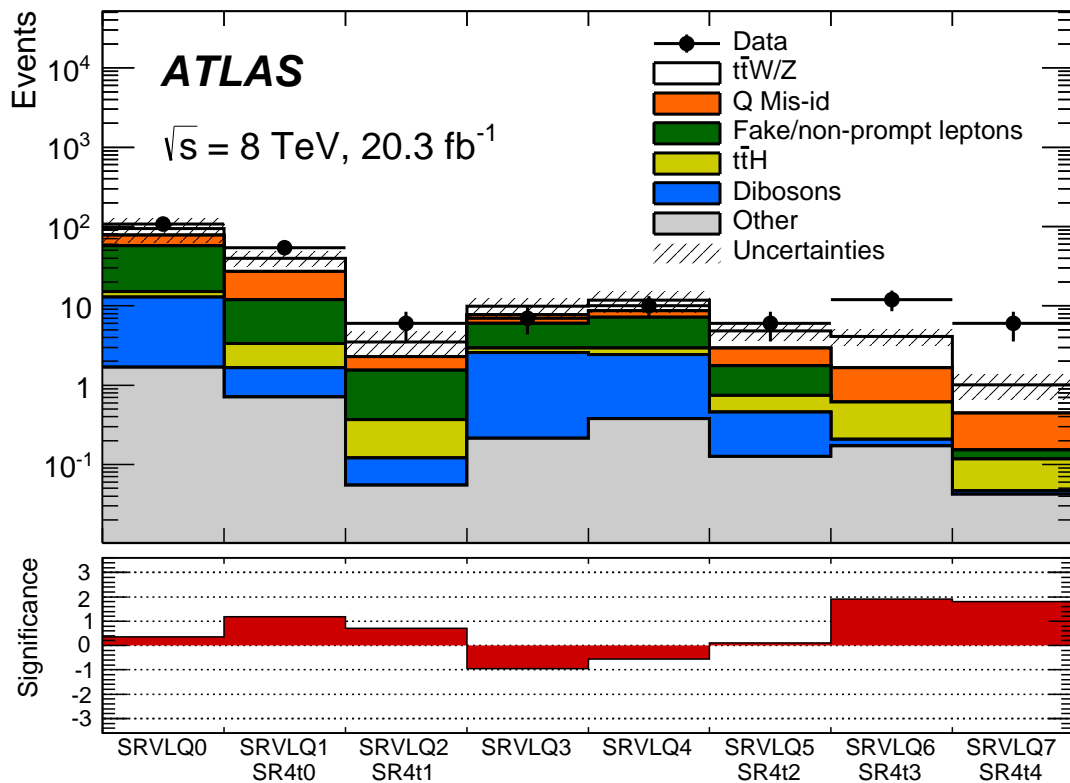


Figure 3: Expected background yields and observed data events in various signal regions. Uncertainties include both the statistical and systematic errors. The difference between data and expectations is quantified by the means of the significance, computed from the p -values in tables 8 and 9.

regions are considered (as is the case for VLQ and b' models), the significance is above one standard deviation but less than two. For signals for which only SR4t0–SR4t4 are considered (as is the case for four-top-quark production models) the significance reaches 2.5 standard deviations. Several checks (detailed in section 8) of the background estimates were performed. Some features of the events in the signal regions that exhibit the most significant excesses (SR4t3 and SR4t4) are presented in section 9.

The excess is not significant enough to support a claim of BSM physics. Therefore 95% CL limits (upper limits on cross sections, or lower limits on masses) relevant for each model are calculated. The observed excess causes these limits to be less restrictive than expected for the background-only hypothesis. The data place 95% CL upper limits on the b' -quark pair production cross section that vary with the mass of the b' -quark. Limits obtained assuming a 100% branching ratio to Wt are presented in figure 6a (expected mass limit at 0.79 TeV, observed at 0.73 TeV), and limits where decays to u - or c -quarks are also considered are shown in figures 6b and 6c.

Limits on the VLQ pair-production cross section, assuming the branching fractions to

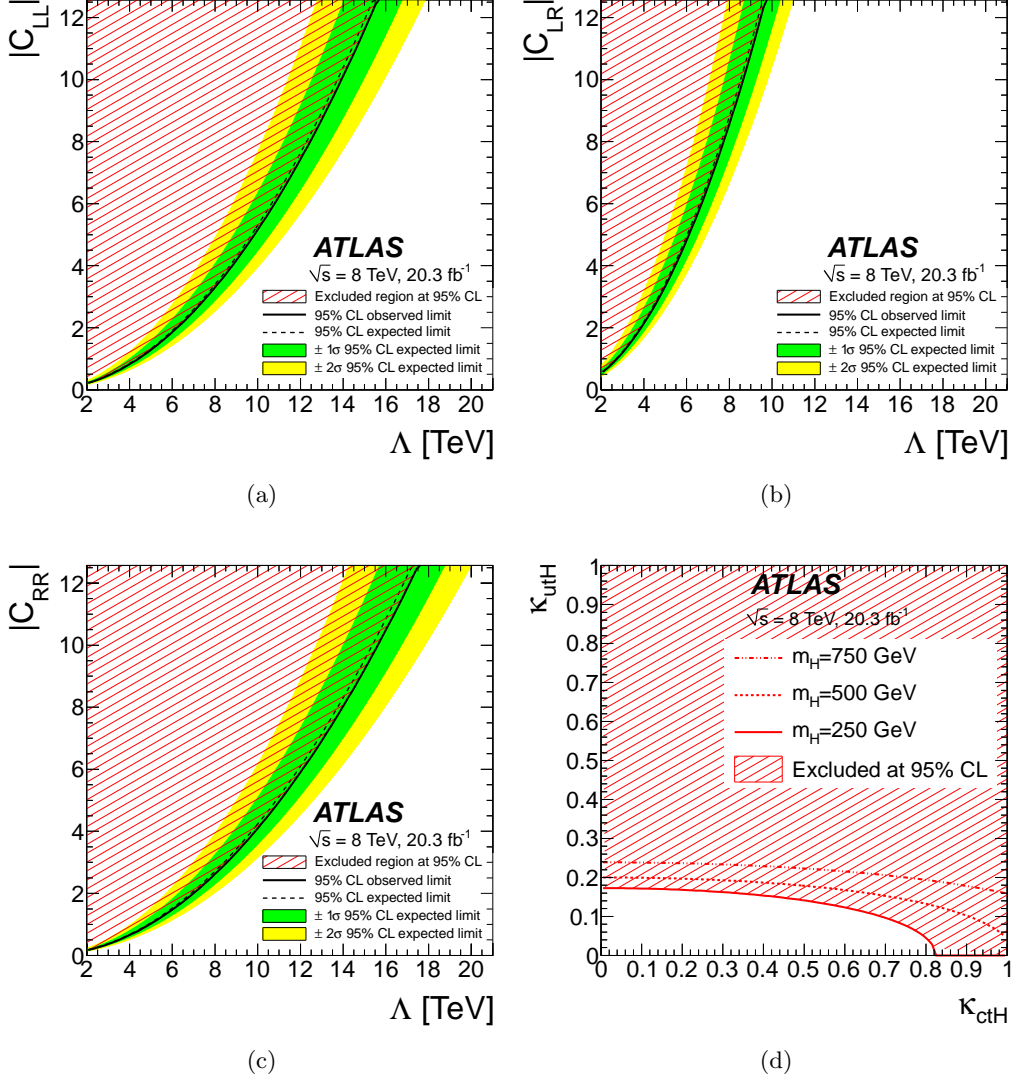


Figure 4: Expected and observed limits on the coupling constant $|C|$ in the contact interaction model for same-sign top quark pair production as a function of the BSM physics energy scale Λ for the (a) left–left, (b) left–right and (c) right–right terms. Plot (d) shows the observed limits on the Higgs-like exchange with FCNC coupling in the plane $(\kappa_{utH}, \kappa_{ctH})$ for three different hypotheses on the mass of the heavy Higgs-like particle.

W , Z , and H modes prescribed by the singlet model, are shown in figure 7. Comparison with the calculated cross-section results in lower limits on the B -quark mass of 0.62 TeV and on the T quark mass of 0.59 TeV at 95% CL. The expected limits in the absence of a signal contribution are 0.69 TeV for the B -quark mass and 0.66 TeV for the T -quark mass. If the three branching fractions are allowed to vary independently (subject to the constraint that they sum to one), the data can be interpreted as excluding at 95% CL some

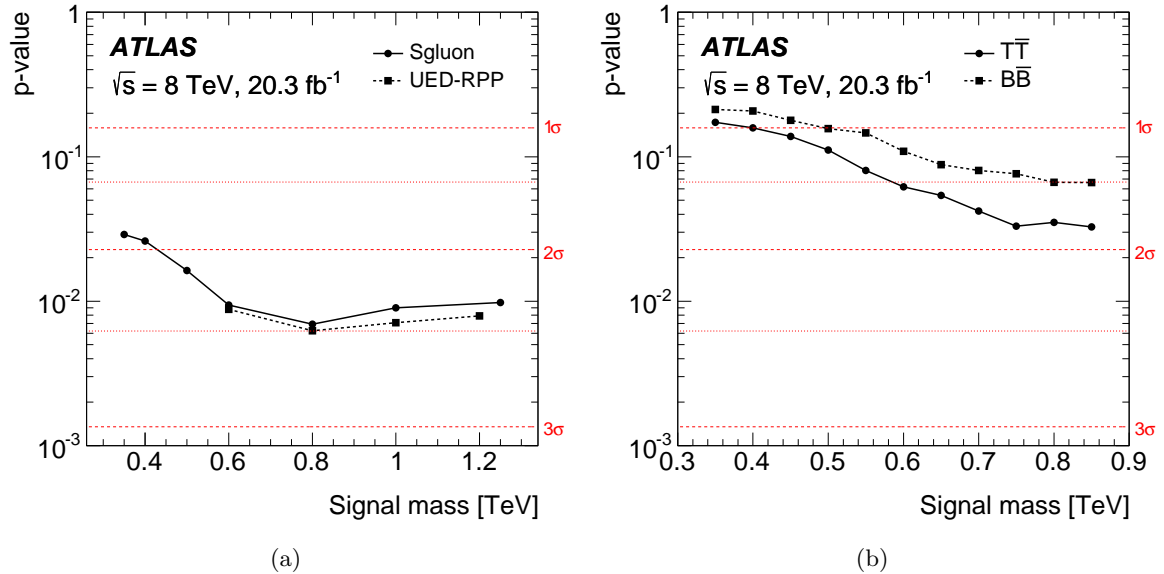
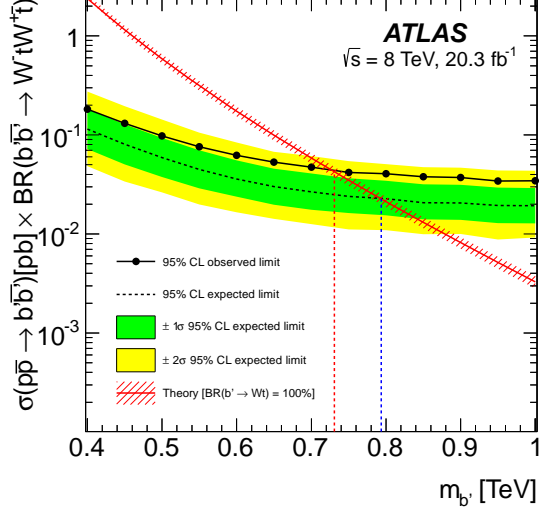


Figure 5: (a) Probability for the data in the four-top-quark signal regions (SR4t0–SR4t4) to be consistent with a zero cross section for anomalous four-top-quark production under two model scenarios, as a function of the characteristic mass scale of the models. (b) Probability for the data in the VLQ/ b' -quark signal regions (SRVLQ0–SRVLQ7) to be consistent with a zero cross section for various heavy quarks, as a function of the quark mass.

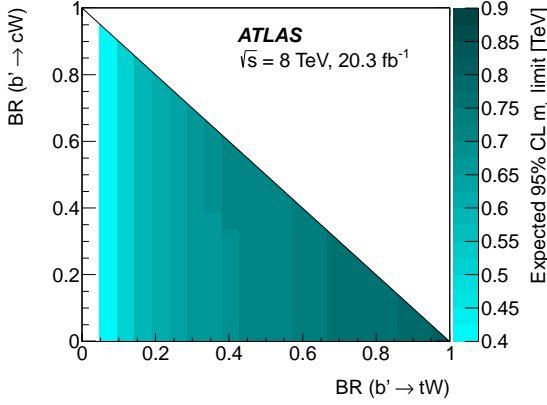
of the possible sets of branching ratios for a given B - or T -quark mass. These exclusions are shown in figures 8 and 9.

Limits on $T_{5/3}$ production are set for pair production only, and for the sum of pair and single production for two different values of the coupling λ of the $T_{5/3}$ to Wt ($\lambda = 0.5$ and 1.0) [89]. This coupling is related to the mixing parameter g^* used by the model in refs. [90, 91]: $\lambda = m_{T_{5/3}} g g^* / m_W \sqrt{2}$. The pair-production limits are shown in figure 10a, and correspond to a mass limit of 0.74 TeV (0.81 TeV expected). The limits on pair plus single production with $\lambda = 0.5$ are shown in figure 10b, where the observed mass limit is 0.75 TeV and the expected limit is 0.81 TeV. Finally, limits on pair plus single production with $\lambda = 1.0$ are shown in figure 10c, where again the observed mass limit is 0.75 TeV and the expected limit is 0.81 TeV.

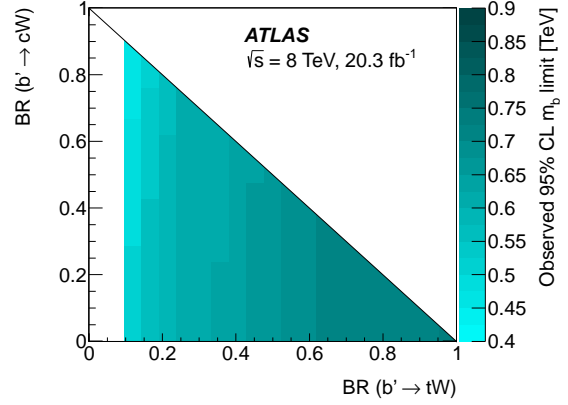
The upper limit on the cross section for four-top-quark production is 70 fb assuming SM kinematics, and 61 fb for production with a BSM-physics contact interaction (expected limits are respectively 27 fb and 22 fb). The cross-section limit for the contact interaction case is lower than for the SM since the contact interaction tends to result in final-state objects with larger p_T , which increases the selection efficiency. The limits are also interpreted in the context of specific BSM physics models. For the contact interaction model, the upper limit on $|C_{4t}|/\Lambda^2$ is 15.1 TeV $^{-2}$, as illustrated in figure 11a. The lower limit on



(a)



(b)



(c)

Figure 6: Limits on b' -quark pair production: (a) Expected and observed upper limits on the b' pair-production cross section times the branching ratio for $b'\bar{b}' \rightarrow W^-tW^+\bar{t}$, as a function of the b' -quark mass (the vertical dashed lines indicate the expected and observed limits on the b' -quark mass, and the shaded band around the theory cross section indicates the total uncertainty on the calculation); (b) expected and (c) observed exclusion limits on the b' -quark mass as a function of the assumed branching ratios into c - and t -quarks.

the sgluon mass is 0.83 TeV, assuming that the sgluons are pair-produced and always decay to $t\bar{t}$ (for an expected limit of 0.94 TeV), as shown in figure 11b. The observed limits on the cross section times branching ratio for the 2UED/RPP signal are shown in figures 11c, 11d and 12. These imply the following limits on m_{KK} : in the symmetric case ($R_4 = R_5$), the observed limit coming from tier (1, 1) is 0.96 TeV (where the expected limit is 1.05 TeV). The observed limit coming from tiers (2, 0) + (0, 2) alone ($\text{BR}(A^{(1,1)} \mapsto t\bar{t}t) = 0$) is 0.50 TeV

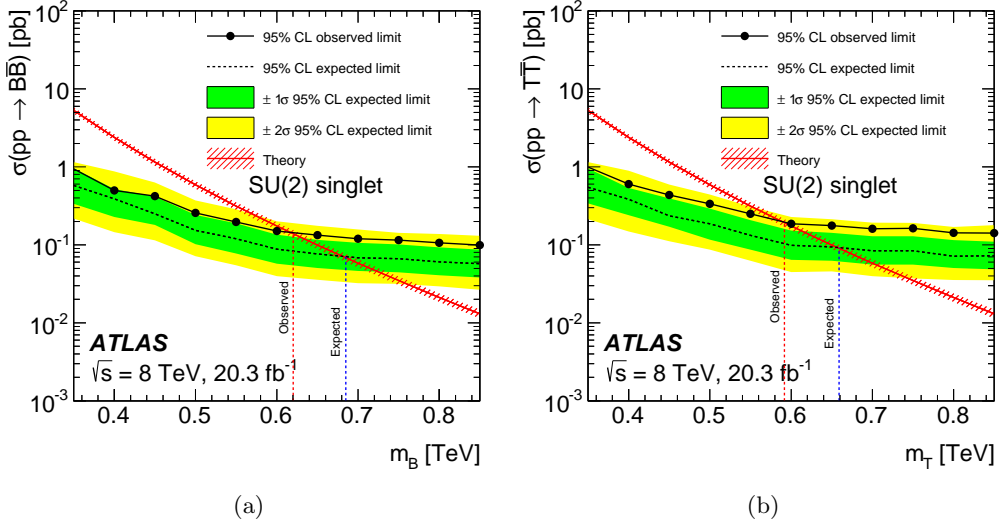


Figure 7: Expected and observed limits on the pair production cross section as a function of mass for (a) vector-like B and (b) vector-like T quarks. The vertical dashed lines indicate the expected and observed limits on the vector-like quark mass. These limits assume branching ratios given by the model where the B and T quarks exist as singlets [25]. The shaded band around the theory cross section indicates the total uncertainty on the calculation.

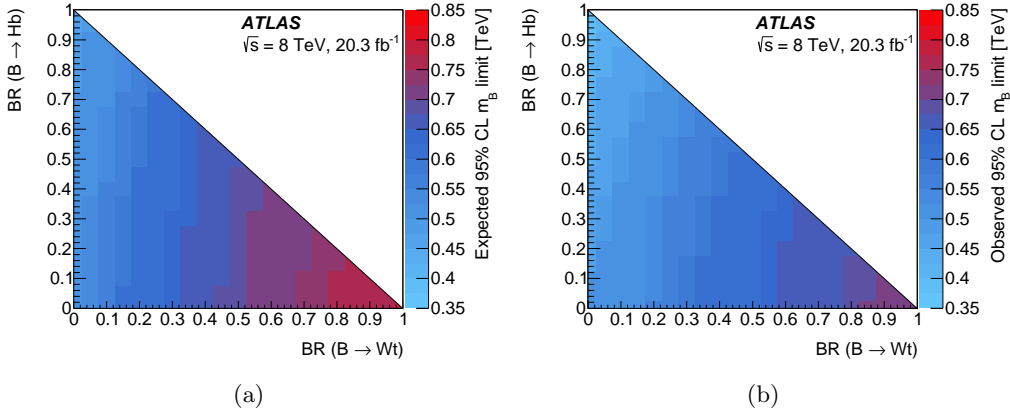


Figure 8: Expected (a) and observed (b) vector-like B quark mass hypotheses excluded at 95% CL as a function of the assumed branching ratios.

(where the expected limit is 0.55 TeV). In the highly asymmetric case ($R_4 > R_5$), tier (0, 2) does not contribute any longer and the observed limit on m_{KK} from tier (2, 0) alone is 0.45 TeV (where the expected limit is 0.51 TeV). Figure 12 shows the limits in the m_{KK} - ξ plane, with the constraints from cosmological considerations superimposed.

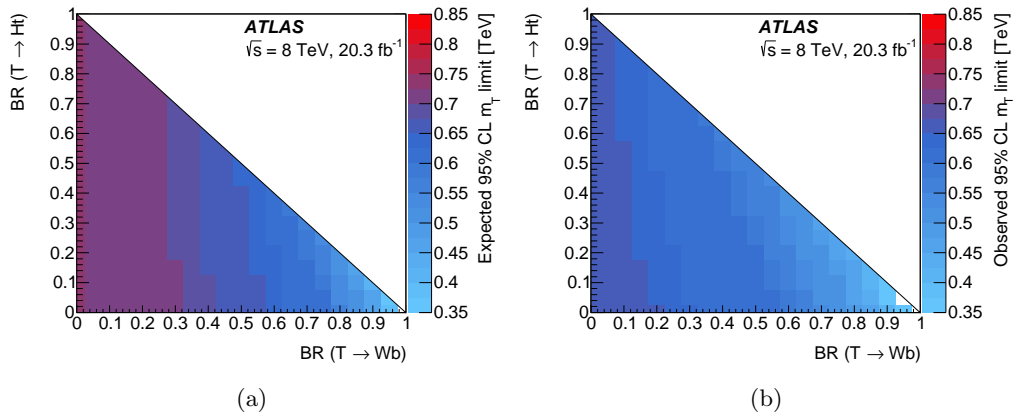
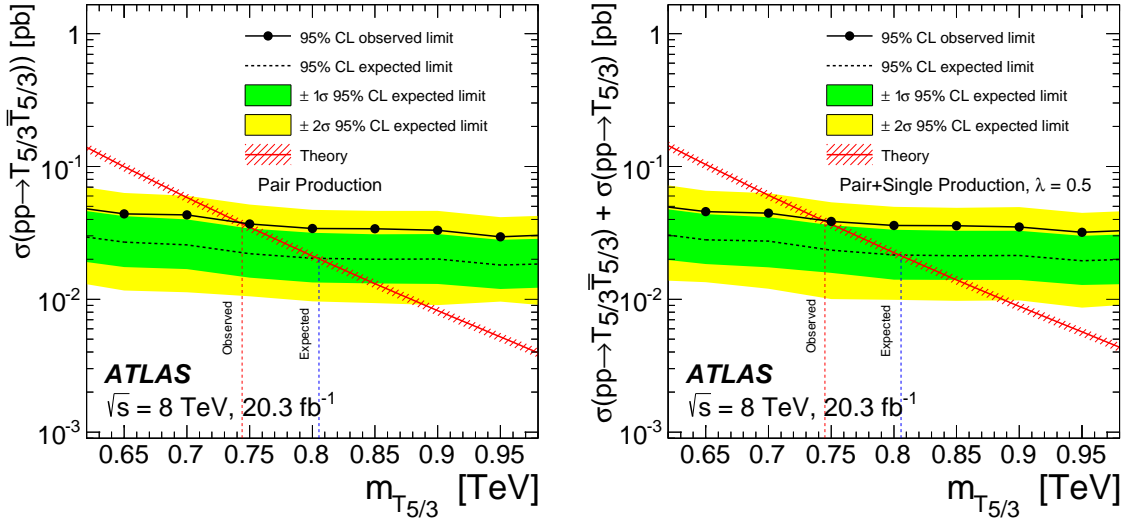
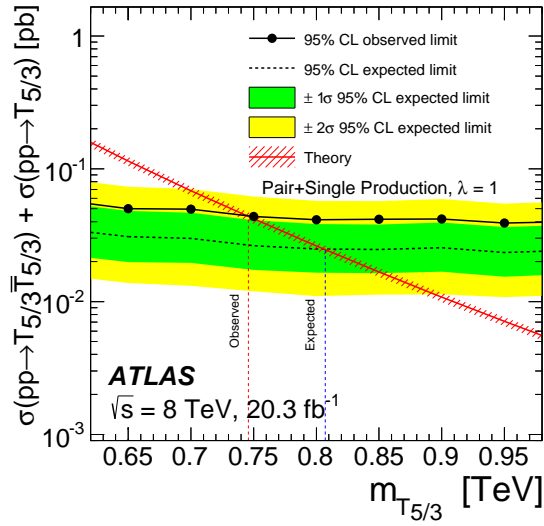


Figure 9: Expected (a) and observed (b) vector-like T quark mass hypotheses excluded at 95% CL as a function of the assumed branching ratios.



(a)

(b)



(c)

Figure 10: Expected and observed cross section limits as a function of mass on (a) $T_{5/3}$ pair production, (b) $T_{5/3}$ pair plus single production for coupling $\lambda = 0.5$, and (c) $T_{5/3}$ pair plus single production for $\lambda = 1.0$. The vertical dashed lines indicate the expected and observed limits on the $T_{5/3}$ mass, and the shaded band around the theory cross section indicates the total uncertainty on the calculation.

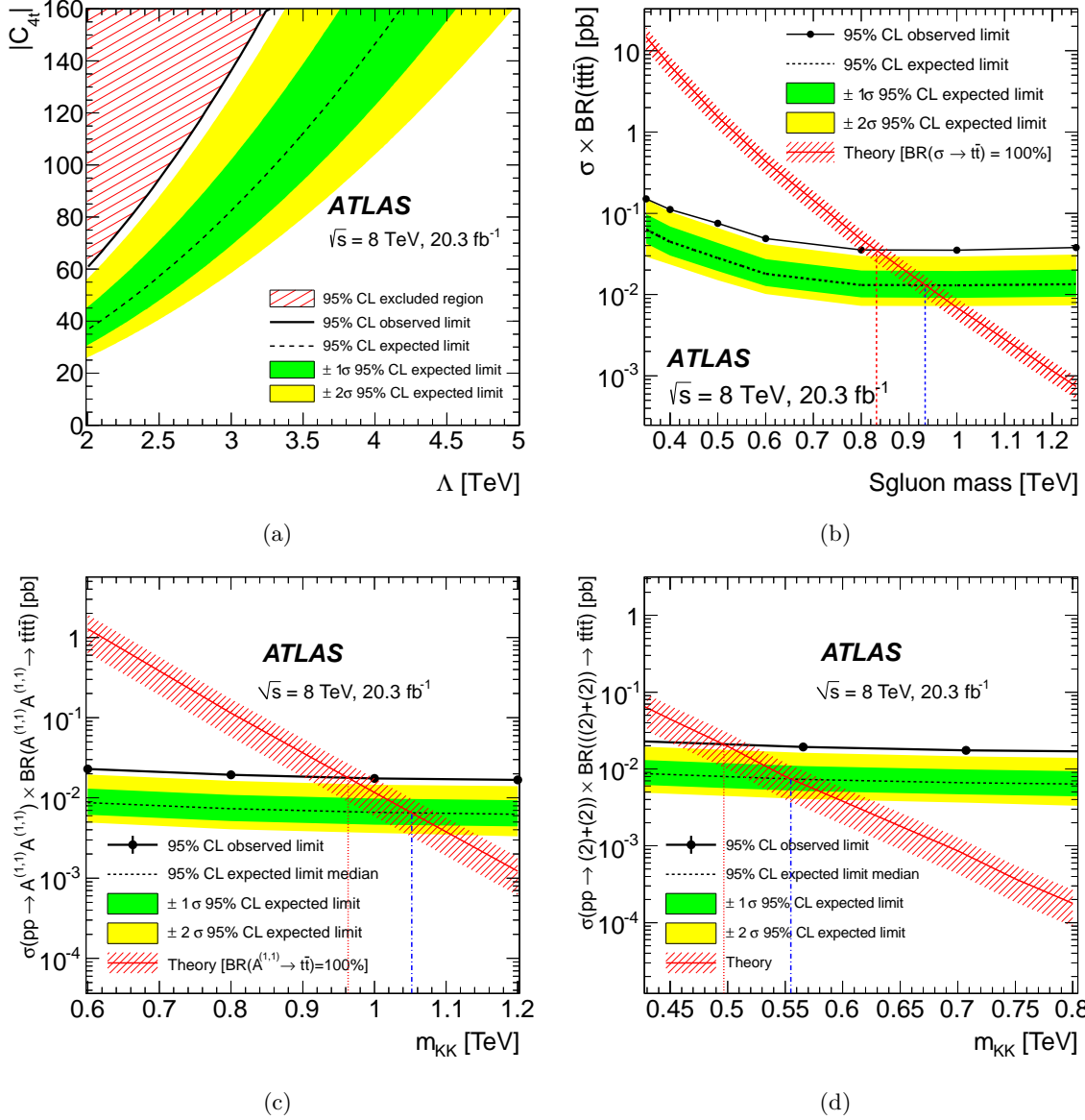


Figure 11: Limits obtained from the search for four-top-quark production. (a) Expected and observed limits on the coupling constant $|C_{4t}|$ in the contact interaction model for four-top production as a function of the BSM physics energy scale Λ . The region in the top left corner, corresponding to $|C_{4t}|/\Lambda^2 > 15.1 \text{ TeV}^{-2}$, is excluded at 95% CL. (b) Expected and observed limits for the sgluon pair-production cross section times branching ratio to four top quarks as a function of the sgluon mass. (c) Expected and observed limits on the four-top-quark production rate for the 2UED/RPP model in the symmetric case. The theory line corresponds to the production of four-top-quark events by tier (1, 1) with a branching ratio of $A^{(1,1)}$ to $t\bar{t}\bar{t}\bar{t}$ of 100%. (d) Expected and observed limits on the four-top-quark production rate for the 2UED/RPP model in the symmetric case. The notation (2) + (2) is a shorthand for $A^{(2,0)}A^{(2,0)} + A^{(0,2)}A^{(0,2)}$. The theory line corresponds to the four-top-quark production by tiers (2, 0) + (0, 2) alone ($\text{BR}(A^{(1,1)} \mapsto t\bar{t}\bar{t}\bar{t}) = 0$). The vertical dashed lines in (b), (c), and (d) indicate the expected and observed limits on the sgluon mass or on m_{KK} , and the shaded band around the theory cross section indicates the total uncertainty on the calculation.

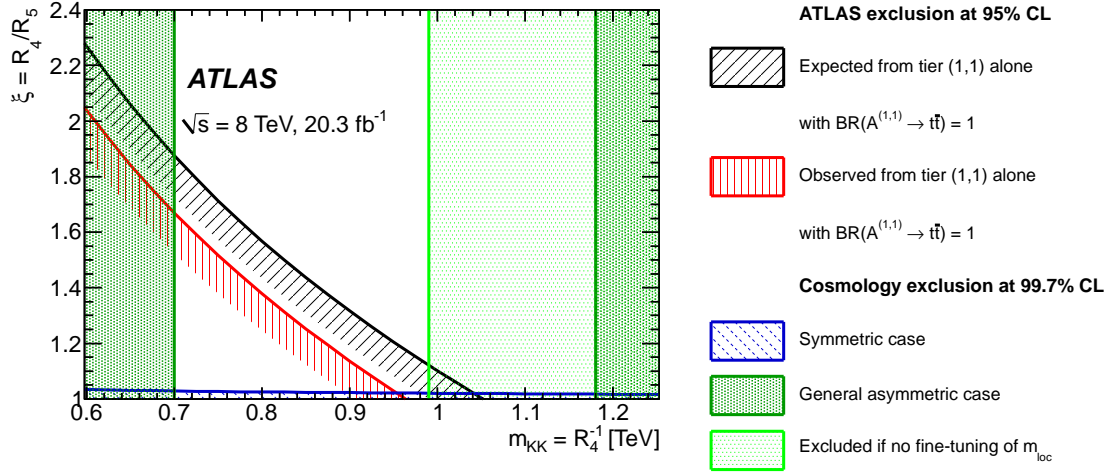


Figure 12: Expected and observed limits in the $(m_{\text{KK}} = 1/R_4, \xi = R_4/R_5)$ plane for the 2UED/RPP model. Cosmological constraints are also shown. They are due both to direct searches for dark matter and from constraints on its relic density (see ref. [43] for more details). The m_{loc} parameter from ref. [43] affects the dark-matter relic density predicted by the 2UED/RPP model.

8 Checks of the background estimate

Several checks were performed to assess the validity of the background estimate. The most important tests are summarized here. For the simulation-based background estimates: variations in the cross section, in the generators, and their settings that span the range consistent with theoretical expectations or direct measurements were applied. Variations in the expected yield are part of the systematic uncertainty. The data-driven estimates (for the charge misidentification and fake/non-prompt lepton backgrounds) were checked in several ways. The particular leptons observed in SRVLQ6 and SRVLQ7 were scrutinized, and their quality was found to be consistent with a sample dominated by real leptons. Similarly, the multivariate discriminant for b -tagging is well above the required threshold for tagged jets found in the sample. In addition, the expected contribution from charge misidentification and from fake/non-prompt leptons was assessed using samples of simulated events. It is found that the yields are consistent within uncertainties with the expectations from the data-driven estimates. To further investigate whether the matrix method accurately predicts the number of fake/non-prompt leptons in $t\bar{t}$ events, the entire procedure was repeated with samples of simulated events, with r and f measured using simulated single-lepton and multijet samples respectively. The predicted number of fake/non-prompt leptons in simulated $t\bar{t}$ samples is consistent with the actual number present in the MC samples.

9 Features of events in signal regions with most significant excesses

Information about the lepton charges and flavours, as well as some key kinematic information, for the observed events in signal regions SR4t3/SRVLQ6 and SR4t4/SRVLQ7 are presented in tables 11–12. One unexpected feature is the dominance of one electric charge over another: in SR4t3/SRVLQ6 there are 10 negatively charged and 16 positively charged leptons, and in SR4t4/SRVLQ7 there are only 2 negatively charged leptons and 11 positively charged leptons. Similar effects are observed in two other signal regions, with SRVLQ3 being dominated by negatively charged leptons and SR4t2/SRVLQ5 being dominated by positively charged leptons. These charge asymmetries are interpreted as statistical fluctuations. This interpretation is bolstered by the fact that *i*) there is no known mechanism for the selection to favour one electric charge over the other; *ii*) the asymmetry is present only in some of the signal regions (and both negative and positive charges dominate in the various regions); and *iii*) that the asymmetries do not persist in the loose lepton samples selected with the same kinematic criteria as are applied in the signal regions.

Type	N_j	H_T [GeV]	E_T^{miss} [GeV]
e^-e^-	3	807	171
e^+e^+	5	862	268
e^+e^+	5	868	113
μ^-e^-	6	1346	353
$e^+\mu^+$	5	810	106
$e^-\mu^-$	3	707	184
$e^-\mu^-$	2	706	174
μ^+e^+	8	882	150
μ^+e^+	4	860	112
$\mu^+\mu^+$	5	888	111
$\mu^-e^+e^+$	5	773	197
$\mu^-e^+e^+$	9	968	355

Table 11: List of data events in the SR4t3/SRVLQ6 category (by definition, all events have exactly two b -jets, the E_T^{miss} is above 100 GeV and the H_T above 700 GeV).

Type	N_j	N_b	H_T [GeV]	E_T^{miss} [GeV]
e^+e^+	4	3	709	298
e^+e^+	6	3	800	137
$e^+\mu^+$	5	3	744	216
$e^+\mu^+$	4	3	888	155
μ^+e^+	3	3	1439	239
$\mu^-\mu^+\mu^-$	4	4	1072	176

Table 12: List of data events in the SR4t4/SRVLQ7 category (by definition, the E_T^{miss} is above 40 GeV and the H_T above 700 GeV).

10 Conclusion

A search for BSM physics has been performed using pp collisions at $\sqrt{s} = 8$ TeV corresponding to an integrated luminosity of 20.3 fb^{-1} recorded by the ATLAS detector at the LHC, where events with at least two leptons, including a pair of the same electric charge, at least one b -tagged jet, sizeable missing transverse momentum, and large H_T were considered. Several BSM physics effects could enhance the yield of such events over the small SM expectation. The search was performed in the context of several BSM physics models, with signal regions defined for different models. The regions of parameter space excluded by the data are quantified by setting 95% CL limits. The observed yield in the signal region for positively charged top quark pair production is consistent with the expected background, resulting in limits of 8.4–62 fb on the cross section of this process (depending on the model considered) and a limit $\text{BR}(t \rightarrow uH) < 1\%$. In the set of signal regions

defined for vector-like quark, four-top-quark, and chiral b' -quark searches there is an excess of observed events over the SM prediction, particularly in the subset of those signal regions that require at least two b -tagged jets (and thus are relevant to the search for four-top-quark production). The significance of the excess varies with the signal being considered, reaching 2.5 standard deviations for hypotheses involving heavy resonances decaying to four top quarks. Nonetheless the data can still constrain some of the BSM physics models considered; 95% CL limits are set as follows: the mass of the chiral b' -quark is constrained as a function of the branching ratio to Wt , the masses of vector-like B and T quarks are constrained to $m_B > 0.62$ TeV, $m_T > 0.59$ TeV (assuming branching fractions to the W , Z , and H decay modes arising from a singlet model), the mass of the $T_{5/3}$ quark is greater than 0.75 TeV, the SM four-top production cross section is less than 70 fb, the sgluon mass is greater than 0.83 TeV and the Kaluza–Klein mass (in the context of models with two universal extra dimensions) is greater than 0.96 TeV.

Acknowledgements

We thank CERN for the very successful operation of the LHC, as well as the support staff from our institutions without whom ATLAS could not be operated efficiently.

We acknowledge the support of ANPCyT, Argentina; YerPhI, Armenia; ARC, Australia; BMWFW and FWF, Austria; ANAS, Azerbaijan; SSTC, Belarus; CNPq and FAPESP, Brazil; NSERC, NRC and CFI, Canada; CERN; CONICYT, Chile; CAS, MOST and NSFC, China; COLCIENCIAS, Colombia; MSMT CR, MPO CR and VSC CR, Czech Republic; DNRF, DNSRC and Lundbeck Foundation, Denmark; EPLANET, ERC and NSRF, European Union; IN2P3-CNRS, CEA-DSM/IRFU, France; GNSF, Georgia; BMBF, DFG, HGF, MPG and AvH Foundation, Germany; GSRT and NSRF, Greece; RGC, Hong Kong SAR, China; ISF, MINERVA, GIF, I-CORE and Benoziyo Center, Israel; INFN, Italy; MEXT and JSPS, Japan; CNRST, Morocco; FOM and NWO, Netherlands; BRF and RCN, Norway; MNiSW and NCN, Poland; GRICES and FCT, Portugal; MNE/IFA, Romania; MES of Russia and NRC KI, Russian Federation; JINR; MSTD, Serbia; MSSR, Slovakia; ARRS and MIZŠ, Slovenia; DST/NRF, South Africa; MINECO, Spain; SRC and Wallenberg Foundation, Sweden; SER, SNSF and Cantons of Bern and Geneva, Switzerland; NSC, Taiwan; TAEK, Turkey; STFC, the Royal Society and Leverhulme Trust, United Kingdom; DOE and NSF, United States of America.

The crucial computing support from all WLCG partners is acknowledged gratefully, in particular from CERN and the ATLAS Tier-1 facilities at TRIUMF (Canada), NDGF (Denmark, Norway, Sweden), CC-IN2P3 (France), KIT/GridKA (Germany), INFN-CNAF (Italy), NL-T1 (Netherlands), PIC (Spain), ASGC (Taiwan), RAL (UK) and BNL (USA) and in the Tier-2 facilities worldwide.

References

- [1] ATLAS Collaboration, Observation of a new particle in the search for the Standard Model Higgs boson with the ATLAS detector at the LHC, [Phys. Lett. B 716 \(2012\) 1–29](#).
[arXiv:1207.7214](#).

- [2] CMS Collaboration, Observation of a new boson at a mass of 125 GeV with the CMS experiment at the LHC, *Phys. Lett. B* **716** (2012) 30–61. [arXiv:1207.7235](#).
- [3] B. A. Dobrescu, C. T. Hill, Electroweak symmetry breaking via top condensation seesaw, *Phys. Rev. Lett.* **81** (1998) 2634–2637. [arXiv:hep-ph/9712319](#).
- [4] R. S. Chivukula, B. A. Dobrescu, H. Georgi, C. T. Hill, Top quark seesaw theory of electroweak symmetry breaking, *Phys. Rev. D* **59** (1999) 075003. [arXiv:hep-ph/9809470](#).
- [5] H.-J. He, C. T. Hill, T. M. Tait, Top quark seesaw, vacuum structure and electroweak precision constraints, *Phys. Rev. D* **65** (2002) 055006. [arXiv:hep-ph/0108041](#).
- [6] C. T. Hill, E. H. Simmons, Strong dynamics and electroweak symmetry breaking, *Phys. Rept.* **381** (2003) 235–402. [arXiv:hep-ph/0203079](#).
- [7] R. Contino, L. Da Rold, A. Pomarol, Light custodians in natural composite Higgs models, *Phys. Rev. D* **75** (2007) 055014. [arXiv:hep-ph/0612048](#).
- [8] C. Anastasiou, E. Furlan, J. Santiago, Realistic composite Higgs models, *Phys. Rev. D* **79** (2009) 075003. [arXiv:0901.2117](#).
- [9] K. Kong, M. McCaskey, G. W. Wilson, Multi-lepton signals from the top-prime quark at the LHC, *JHEP* **1204** (2012) 079. [arXiv:1112.3041](#).
- [10] A. Carmona, M. Chala, J. Santiago, New Higgs production mechanism in composite Higgs models, *JHEP* **1207** (2012) 049. [arXiv:1205.2378](#).
- [11] M. Gillioz, et al., Higgs low-energy theorem (and its corrections) in composite models, *JHEP* **1210** (2012) 004. [arXiv:1206.7120](#).
- [12] A. Davidson, K. C. Wali, Family mass hierarchy from universal seesaw mechanism, *Phys. Rev. Lett.* **60** (1988) 1813–1816.
- [13] K. S. Babu, R. N. Mohapatra, Solution to the strong CP problem without an axion, *Phys. Rev. D* **41** (1990) 1286–1291.
- [14] B. Grinstein, M. Redi, G. Villadoro, Low scale flavor gauge symmetries, *JHEP* **1011** (2010) 067. [arXiv:1009.2049](#).
- [15] D. Guadagnoli, R. N. Mohapatra, I. Sung, Gauged flavor group with left-right symmetry, *JHEP* **1104** (2011) 093. [arXiv:1103.4170](#).
- [16] N. Arkani-Hamed, A. G. Cohen, E. Katz, A. E. Nelson, The littlest Higgs, *JHEP* **0207** (2002) 034. [arXiv:hep-ph/0206021](#).
- [17] T. Han, H. E. Logan, B. McElrath, L.-T. Wang, Phenomenology of the little Higgs model, *Phys. Rev. D* **67** (2003) 095004. [arXiv:hep-ph/0301040](#).
- [18] M. Perelstein, M. E. Peskin, A. Pierce, Top quarks and electroweak symmetry breaking in little Higgs models, *Phys. Rev. D* **69** (2004) 075002. [arXiv:hep-ph/0310039](#).
- [19] M. Schmaltz, D. Tucker-Smith, Little Higgs theories, *Ann. Rev. Nucl. Part. Sci.* **55** (2005) 229–270. [arXiv:hep-ph/0502182](#).
- [20] M. S. Carena, J. Hubisz, M. Perelstein, P. Verdier, Collider signatures for new T -parity-odd quarks in little Higgs models, *Phys. Rev. D* **75** (2007) 091701. [arXiv:hep-ph/0610156](#).
- [21] S. Matsumoto, T. Moroi, K. Tobe, Testing the Littlest Higgs Model with T -parity at the Large Hadron Collider, *Phys. Rev. D* **78** (2008) 055018. [arXiv:0806.3837](#).

- [22] J. A. Aguilar-Saavedra, R. Benbrik, S. Heinemeyer, M. Pérez-Victoria, Handbook of vectorlike quarks: Mixing and single production, *Phys. Rev. D* **88** (9) (2013) 094010. [arXiv:1306.0572](#).
- [23] J. A. Aguilar-Saavedra, Effects of mixing with quark singlets, *Phys. Rev. D* **67** (2003) 035003. [Erratum-ibid D 69 (2004) 099901.]
- [24] Y. Okada, L. Panizzi, LHC signatures of vector-like quarks, *Adv. High Energy Phys.* **2013** (2013) 364936. [arXiv:1207.5607](#).
- [25] J. A. Aguilar-Saavedra, Identifying top partners at LHC, *JHEP* **0911** (2009) 030. [arXiv:0907.3155](#).
- [26] M. Czakon, P. Fiedler, A. Mitov, Total top-quark pair-production cross section at hadron colliders through $O(\alpha_s^4)$, *Phys. Rev. Lett.* **110** (2013) 252004. [arXiv:1303.6254](#).
- [27] M. Czakon, A. Mitov, Top++: A program for the calculation of the top-pair cross-section at hadron colliders, *Comput. Phys. Commun.* **185** (2014) 2930. [arXiv:1112.5675](#).
- [28] V. Barger, A. L. Stange, R. J. N. Phillips, Four-heavy-quark hadroproduction, *Phys. Rev. D* **44** (1991) 1987–1996.
- [29] V. Barger, W.-Y. Keung, B. Yencho, Triple-top signal of new physics at the LHC, *Phys. Lett. B* **687** (2010) 70–74. [arXiv:1001.0221](#).
- [30] B. Lillie, J. Shu, T. M. P. Tait, Top compositeness at the Tevatron and LHC, *JHEP* **804** (2008) 87. [arXiv:0712.3057](#).
- [31] A. Pomarol, J. Serra, Top quark compositeness: Feasibility and implications, *Phys. Rev. D* **78** (2008) 074026. [arXiv:0806.3247](#).
- [32] C. Degrande, et al., Non-resonant new physics in top pair production at hadron colliders, *JHEP* **1103** (2011) 125. [arXiv:1010.6304](#).
- [33] M. Guchait, F. Mahmoudi, K. Sridhar, Associated production of a Kaluza-Klein excitation of a gluon with a $t\bar{t}$ pair at the LHC, *Phys. Lett. B* **666** (2008) 347. [arXiv:0710.2234](#).
- [34] T. Plehn, T. M. P. Tait, Seeking sgluons, *J. Phys. G* **36** (2009) 075001. [arXiv:0810.3919](#).
- [35] S. Y. Choi, et al., Color-octet scalars of $N = 2$ supersymmetry at the LHC, *Phys. Lett. B* **672** (2009) 246–252. [arXiv:0812.3586](#).
- [36] C. Kilic, T. Okui, R. Sundrum, Vectorlike confinement at the LHC, *JHEP* **1002** (2010) 018. [arXiv:0906.0577](#).
- [37] C. Kilic, T. Okui, R. Sundrum, Colored resonances at the Tevatron: phenomenology and discovery potential in multijets, *JHEP* **0807** (2008) 038. [arXiv:0802.2568](#).
- [38] G. Burdman, B. A. Dobrescu, E. Pónton, Resonances from two universal extra dimensions, *Phys. Rev. D* **74** (2006) 075008. [arXiv:hep-ph/0601186](#).
- [39] S. Calvet, B. Fuks, P. Gris, L. Valéry, Searching for sgluons in multitop events at a center-of-mass energy of 8 TeV, *JHEP* **1304** (2013) 043. [arXiv:1212.3360](#).
- [40] L. Beck et. al., Probing top-philic sgluons with LHC Run I data, *Phys. Lett. B* **746** (2015) 48. [arXiv:1501.07580](#).
- [41] D. Goncalves-Netto, et al., Sgluon pair production to next-to-leading order, *Phys. Rev. D* **85** (2012) 114024. [arXiv:1203.6358](#).

- [42] G. Cacciapaglia, A. Deandrea, J. Llodra-Perez, A Dark Matter candidate from Lorentz Invariance in 6D, *JHEP* 1003 (2010) 083. [arXiv:0907.4993](#).
- [43] A. Arbey, G. Cacciapaglia, A. Deandrea, B. Kubik, Dark Matter in a twisted bottle, *JHEP* 1301 (2013) 147. [arXiv:1210.0384](#).
- [44] P. H. Frampton, P. Q. Hung, M. Sher, Quarks and leptons beyond the third generation, *Phys. Rept.* 330 (2000) 263. [arXiv:hep-ph/9903387](#).
- [45] B. Holdom, The discovery of the fourth family at the LHC: What if?, *JHEP* 0608 (2006) 076. [arXiv:hep-ph/0606146](#).
- [46] P. Q. Hung, Minimal SU(5) resuscitated by new quarks and leptons, *Phys. Rev. Lett.* 80 (1998) 3000–3003. [arXiv:hep-ph/9712338](#).
- [47] W.-S. Hou, Source of CP violation for the baryon asymmetry of the universe, *Chin. J. Phys.* 47 (2009) 134.
- [48] O. Eberhardt, et al., Impact of a Higgs boson at a mass of 126 GeV on the Standard Model with three and four fermion generations, *Phys. Rev. Lett.* 109 (2012) 241802. [arXiv:1209.1101](#).
- [49] A. Djouadi, A. Lenz, Sealing the fate of a fourth generation of fermions, *Phys. Lett. B* 715 (2012) 310–314. [arXiv:1204.1252](#).
- [50] O. Eberhardt, et al., Joint analysis of Higgs decays and electroweak precision observables in the Standard Model with a sequential fourth generation, *Phys. Rev. D* 86 (2012) 013011. [arXiv:1204.3872](#).
- [51] O. Eberhardt, et al., Status of the fourth fermion generation before ICHEP2012: Higgs data and electroweak precision observables, *Phys. Rev. D* 86 (2012) 074014. [arXiv:1207.0438](#).
- [52] A. Denner, et al., Higgs production and decay with a fourth Standard-Model-like fermion generation, *Eur. Phys. J. C* 72 (2012) 1992. [arXiv:1111.6395](#).
- [53] G. Passarino, C. Sturm, S. Uccirati, Complete electroweak corrections to Higgs production in a Standard Model with four generations at the LHC, *Phys. Lett. B* 706 (2011) 195–199. [arXiv:1108.2025](#).
- [54] S. Bar-Shalom, M. Geller, S. Nandi, A. Soni, Two Higgs doublets, a 4th generation and a 125 GeV Higgs: A review., *Adv. High Energy Phys.* 2013 (2013) 672972. [arXiv:1208.3195](#).
- [55] J. A. Aguilar-Saavedra, M. Pérez-Victoria, No like-sign tops at Tevatron: Constraints on extended models and implications for the $t\bar{t}$ asymmetry, *Phys. Lett. B* 701 (2011) 93–100. [arXiv:1104.1385](#).
- [56] E. L. Berger, Q.-H. Cao, C.-R. Chen, C. S. Li, H. Zhang, Top quark forward-backward asymmetry and same-sign top quark pairs, *Phys. Rev. Lett.* 106 (2011) 201801. [arXiv:1101.5625](#).
- [57] M. Buchkremer, G. Cacciapaglia, A. Deandrea, L. Panizzi, [Feynrules Top FCNC model](#).
- [58] ATLAS Collaboration, Search for same-sign top-quark production and fourth-generation down-type quarks in pp collisions at $\sqrt{s} = 7$ TeV with the ATLAS detector, *JHEP* 1204 (2012) 069. [arXiv:1202.5520](#).
- [59] CMS Collaboration, Search for new physics in events with same-sign dileptons and jets in pp collisions at $\sqrt{s} = 8$ TeV, *JHEP* 1401 (2014) 163. [arXiv:1311.6736](#).

- [60] CMS Collaboration, Search for top-quark partners with charge 5/3 in the same-sign dilepton final state, *Phys. Rev. Lett.* **112** (2014), 171801. [arXiv:1312.2391](#).
- [61] CMS Collaboration, Inclusive search for a vector-like T quark with charge $\frac{2}{3}$ in pp collisions at $\sqrt{s} = 8$ TeV, *Phys. Lett. B* **729** (2014) 149–171. [arXiv:1311.7667](#).
- [62] ATLAS Collaboration, Search for supersymmetry at $\sqrt{s}=8$ TeV in final states with jets and two same-sign leptons or three leptons with the ATLAS detector, *JHEP* **1406** (2014) 035. [arXiv:1404.2500](#).
- [63] ATLAS Collaboration, The ATLAS experiment at the CERN Large Hadron Collider, *JINST* **3** (2008) S08003.
- [64] A.D. Martin, W. J. Stirling, R. S. Thorne, and G. Watt, Parton distributions for the LHC, *Eur. Phys. J. C* **63** (2009) 189–285. [arXiv:0901.0002](#).
- [65] T. Sjöstrand and S. Mrenna and P.Z. Skands, Pythia 6.4 physics and manual, *JHEP* **05** (2006) 026. [arXiv:hep-ph/0603175](#).
- [66] J. Alwall, M. Herquet, F. Maltoni, O. Mattelaer, T. Stelzer, MadGraph 5 : Going beyond, *JHEP* **1106** (2011) 128. [arXiv:1106.0522](#).
- [67] J. Pumplin, et al., New generation of parton distributions with uncertainties from global QCD analysis, *JHEP* **07** (2002) 012. [arXiv:hep-ph/0201195](#).
- [68] T. Sjöstrand, S. Mrenna, P. Skands, A brief introduction to PYTHIA 8.1, *Comput. Phys. Commun.* **178** (2008) 852–867. [arXiv:0710.3820](#).
- [69] P. Meade, M. Reece, BRIDGE: Branching ratio inquiry / decay generated events, [arXiv:hep-ph/0703031](#).
- [70] G. Cacciapaglia, A. Deandrea, J. Llodra-Perez, The Universal Real Projective Plane: LHC phenomenology at one loop, *JHEP* **1110** (2011) 146. [arXiv:1104.3800](#).
- [71] J. A. Aguilar-Saavedra, Effective four-fermion operators in top physics: A roadmap, *Nuclear Physics B* **843** (3) (2011) 638 – 672. [Erratum-ibid B 851 (2) (2011) 443-444.]
- [72] T. Gleisberg, et al., Event generation with SHERPA 1.1, *JHEP* **0902** (2009) 007. [arXiv:0811.4622](#).
- [73] H.-L. Lai, et al., New parton distributions for collider physics, *Phys. Rev. D* **82** (2010) 074024. [arXiv:1007.2241](#).
- [74] GEANT4 Collaboration, S. Agostinelli et al., GEANT4: A Simulation toolkit, *Nucl. Instrum. Meth. A* **506** (2003) 250–303.
- [75] ATLAS Collaboration, The ATLAS simulation infrastructure, *Eur. Phys. J. C* **70** (2010) 823–874. [arXiv:1005.4568](#).
- [76] ATLAS Collaboration, The simulation principle and performance of the ATLAS fast calorimeter simulation FastCaloSim, [ATL-PHYS-PUB-2010-013](#).
- [77] ATLAS Collaboration, Electron efficiency measurements with the ATLAS detector using the 2012 LHC proton-proton collision data, [ATLAS-CONF-2014-032](#).
- [78] K. Rehermann, B. Tweedie, Efficient identification of boosted semileptonic top quarks at the LHC, *JHEP* **1103** (2011) 059. [arXiv:1007.2221](#).
- [79] ATLAS Collaboration, Measurement of the muon reconstruction performance of the ATLAS

- detector using 2011 and 2012 LHC proton-proton collision data, [Eur. Phys. J. C 74 \(2014\) 3130](#). [arXiv:1407.3935](#).
- [80] M. Cacciari, G. P. Salam, G. Soyez, The anti- k_t jet clustering algorithm, [JHEP 0804 \(2008\) 063](#). [arXiv:0802.1189](#).
- [81] M. Cacciari, G. P. Salam, Dispelling the N^3 myth for the k_t jet-finder, [Phys. Lett. B 641 \(2006\) 57–61](#). [arXiv:hep-ph/0512210](#).
- [82] M. Cacciari, G. P. Salam, G. Soyez, FastJet User Manual, [Eur. Phys. J. C 72 \(2012\) 1896](#). [arXiv:1111.6097](#).
- [83] ATLAS Collaboration, Jet energy measurement with the ATLAS detector in proton-proton collisions at $\sqrt{s} = 7$ TeV, [Eur. Phys. J. C 73 \(2013\) 2304](#). [arXiv:1112.6426](#).
- [84] ATLAS Collaboration, Commissioning of the ATLAS high-performance b-tagging algorithms in the 7 TeV collision data, [ATLAS-CONF-2011-102](#).
- [85] J. M. Campbell, R. K. Ellis, $t\bar{t}W^\pm$ production and decay at NLO, [JHEP 1207 \(2012\) 052](#). [arXiv:1204.5678](#).
- [86] ATLAS Collaboration, Improved luminosity determination in pp collisions at $\sqrt{s} = 7$ TeV using the ATLAS detector at the LHC, [Eur. Phys. J. C 73 \(2013\) 2518](#). [arXiv:1302.4393](#).
- [87] T. Junk, Confidence level computation for combining searches with small statistics, [Nucl. Instrum. Meth. A 434 \(1999\) 435–443](#). [arXiv:hep-ex/9902006](#).
- [88] A. L. Read, Presentation of search results: The CL(s) technique, [J. Phys. G 28 \(2002\) 2693–2704](#).
- [89] R. Contino, G. Servant, Discovering the top partners at the LHC using same-sign dilepton final states, [JHEP 0806 \(2008\) 026](#). [arXiv:0801.1679](#).
- [90] M. Buchkremer, G. Cacciapaglia, A. Deandrea, L. Panizzi, [Feynrules exotic \(X,T\) doublet model](#).
- [91] M. Buchkremer, G. Cacciapaglia, A. Deandrea, L. Panizzi, Model independent framework for searches of top partners, [Nucl. Phys. B 876 \(2013\) 376–417](#). [arXiv:1305.4172](#).

The ATLAS Collaboration

G. Aad⁸⁵, B. Abbott¹¹³, J. Abdallah¹⁵², O. Abdinov¹¹, R. Aben¹⁰⁷, M. Abolins⁹⁰, O.S. AbouZeid¹⁵⁹, H. Abramowicz¹⁵⁴, H. Abreu¹⁵³, R. Abreu³⁰, Y. Abulaiti^{147a,147b}, B.S. Acharya^{165a,165b,a}, L. Adamczyk^{38a}, D.L. Adams²⁵, J. Adelman¹⁰⁸, S. Adomeit¹⁰⁰, T. Adye¹³¹, A.A. Affolder⁷⁴, T. Agatonovic-Jovin¹³, J.A. Aguilar-Saavedra^{126a,126f}, M. Agustoni¹⁷, S.P. Ahlen²², F. Ahmadov^{65,b}, G. Aielli^{134a,134b}, H. Akerstedt^{147a,147b}, T.P.A. Åkesson⁸¹, G. Akimoto¹⁵⁶, A.V. Akimov⁹⁶, G.L. Alberghi^{20a,20b}, J. Albert¹⁷⁰, S. Albrand⁵⁵, M.J. Alconada Verzini⁷¹, M. Aleksa³⁰, I.N. Aleksandrov⁶⁵, C. Alexa^{26a}, G. Alexander¹⁵⁴, T. Alexopoulos¹⁰, M. Alhroob¹¹³, G. Alimonti^{91a}, L. Alio⁸⁵, J. Alison³¹, S.P. Alkire³⁵, B.M.M. Allbrooke¹⁸, P.P. Allport⁷⁴, A. Aloisio^{104a,104b}, A. Alonso³⁶, F. Alonso⁷¹, C. Alpigiani⁷⁶, A. Altheimer³⁵, B. Alvarez Gonzalez⁹⁰, D. Álvarez Piqueras¹⁶⁸, M.G. Alviggi^{104a,104b}, K. Amako⁶⁶, Y. Amaral Coutinho^{24a}, C. Amelung²³, D. Amidei⁸⁹, S.P. Amor Dos Santos^{126a,126c}, A. Amorim^{126a,126b}, S. Amoroso⁴⁸, N. Amram¹⁵⁴, G. Amundsen²³, C. Anastopoulos¹⁴⁰, L.S. Ancu⁴⁹, N. Andari³⁰, T. Andeen³⁵, C.F. Anders^{58b}, G. Anders³⁰, K.J. Anderson³¹, A. Andreazza^{91a,91b}, V. Andrei^{58a}, S. Angelidakis⁹, I. Angelozzi¹⁰⁷, P. Anger⁴⁴, A. Angerami³⁵, F. Anghinolfi³⁰, A.V. Anisenkov^{109,c}, N. Anjos¹², A. Annovi^{124a,124b}, M. Antonelli⁴⁷, A. Antonov⁹⁸, J. Antos^{145b}, F. Anulli^{133a}, M. Aoki⁶⁶, L. Aperio Bella¹⁸, G. Arabidze⁹⁰, Y. Arai⁶⁶, J.P. Araque^{126a}, A.T.H. Arce⁴⁵, F.A. Arduh⁷¹, J-F. Arguin⁹⁵, S. Argyropoulos⁴², M. Arik^{19a}, A.J. Armbruster³⁰, O. Arnaez³⁰, V. Arnal⁸², H. Arnold⁴⁸, M. Arratia²⁸, O. Arslan²¹, A. Artamonov⁹⁷, G. Artoni²³, S. Asai¹⁵⁶, N. Asbah⁴², A. Ashkenazi¹⁵⁴, B. Åsman^{147a,147b}, L. Asquith¹⁵⁰, K. Assamagan²⁵, R. Astalos^{145a}, M. Atkinson¹⁶⁶, N.B. Atlay¹⁴², B. Auerbach⁶, K. Augsten¹²⁸, M. Aourousseau^{146b}, G. Avolio³⁰, B. Axen¹⁵, M.K. Ayoub¹¹⁷, G. Azuelos^{95,d}, M.A. Baak³⁰, A.E. Baas^{58a}, C. Bacci^{135a,135b}, H. Bachacou¹³⁷, K. Bachas¹⁵⁵, M. Backes³⁰, M. Backhaus³⁰, E. Badescu^{26a}, P. Bagiacchi^{133a,133b}, P. Bagnaia^{133a,133b}, Y. Bai^{33a}, T. Bain³⁵, J.T. Baines¹³¹, O.K. Baker¹⁷⁷, P. Balek¹²⁹, T. Balestri¹⁴⁹, F. Balli⁸⁴, E. Banas³⁹, Sw. Banerjee¹⁷⁴, A.A.E. Bannoura¹⁷⁶, H.S. Bansil¹⁸, L. Barak³⁰, S.P. Baranov⁹⁶, E.L. Barberio⁸⁸, D. Barberis^{50a,50b}, M. Barbero⁸⁵, T. Barillari¹⁰¹, M. Barisonzi^{165a,165b}, T. Barklow¹⁴⁴, N. Barlow²⁸, S.L. Barnes⁸⁴, B.M. Barnett¹³¹, R.M. Barnett¹⁵, Z. Barnovska⁵, A. Baroncelli^{135a}, G. Barone⁴⁹, A.J. Barr¹²⁰, F. Barreiro⁸², J. Barreiro Guimarães da Costa⁵⁷, R. Bartoldus¹⁴⁴, A.E. Barton⁷², P. Bartos^{145a}, A. Bassalat¹¹⁷, A. Basye¹⁶⁶, R.L. Bates⁵³, S.J. Batista¹⁵⁹, J.R. Batley²⁸, M. Battaglia¹³⁸, M. Bause^{133a,133b}, F. Bauer¹³⁷, H.S. Bawa^{144,e}, J.B. Beacham¹¹¹, M.D. Beattie⁷², T. Beau⁸⁰, P.H. Beauchemin¹⁶², R. Beccherle^{124a,124b}, P. Bechtel²¹, H.P. Beck^{17,f}, K. Becker¹²⁰, M. Becker⁸³, S. Becker¹⁰⁰, M. Beckingham¹⁷¹, C. Becot¹¹⁷, A.J. Beddall^{19c}, A. Beddall^{19c}, V.A. Bednyakov⁶⁵, C.P. Bee¹⁴⁹, L.J. Beamster¹⁰⁷, T.A. Beermann¹⁷⁶, M. Beger²⁵, J.K. Behr¹²⁰, C. Belanger-Champagne⁸⁷, P.J. Bell⁴⁹, W.H. Bell⁴⁹, G. Bella¹⁵⁴, L. Bellagamba^{20a}, A. Bellerive²⁹, M. Bellomo⁸⁶, K. Belotskiy⁹⁸, O. Beltramello³⁰, O. Benary¹⁵⁴, D. Bencheikroun^{136a}, M. Bender¹⁰⁰, K. Bendtz^{147a,147b}, N. Benekos¹⁰, Y. Benhammou¹⁵⁴, E. Benhar Nocchioli⁴⁹, J.A. Benitez Garcia^{160b}, D.P. Benjamin⁴⁵, J.R. Bensinger²³, S. Bentvelsen¹⁰⁷, L. Beresford¹²⁰, M. Beretta⁴⁷,

D. Berge¹⁰⁷, E. Bergeaas Kuutmann¹⁶⁷, N. Berger⁵, F. Berghaus¹⁷⁰, J. Beringer¹⁵,
 C. Bernard²², N.R. Bernard⁸⁶, C. Bernius¹¹⁰, F.U. Bernlochner²¹, T. Berry⁷⁷,
 P. Berta¹²⁹, C. Bertella⁸³, G. Bertoli^{147a,147b}, F. Bertolucci^{124a,124b}, C. Bertsche¹¹³,
 D. Bertsche¹¹³, M.I. Besana^{91a}, G.J. Besjes¹⁰⁶, O. Bessidskaia Bylund^{147a,147b},
 M. Bessner⁴², N. Besson¹³⁷, C. Betancourt⁴⁸, S. Bethke¹⁰¹, A.J. Bevan⁷⁶, W. Bhimji⁴⁶,
 R.M. Bianchi¹²⁵, L. Bianchini²³, M. Bianco³⁰, O. Biebel¹⁰⁰, S.P. Bieniek⁷⁸,
 M. Biglietti^{135a}, J. Bilbao De Mendizabal⁴⁹, H. Bilokon⁴⁷, M. Bindi⁵⁴, S. Binet¹¹⁷,
 A. Bingul^{19c}, C. Bini^{133a,133b}, C.W. Black¹⁵¹, J.E. Black¹⁴⁴, K.M. Black²²,
 D. Blackburn¹³⁹, R.E. Blair⁶, J.-B. Blanchard¹³⁷, J.E. Blanco⁷⁷, T. Blazek^{145a}, I. Bloch⁴²,
 C. Blocker²³, W. Blum^{83,*}, U. Blumenschein⁵⁴, G.J. Bobbink¹⁰⁷, V.S. Bobrovnikov^{109,c},
 S.S. Bocchetta⁸¹, A. Bocci⁴⁵, C. Bock¹⁰⁰, M. Boehler⁴⁸, J.A. Bogaerts³⁰,
 A.G. Bogdanchikov¹⁰⁹, C. Boehm^{147a}, V. Boisvert⁷⁷, T. Bold^{38a}, V. Boldea^{26a},
 A.S. Boldyrev⁹⁹, M. Bomben⁸⁰, M. Bona⁷⁶, M. Boonekamp¹³⁷, A. Borisov¹³⁰,
 G. Borissov⁷², S. Borroni⁴², J. Bortfeldt¹⁰⁰, V. Bortolotto^{60a,60b,60c}, K. Bos¹⁰⁷,
 D. Boscherini^{20a}, M. Bosman¹², J. Boudreau¹²⁵, J. Bouffard², E.V. Bouhova-Thacker⁷²,
 D. Boumediene³⁴, C. Bourdarios¹¹⁷, N. Bousson¹¹⁴, S. Boutouil^{136d}, A. Boveia³⁰,
 J. Boyd³⁰, I.R. Boyko⁶⁵, I. Bozic¹³, J. Bracinik¹⁸, A. Brandt⁸, G. Brandt¹⁵, O. Brandt^{58a},
 U. Bratzler¹⁵⁷, B. Brau⁸⁶, J.E. Brau¹¹⁶, H.M. Braun^{176,*}, S.F. Brazzale^{165a,165c},
 K. Brendlinger¹²², A.J. Brennan⁸⁸, L. Brenner¹⁰⁷, R. Brenner¹⁶⁷, S. Bressler¹⁷³,
 K. Bristow^{146c}, T.M. Bristow⁴⁶, D. Britton⁵³, D. Britzger⁴², F.M. Brochu²⁸, I. Brock²¹,
 R. Brock⁹⁰, J. Bronner¹⁰¹, G. Brooijmans³⁵, T. Brooks⁷⁷, W.K. Brooks^{32b}, J. Brosamer¹⁵,
 E. Brost¹¹⁶, J. Brown⁵⁵, P.A. Bruckman de Renstrom³⁹, D. Bruncko^{145b}, R. Bruneliere⁴⁸,
 A. Bruni^{20a}, G. Bruni^{20a}, M. Bruschi^{20a}, L. Bryngemark⁸¹, T. Buanes¹⁴, Q. Buat¹⁴³,
 P. Buchholz¹⁴², A.G. Buckley⁵³, S.I. Buda^{26a}, I.A. Budagov⁶⁵, F. Buehrer⁴⁸, L. Bugge¹¹⁹,
 M.K. Bugge¹¹⁹, O. Bulekov⁹⁸, H. Burckhart³⁰, S. Burdin⁷⁴, B. Burghgrave¹⁰⁸,
 S. Burke¹³¹, I. Burmeister⁴³, E. Busato³⁴, D. Buescher⁴⁸, V. Buescher⁸³, P. Bussey⁵³,
 C.P. Buszello¹⁶⁷, J.M. Butler²², A.I. Butt³, C.M. Buttar⁵³, J.M. Butterworth⁷⁸,
 P. Butti¹⁰⁷, W. Buttinger²⁵, A. Buzatu⁵³, R. Buzykaev^{109,c}, S. Cabrera Urbán¹⁶⁸,
 D. Caforio¹²⁸, O. Cakir^{4a}, P. Calafiura¹⁵, A. Calandri¹³⁷, G. Calderini⁸⁰, P. Calfayan¹⁰⁰,
 L.P. Caloba^{24a}, D. Calvet³⁴, S. Calvet³⁴, R. Camacho Toro⁴⁹, S. Camarda⁴²,
 D. Cameron¹¹⁹, L.M. Caminada¹⁵, R. Caminal Armadans¹², S. Campana³⁰,
 M. Campanelli⁷⁸, A. Campoverde¹⁴⁹, V. Canale^{104a,104b}, A. Canepa^{160a}, M. Cano Bret⁷⁶,
 J. Cantero⁸², R. Cantrill^{126a}, T. Cao⁴⁰, M.D.M. Capeans Garrido³⁰, I. Caprini^{26a},
 M. Caprini^{26a}, M. Capua^{37a,37b}, R. Caputo⁸³, R. Cardarelli^{134a}, T. Carli³⁰,
 G. Carlino^{104a}, L. Carminati^{91a,91b}, S. Caron¹⁰⁶, E. Carquin^{32a}, G.D. Carrillo-Montoya⁸,
 J.R. Carter²⁸, J. Carvalho^{126a,126c}, D. Casadei⁷⁸, M.P. Casado¹², M. Casolino¹²,
 E. Castaneda-Miranda^{146b}, A. Castelli¹⁰⁷, V. Castillo Gimenez¹⁶⁸, N.F. Castro^{126a,g},
 P. Catastini⁵⁷, A. Catinaccio³⁰, J.R. Catmore¹¹⁹, A. Cattai³⁰, J. Caudron⁸³,
 V. Cavaliere¹⁶⁶, D. Cavalli^{91a}, M. Cavalli-Sforza¹², V. Cavalinni^{124a,124b},
 F. Ceradini^{135a,135b}, B.C. Cerio⁴⁵, K. Cerny¹²⁹, A.S. Cerqueira^{24b}, A. Cerri¹⁵⁰,
 L. Cerrito⁷⁶, F. Cerutti¹⁵, M. Cerv³⁰, A. Cervelli¹⁷, S.A. Cetin^{19b}, A. Chafaq^{136a},
 D. Chakraborty¹⁰⁸, I. Chalupkova¹²⁹, P. Chang¹⁶⁶, B. Chapleau⁸⁷, J.D. Chapman²⁸,
 D.G. Charlton¹⁸, C.C. Chau¹⁵⁹, C.A. Chavez Barajas¹⁵⁰, S. Cheatham¹⁵³,

A. Chegwidden⁹⁰, S. Chekanov⁶, S.V. Chekulaev^{160a}, G.A. Chelkov^{65,h},
 M.A. Chelstowska⁸⁹, C. Chen⁶⁴, H. Chen²⁵, K. Chen¹⁴⁹, L. Chen^{33d,i}, S. Chen^{33c},
 X. Chen^{33f}, Y. Chen⁶⁷, H.C. Cheng⁸⁹, Y. Cheng³¹, A. Cheplakov⁶⁵, E. Cheremushkina¹³⁰,
 R. Cherkaoui El Moursli^{136e}, V. Chernyatin^{25,*}, E. Cheu⁷, L. Chevalier¹³⁷, V. Chiarella⁴⁷,
 J.T. Childers⁶, G. Chiodini^{73a}, A.S. Chisholm¹⁸, R.T. Chislett⁷⁸, A. Chitan^{26a},
 M.V. Chizhov⁶⁵, K. Choi⁶¹, S. Chouridou⁹, B.K.B. Chow¹⁰⁰, V. Christodoulou⁷⁸,
 D. Chromek-Burckhart³⁰, M.L. Chu¹⁵², J. Chudoba¹²⁷, A.J. Chuinard⁸⁷,
 J.J. Chwastowski³⁹, L. Chytka¹¹⁵, G. Ciapetti^{133a,133b}, A.K. Ciftci^{4a}, D. Cinca⁵³,
 V. Cindro⁷⁵, I.A. Cioara²¹, A. Ciocio¹⁵, Z.H. Citron¹⁷³, M. Ciubancan^{26a}, A. Clark⁴⁹,
 B.L. Clark⁵⁷, P.J. Clark⁴⁶, R.N. Clarke¹⁵, W. Cleland¹²⁵, C. Clement^{147a,147b},
 Y. Coadou⁸⁵, M. Cobal^{165a,165c}, A. Coccaro¹³⁹, J. Cochran⁶⁴, L. Coffey²³, J.G. Cogan¹⁴⁴,
 B. Cole³⁵, S. Cole¹⁰⁸, A.P. Colijn¹⁰⁷, J. Collot⁵⁵, T. Colombo^{58c}, G. Compostella¹⁰¹,
 P. Conde Muiño^{126a,126b}, E. Coniavitis⁴⁸, S.H. Connell^{146b}, I.A. Connelly⁷⁷,
 S.M. Consonni^{91a,91b}, V. Consorti⁴⁸, S. Constantinescu^{26a}, C. Conta^{121a,121b}, G. Conti³⁰,
 F. Conventi^{104a,j}, M. Cooke¹⁵, B.D. Cooper⁷⁸, A.M. Cooper-Sarkar¹²⁰, K. Copic¹⁵,
 T. Cornelissen¹⁷⁶, M. Corradi^{20a}, F. Corriveau^{87,k}, A. Corso-Radu¹⁶⁴,
 A. Cortes-Gonzalez¹², G. Cortiana¹⁰¹, G. Costa^{91a}, M.J. Costa¹⁶⁸, D. Costanzo¹⁴⁰,
 D. Côté⁸, G. Cottin²⁸, G. Cowan⁷⁷, B.E. Cox⁸⁴, K. Cranmer¹¹⁰, G. Cree²⁹,
 S. Crépe-Renaudin⁵⁵, F. Crescioli⁸⁰, W.A. Cribbs^{147a,147b}, M. Crispin Ortuzar¹²⁰,
 M. Cristinziani²¹, V. Croft¹⁰⁶, G. Crosetti^{37a,37b}, T. Cuhadar Donszelmann¹⁴⁰,
 J. Cummings¹⁷⁷, M. Curatolo⁴⁷, C. Cuthbert¹⁵¹, H. Czirr¹⁴², P. Czodrowski³,
 S. D'Auria⁵³, M. D'Onofrio⁷⁴, M.J. Da Cunha Sargedas De Sousa^{126a,126b}, C. Da Via⁸⁴,
 W. Dabrowski^{38a}, A. Dafinca¹²⁰, T. Dai⁸⁹, O. Dale¹⁴, F. Dallaire⁹⁵, C. Dallapiccola⁸⁶,
 M. Dam³⁶, J.R. Dandoy³¹, A.C. Daniells¹⁸, M. Danninger¹⁶⁹, M. Dano Hoffmann¹³⁷,
 V. Dao⁴⁸, G. Darbo^{50a}, S. Darmora⁸, J. Dassoulas³, A. Dattagupta⁶¹, W. Davey²¹,
 C. David¹⁷⁰, T. Davidek¹²⁹, E. Davies^{120,l}, M. Davies¹⁵⁴, P. Davison⁷⁸, Y. Davygora^{58a},
 E. Dawe⁸⁸, I. Dawson¹⁴⁰, R.K. Daya-Ishmukhametova⁸⁶, K. De⁸, R. de Asmundis^{104a},
 S. De Castro^{20a,20b}, S. De Cecco⁸⁰, N. De Groot¹⁰⁶, P. de Jong¹⁰⁷, H. De la Torre⁸²,
 F. De Lorenzi⁶⁴, L. De Nooij¹⁰⁷, D. De Pedis^{133a}, A. De Salvo^{133a}, U. De Sanctis¹⁵⁰,
 A. De Santo¹⁵⁰, J.B. De Vivie De Regie¹¹⁷, W.J. Dearnaley⁷², R. Debbe²⁵,
 C. Debenedetti¹³⁸, D.V. Dedovich⁶⁵, I. Deigaard¹⁰⁷, J. Del Peso⁸², T. Del Prete^{124a,124b},
 D. Delgove¹¹⁷, F. Deliot¹³⁷, C.M. Delitzsch⁴⁹, M. Deliyergiyev⁷⁵, A. Dell'Acqua³⁰,
 L. Dell'Asta²², M. Dell'Orso^{124a,124b}, M. Della Pietra^{104a,j}, D. della Volpe⁴⁹,
 M. Delmastro⁵, P.A. Delsart⁵⁵, C. Deluca¹⁰⁷, D.A. DeMarco¹⁵⁹, S. Demers¹⁷⁷,
 M. Demichev⁶⁵, A. Demilly⁸⁰, S.P. Denisov¹³⁰, D. Derendarz³⁹, J.E. Derkaoui^{136d},
 F. Derue⁸⁰, P. Dervan⁷⁴, K. Desch²¹, C. Deterre⁴², P.O. Deviveiros³⁰, A. Dewhurst¹³¹,
 S. Dhaliwal¹⁰⁷, A. Di Ciaccio^{134a,134b}, L. Di Ciaccio⁵, A. Di Domenico^{133a,133b},
 C. Di Donato^{104a,104b}, A. Di Girolamo³⁰, B. Di Girolamo³⁰, A. Di Mattia¹⁵³,
 B. Di Micco^{135a,135b}, R. Di Nardo⁴⁷, A. Di Simone⁴⁸, R. Di Sipio¹⁵⁹, D. Di Valentino²⁹,
 C. Diaconu⁸⁵, M. Diamond¹⁵⁹, F.A. Dias⁴⁶, M.A. Diaz^{32a}, E.B. Diehl⁸⁹, J. Dietrich¹⁶,
 S. Diglio⁸⁵, A. Dimitrievska¹³, J. Dingfelder²¹, F. Dittus³⁰, F. Djama⁸⁵, T. Djobava^{51b},
 J.I. Djuvsland^{58a}, M.A.B. do Vale^{24c}, D. Dobos³⁰, M. Dobre^{26a}, C. Doglioni⁴⁹,
 T. Dohmae¹⁵⁶, J. Dolejsi¹²⁹, Z. Dolezal¹²⁹, B.A. Dolgoshein^{98,*}, M. Donadelli^{24d},

S. Donati^{124a,124b}, P. Dondero^{121a,121b}, J. Donini³⁴, J. Dopke¹³¹, A. Doria^{104a},
 M.T. Dova⁷¹, A.T. Doyle⁵³, E. Drechsler⁵⁴, M. Dris¹⁰, E. Dubreuil³⁴, E. Duchovni¹⁷³,
 G. Duckeck¹⁰⁰, O.A. Ducu^{26a,85}, D. Duda¹⁷⁶, A. Dudarev³⁰, L. Duflot¹¹⁷, L. Duguid⁷⁷,
 M. Dührssen³⁰, M. Dunford^{58a}, H. Duran Yildiz^{4a}, M. Düren⁵², A. Durglishvili^{51b},
 D. Duschinger⁴⁴, M. Dwuznik^{38a}, M. Dyndal^{38a}, C. Eckardt⁴², K.M. Ecker¹⁰¹, W. Edson²,
 N.C. Edwards⁴⁶, W. Ehrenfeld²¹, T. Eifert³⁰, G. Eigen¹⁴, K. Einsweiler¹⁵, T. Ekelof¹⁶⁷,
 M. El Kacimi^{136c}, M. Ellert¹⁶⁷, S. Elles⁵, F. Ellinghaus⁸³, A.A. Elliot¹⁷⁰, N. Ellis³⁰,
 J. Elmsheuser¹⁰⁰, M. Elsing³⁰, D. Emeliyanov¹³¹, Y. Enari¹⁵⁶, O.C. Endner⁸³,
 M. Endo¹¹⁸, R. Engelmann¹⁴⁹, J. Erdmann⁴³, A. Ereditato¹⁷, G. Ernis¹⁷⁶, J. Ernst²,
 M. Ernst²⁵, S. Errede¹⁶⁶, E. Ertel⁸³, M. Escalier¹¹⁷, H. Esch⁴³, C. Escobar¹²⁵,
 B. Esposito⁴⁷, A.I. Etienne¹³⁷, E. Etzion¹⁵⁴, H. Evans⁶¹, A. Ezhilov¹²³, L. Fabbri^{20a,20b},
 G. Facini³¹, R.M. Fakhruddinov¹³⁰, S. Falciano^{133a}, R.J. Falla⁷⁸, J. Faltova¹²⁹,
 Y. Fang^{33a}, M. Fanti^{91a,91b}, A. Farbin⁸, A. Farilla^{135a}, T. Farooque¹², S. Farrell¹⁵,
 S.M. Farrington¹⁷¹, P. Farthouat³⁰, F. Fassi^{136e}, P. Fassnacht³⁰, D. Fassouliotis⁹,
 A. Favareto^{50a,50b}, L. Fayard¹¹⁷, P. Federic^{145a}, O.L. Fedin^{123,m}, W. Fedorko¹⁶⁹,
 S. Feigl³⁰, L. Feligioni⁸⁵, C. Feng^{33d}, E.J. Feng⁶, H. Feng⁸⁹, A.B. Fenyuk¹³⁰,
 P. Fernandez Martinez¹⁶⁸, S. Fernandez Perez³⁰, S. Ferrag⁵³, J. Ferrando⁵³, A. Ferrari¹⁶⁷,
 P. Ferrari¹⁰⁷, R. Ferrari^{121a}, D.E. Ferreira de Lima⁵³, A. Ferrer¹⁶⁸, D. Ferrere⁴⁹,
 C. Ferretti⁸⁹, A. Ferretto Parodi^{50a,50b}, M. Fiassaric³¹, F. Fiedler⁸³, A. Filipčič⁷⁵,
 M. Filipuzzi⁴², F. Filthaut¹⁰⁶, M. Fincke-Keeler¹⁷⁰, K.D. Finelli¹⁵¹,
 M.C.N. Fiolhais^{126a,126c}, L. Fiorini¹⁶⁸, A. Firan⁴⁰, A. Fischer², C. Fischer¹², J. Fischer¹⁷⁶,
 W.C. Fisher⁹⁰, E.A. Fitzgerald²³, M. Flechl⁴⁸, I. Fleck¹⁴², P. Fleischmann⁸⁹,
 S. Fleischmann¹⁷⁶, G.T. Fletcher¹⁴⁰, G. Fletcher⁷⁶, T. Flick¹⁷⁶, A. Floderus⁸¹,
 L.R. Flores Castillo^{60a}, M.J. Flowerdew¹⁰¹, A. Formica¹³⁷, A. Forti⁸⁴, D. Fournier¹¹⁷,
 H. Fox⁷², S. Fracchia¹², P. Francavilla⁸⁰, M. Franchini^{20a,20b}, D. Francis³⁰, L. Franconi¹¹⁹,
 M. Franklin⁵⁷, M. Fraternali^{121a,121b}, D. Freeborn⁷⁸, S.T. French²⁸, F. Friedrich⁴⁴,
 D. Froidevaux³⁰, J.A. Frost¹²⁰, C. Fukunaga¹⁵⁷, E. Fullana Torregrosa⁸³, B.G. Fulsom¹⁴⁴,
 J. Fuster¹⁶⁸, C. Gabaldon⁵⁵, O. Gabizon¹⁷⁶, A. Gabrielli^{20a,20b}, A. Gabrielli^{133a,133b},
 S. Gadatsch¹⁰⁷, S. Gadomski⁴⁹, G. Gagliardi^{50a,50b}, P. Gagnon⁶¹, C. Galea¹⁰⁶,
 B. Galhardo^{126a,126c}, E.J. Gallas¹²⁰, B.J. Gallop¹³¹, P. Gallus¹²⁸, G. Galster³⁶,
 K.K. Gan¹¹¹, J. Gao^{33b,85}, Y. Gao⁴⁶, Y.S. Gao^{144,e}, F.M. Garay Walls⁴⁶, F. Garbers¹⁷⁷,
 C. García¹⁶⁸, J.E. García Navarro¹⁶⁸, M. Garcia-Sciveres¹⁵, R.W. Gardner³¹,
 N. Garelli¹⁴⁴, V. Garonne¹¹⁹, C. Gatti⁴⁷, A. Gaudiello^{50a,50b}, G. Gaudio^{121a}, B. Gaur¹⁴²,
 L. Gauthier⁹⁵, P. Gauzzi^{133a,133b}, I.L. Gavrilenko⁹⁶, C. Gay¹⁶⁹, G. Gaycken²¹,
 E.N. Gazis¹⁰, P. Ge^{33d}, Z. Gece¹⁶⁹, C.N.P. Gee¹³¹, D.A.A. Geerts¹⁰⁷,
 Ch. Geich-Gimbel²¹, M.P. Geisler^{58a}, C. Gemme^{50a}, M.H. Genest⁵⁵, S. Gentile^{133a,133b},
 M. George⁵⁴, S. George⁷⁷, D. Gerbaudo¹⁶⁴, A. Gershon¹⁵⁴, H. Ghazlane^{136b},
 N. Ghodbane³⁴, B. Giacobbe^{20a}, S. Giagu^{133a,133b}, V. Giangiobbe¹², P. Giannetti^{124a,124b},
 B. Gibbard²⁵, S.M. Gibson⁷⁷, M. Gilchriese¹⁵, T.P.S. Gillam²⁸, D. Gillberg³⁰, G. Gilles³⁴,
 D.M. Gingrich^{3,d}, N. Giokaris⁹, M.P. Giordani^{165a,165c}, F.M. Giorgi^{20a}, F.M. Giorgi¹⁶,
 P.F. Giraud¹³⁷, P. Giromini⁴⁷, D. Giugni^{91a}, C. Giuliani⁴⁸, M. Giuliani^{58b},
 B.K. Gjelsten¹¹⁹, S. Gkaitatzis¹⁵⁵, I. Gkialas¹⁵⁵, E.L. Gkougkousis¹¹⁷, L.K. Gladilin⁹⁹,
 C. Glasman⁸², J. Glatzer³⁰, P.C.F. Glaysher⁴⁶, A. Glazov⁴², M. Goblirsch-Kolb¹⁰¹,

J.R. Goddard⁷⁶, J. Godlewski³⁹, S. Goldfarb⁸⁹, T. Golling⁴⁹, D. Golubkov¹³⁰,
 A. Gomes^{126a,126b,126d}, R. Gonalo^{126a}, J. Goncalves Pinto Firmino Da Costa¹³⁷,
 L. Gonella²¹, S. Gonzalez de la Hoz¹⁶⁸, G. Gonzalez Parra¹², S. Gonzalez-Sevilla⁴⁹,
 L. Goossens³⁰, P.A. Gorbounov⁹⁷, H.A. Gordon²⁵, I. Gorelov¹⁰⁵, B. Gorini³⁰,
 E. Gorini^{73a,73b}, A. Goriřek⁷⁵, E. Gornicki³⁹, A.T. Goshaw⁴⁵, C. Gossling⁴³,
 M.I. Gostkin⁶⁵, D. Goujdami^{136c}, A.G. Goussiou¹³⁹, N. Govender^{146b}, H.M.X. Grabas¹³⁸,
 L. Graber⁵⁴, I. Grabowska-Bold^{38a}, P. Grafstrom^{20a,20b}, K-J. Grahn⁴², J. Gramling⁴⁹,
 E. Gramstad¹¹⁹, S. Grancagnolo¹⁶, V. Grassi¹⁴⁹, V. Gratchev¹²³, H.M. Gray³⁰,
 E. Graziani^{135a}, Z.D. Greenwood^{79,n}, K. Gregersen⁷⁸, I.M. Gregor⁴², P. Grenier¹⁴⁴,
 J. Griffiths⁸, A.A. Grillo¹³⁸, K. Grimm⁷², S. Grinstein^{12,o}, Ph. Gris³⁴, J.-F. Grivaz¹¹⁷,
 J.P. Grohs⁴⁴, A. Grohsjean⁴², E. Gross¹⁷³, J. Grosse-Knetter⁵⁴, G.C. Grossi⁷⁹,
 Z.J. Grout¹⁵⁰, L. Guan^{33b}, J. Guenther¹²⁸, F. Guescini⁴⁹, D. Guest¹⁷⁷, O. Gueta¹⁵⁴,
 E. Guido^{50a,50b}, T. Guillemin¹¹⁷, S. Guindon², U. Gul⁵³, C. Gumpert⁴⁴, J. Guo^{33e},
 S. Gupta¹²⁰, P. Gutierrez¹¹³, N.G. Gutierrez Ortiz⁵³, C. Gutsche⁴⁴, C. Guyot¹³⁷,
 C. Gwenlan¹²⁰, C.B. Gwilliam⁷⁴, A. Haas¹¹⁰, C. Haber¹⁵, H.K. Hadavand⁸,
 N. Haddad^{136e}, P. Haefner²¹, S. Hagebock²¹, Z. Hajduk³⁹, H. Hakobyan¹⁷⁸, M. Haleem⁴²,
 J. Haley¹¹⁴, D. Hall¹²⁰, G. Halladjian⁹⁰, G.D. Hallewell⁸⁵, K. Hamacher¹⁷⁶, P. Hamal¹¹⁵,
 K. Hamano¹⁷⁰, M. Hamer⁵⁴, A. Hamilton^{146a}, S. Hamilton¹⁶², G.N. Hamity^{146c},
 P.G. Hamnett⁴², L. Han^{33b}, K. Hanagaki¹¹⁸, K. Hanawa¹⁵⁶, M. Hance¹⁵, P. Hanke^{58a},
 R. Hanna¹³⁷, J.B. Hansen³⁶, J.D. Hansen³⁶, M.C. Hansen²¹, P.H. Hansen³⁶, K. Hara¹⁶¹,
 A.S. Hard¹⁷⁴, T. Harenberg¹⁷⁶, F. Hariri¹¹⁷, S. Harkusha⁹², R.D. Harrington⁴⁶,
 P.F. Harrison¹⁷¹, F. Hartjes¹⁰⁷, M. Hasegawa⁶⁷, S. Hasegawa¹⁰³, Y. Hasegawa¹⁴¹,
 A. Hasib¹¹³, S. Hassani¹³⁷, S. Haug¹⁷, R. Hauser⁹⁰, L. Hauswald⁴⁴, M. Havranek¹²⁷,
 C.M. Hawkes¹⁸, R.J. Hawkings³⁰, A.D. Hawkins⁸¹, T. Hayashi¹⁶¹, D. Hayden⁹⁰,
 C.P. Hays¹²⁰, J.M. Hays⁷⁶, H.S. Hayward⁷⁴, S.J. Haywood¹³¹, S.J. Head¹⁸, T. Heck⁸³,
 V. Hedberg⁸¹, L. Heelan⁸, S. Heim¹²², T. Heim¹⁷⁶, B. Heinemann¹⁵, L. Heinrich¹¹⁰,
 J. Hejbal¹²⁷, L. Helary²², S. Hellman^{147a,147b}, D. Hellmich²¹, C. Helsen³⁰,
 J. Henderson¹²⁰, R.C.W. Henderson⁷², Y. Heng¹⁷⁴, C. Hengler⁴², A. Henrichs¹⁷⁷,
 A.M. Henriques Correia³⁰, S. Henrot-Versille¹¹⁷, G.H. Herbert¹⁶,
 Y. Hernandez Jimenez¹⁶⁸, R. Herrberg-Schubert¹⁶, G. Herten⁴⁸, R. Hertenberger¹⁰⁰,
 L. Hervas³⁰, G.G. Hesketh⁷⁸, N.P. Hessey¹⁰⁷, J.W. Hetherly⁴⁰, R. Hickling⁷⁶,
 E. Higon-Rodriguez¹⁶⁸, E. Hill¹⁷⁰, J.C. Hill²⁸, K.H. Hiller⁴², S.J. Hillier¹⁸, I. Hinchliffe¹⁵,
 E. Hines¹²², R.R. Hinman¹⁵, M. Hirose¹⁵⁸, D. Hirschbuehl¹⁷⁶, J. Hobbs¹⁴⁹, N. Hod¹⁰⁷,
 M.C. Hodgkinson¹⁴⁰, P. Hodgson¹⁴⁰, A. Hoecker³⁰, M.R. Hoferkamp¹⁰⁵, F. Hoenig¹⁰⁰,
 M. Hohlfeld⁸³, D. Hohn²¹, T.R. Holmes¹⁵, T.M. Hong¹²², L. Hooft van Huysduynen¹¹⁰,
 W.H. Hopkins¹¹⁶, Y. Horii¹⁰³, A.J. Horton¹⁴³, J-Y. Hostachy⁵⁵, S. Hou¹⁵²,
 A. Houmada^{136a}, J. Howard¹²⁰, J. Howarth⁴², M. Hrabovsky¹¹⁵, I. Hristova¹⁶,
 J. Hrivnac¹¹⁷, T. Hryn'ova⁵, A. Hrynevich⁹³, C. Hsu^{146c}, P.J. Hsu^{152,p}, S.-C. Hsu¹³⁹,
 D. Hu³⁵, Q. Hu^{33b}, X. Hu⁸⁹, Y. Huang⁴², Z. Hubacek³⁰, F. Hubaut⁸⁵, F. Huegging²¹,
 T.B. Huffman¹²⁰, E.W. Hughes³⁵, G. Hughes⁷², M. Huhtinen³⁰, T.A. Hulsing⁸³,
 N. Huseynov^{65,b}, J. Huston⁹⁰, J. Huth⁵⁷, G. Iacobucci⁴⁹, G. Iakovidis²⁵, I. Ibragimov¹⁴²,
 L. Iconomidou-Fayard¹¹⁷, E. Ideal¹⁷⁷, Z. Idrissi^{136e}, P. Iengo³⁰, O. Igonkina¹⁰⁷,
 T. Iizawa¹⁷², Y. Ikegami⁶⁶, K. Ikematsu¹⁴², M. Ikeno⁶⁶, Y. Ilchenko^{31,q}, D. Iliadis¹⁵⁵,

N. Ilic¹⁵⁹, Y. Inamaru⁶⁷, T. Ince¹⁰¹, P. Ioannou⁹, M. Iodice^{135a}, K. Iordanidou⁹,
 V. Ippolito⁵⁷, A. Irlles Quiles¹⁶⁸, C. Isaksson¹⁶⁷, M. Ishino⁶⁸, M. Ishitsuka¹⁵⁸,
 R. Ishmukhametov¹¹¹, C. Issever¹²⁰, S. Istin^{19a}, J.M. Iturbe Ponce⁸⁴, R. Iuppa^{134a,134b},
 J. Ivarsson⁸¹, W. Iwanski³⁹, H. Iwasaki⁶⁶, J.M. Izen⁴¹, V. Izzo^{104a}, S. Jabbar³,
 B. Jackson¹²², M. Jackson⁷⁴, P. Jackson¹, M.R. Jaekel³⁰, V. Jain², K. Jakobs⁴⁸,
 S. Jakobsen³⁰, T. Jakoubek¹²⁷, J. Jakubek¹²⁸, D.O. Jamin¹⁵², D.K. Jana⁷⁹, E. Jansen⁷⁸,
 R.W. Jansky⁶², J. Janssen²¹, M. Janus¹⁷¹, G. Jarlskog⁸¹, N. Javadov^{65,b}, T. Javůrek⁴⁸,
 L. Jeanty¹⁵, J. Jejelava^{51a,r}, G.-Y. Jeng¹⁵¹, D. Jennens⁸⁸, P. Jenni^{48,s}, J. Jentzsch⁴³,
 C. Jeske¹⁷¹, S. Jézéquel⁵, H. Ji¹⁷⁴, J. Jia¹⁴⁹, Y. Jiang^{33b}, S. Jiggins⁷⁸, J. Jimenez Pena¹⁶⁸,
 S. Jin^{33a}, A. Jinaru^{26a}, O. Jinnouchi¹⁵⁸, M.D. Joergensen³⁶, P. Johansson¹⁴⁰,
 K.A. Johns⁷, K. Jon-And^{147a,147b}, G. Jones¹⁷¹, R.W.L. Jones⁷², T.J. Jones⁷⁴,
 J. Jongmanns^{58a}, P.M. Jorge^{126a,126b}, K.D. Joshi⁸⁴, J. Jovicevic^{160a}, X. Ju¹⁷⁴,
 C.A. Jung⁴³, P. Jussel⁶², A. Juste Rozas^{12,o}, M. Kaci¹⁶⁸, A. Kaczmarska³⁹, M. Kado¹¹⁷,
 H. Kagan¹¹¹, M. Kagan¹⁴⁴, S.J. Kahn⁸⁵, E. Kajomovitz⁴⁵, C.W. Kalderon¹²⁰, S. Kama⁴⁰,
 A. Kamenshchikov¹³⁰, N. Kanaya¹⁵⁶, M. Kaneda³⁰, S. Kaneti²⁸, V.A. Kantserov⁹⁸,
 J. Kanzaki⁶⁶, B. Kaplan¹¹⁰, A. Kapliy³¹, D. Kar⁵³, K. Karakostas¹⁰, A. Karamaoun³,
 N. Karastathis^{10,107}, M.J. Kareem⁵⁴, M. Karnevskiy⁸³, S.N. Karpov⁶⁵, Z.M. Karpova⁶⁵,
 K. Karthik¹¹⁰, V. Kartvelishvili⁷², A.N. Karyukhin¹³⁰, L. Kashif¹⁷⁴, R.D. Kass¹¹¹,
 A. Kastanas¹⁴, Y. Kataoka¹⁵⁶, A. Katre⁴⁹, J. Katzy⁴², K. Kawagoe⁷⁰, T. Kawamoto¹⁵⁶,
 G. Kawamura⁵⁴, S. Kazama¹⁵⁶, V.F. Kazanin^{109,c}, M.Y. Kazarinov⁶⁵, R. Keeler¹⁷⁰,
 R. Kehoe⁴⁰, J.S. Keller⁴², J.J. Kempster⁷⁷, H. Keoshkerian⁸⁴, O. Kepka¹²⁷,
 B.P. Kerševan⁷⁵, S. Kersten¹⁷⁶, R.A. Keyes⁸⁷, F. Khalil-zada¹¹, H. Khandanyan^{147a,147b},
 A. Khanov¹¹⁴, A.G. Kharlamov^{109,c}, T.J. Khoo²⁸, V. Khovanskiy⁹⁷, E. Khramov⁶⁵,
 J. Khubua^{51b,t}, H.Y. Kim⁸, H. Kim^{147a,147b}, S.H. Kim¹⁶¹, Y. Kim³¹, N. Kimura¹⁵⁵,
 O.M. Kind¹⁶, B.T. King⁷⁴, M. King¹⁶⁸, R.S.B. King¹²⁰, S.B. King¹⁶⁹, J. Kirk¹³¹,
 A.E. Kiryunin¹⁰¹, T. Kishimoto⁶⁷, D. Kisielewska^{38a}, F. Kiss⁴⁸, K. Kiuchi¹⁶¹,
 O. Kivernyk¹³⁷, E. Kladiva^{145b}, M.H. Klein³⁵, M. Klein⁷⁴, U. Klein⁷⁴, K. Kleinknecht⁸³,
 P. Klimek^{147a,147b}, A. Klimentov²⁵, R. Klingenberg⁴³, J.A. Klinger⁸⁴,
 T. Klioutchnikova³⁰, P.F. Klok¹⁰⁶, E.-E. Kluge^{58a}, P. Kluit¹⁰⁷, S. Kluth¹⁰¹,
 E. Kneringer⁶², E.B.F.G. Knoops⁸⁵, A. Knue⁵³, D. Kobayashi¹⁵⁸, T. Kobayashi¹⁵⁶,
 M. Kobel⁴⁴, M. Kocian¹⁴⁴, P. Kodys¹²⁹, T. Koffas²⁹, E. Koffeman¹⁰⁷, L.A. Kogan¹²⁰,
 S. Kohlmann¹⁷⁶, Z. Kohout¹²⁸, T. Kohriki⁶⁶, T. Koi¹⁴⁴, H. Kolanoski¹⁶, I. Koletsou⁵,
 A.A. Komar^{96,*}, Y. Komori¹⁵⁶, T. Kondo⁶⁶, N. Kondrashova⁴², K. Köneke⁴⁸,
 A.C. König¹⁰⁶, S. König⁸³, T. Kono^{66,u}, R. Konoplich^{110,v}, N. Konstantinidis⁷⁸,
 R. Kopeliansky¹⁵³, S. Koperny^{38a}, L. Köpke⁸³, A.K. Kopp⁴⁸, K. Korcyl³⁹, K. Kordas¹⁵⁵,
 A. Korn⁷⁸, A.A. Korol^{109,c}, I. Korolkov¹², E.V. Korolkova¹⁴⁰, O. Kortner¹⁰¹,
 S. Kortner¹⁰¹, T. Kosek¹²⁹, V.V. Kostyukhin²¹, V.M. Kotov⁶⁵, A. Kotwal⁴⁵,
 A. Kourkoumeli-Charalampidi¹⁵⁵, C. Kourkoumelis⁹, V. Kouskoura²⁵, A. Koutsman^{160a},
 R. Kowalewski¹⁷⁰, T.Z. Kowalski^{38a}, W. Kozanecki¹³⁷, A.S. Kozhin¹³⁰,
 V.A. Kramarenko⁹⁹, G. Kramberger⁷⁵, D. Krasnopevtsev⁹⁸, M.W. Krasny⁸⁰,
 A. Krasznahorkay³⁰, J.K. Kraus²¹, A. Kravchenko²⁵, S. Kreiss¹¹⁰, M. Kretz^{58c},
 J. Kretzschmar⁷⁴, K. Kreutzfeldt⁵², P. Krieger¹⁵⁹, K. Krizka³¹, K. Kroeninger⁴³,
 H. Kroha¹⁰¹, J. Kroll¹²², J. Kroseberg²¹, J. Krstic¹³, U. Kruchonak⁶⁵, H. Krüger²¹,

N. Krumnack⁶⁴, Z.V. Krumshteyn⁶⁵, A. Kruse¹⁷⁴, M.C. Kruse⁴⁵, M. Kruskal²²,
 T. Kubota⁸⁸, H. Kucuk⁷⁸, S. Kuday^{4c}, S. Kuehn⁴⁸, A. Kugel^{58c}, F. Kuger¹⁷⁵, A. Kuhl¹³⁸,
 T. Kuhl⁴², V. Kukhtin⁶⁵, R. Kukla¹³⁷, Y. Kulchitsky⁹², S. Kuleshov^{32b}, M. Kuna^{133a,133b},
 T. Kunigo⁶⁸, A. Kupco¹²⁷, H. Kurashige⁶⁷, Y.A. Kurochkin⁹², R. Kurumida⁶⁷, V. Kus¹²⁷,
 E.S. Kuwertz¹⁴⁸, M. Kuze¹⁵⁸, J. Kvita¹¹⁵, T. Kwan¹⁷⁰, D. Kyriazopoulos¹⁴⁰,
 A. La Rosa⁴⁹, J.L. La Rosa Navarro^{24d}, L. La Rotonda^{37a,37b}, C. Lacasta¹⁶⁸,
 F. Lacava^{133a,133b}, J. Lacey²⁹, H. Lacker¹⁶, D. Lacour⁸⁰, V.R. Lacuesta¹⁶⁸, E. Ladygin⁶⁵,
 R. Lafaye⁵, B. Laforge⁸⁰, T. Lagouri¹⁷⁷, S. Lai⁴⁸, L. Lambourne⁷⁸, S. Lammers⁶¹,
 C.L. Lampen⁷, W. Lampl⁷, E. Lançon¹³⁷, U. Landgraf⁴⁸, M.P.J. Landon⁷⁶, V.S. Lang^{58a},
 J.C. Lange¹², A.J. Lankford¹⁶⁴, F. Lanni²⁵, K. Lantzsch³⁰, S. Laplace⁸⁰, C. Lapoire³⁰,
 J.F. Laporte¹³⁷, T. Lari^{91a}, F. Lasagni Manghi^{20a,20b}, M. Lassnig³⁰, P. Laurelli⁴⁷,
 W. Lavrijsen¹⁵, A.T. Law¹³⁸, P. Laycock⁷⁴, O. Le Dortz⁸⁰, E. Le Guirriec⁸⁵,
 E. Le Menedeu¹², M. LeBlanc¹⁷⁰, T. LeCompte⁶, F. Ledroit-Guillon⁵⁵, C.A. Lee^{146b},
 S.C. Lee¹⁵², L. Lee¹, G. Lefebvre⁸⁰, M. Lefebvre¹⁷⁰, F. Legger¹⁰⁰, C. Leggett¹⁵,
 A. Lehan⁷⁴, G. Lehmann Miotto³⁰, X. Lei⁷, W.A. Leight²⁹, A. Leisos¹⁵⁵, A.G. Leister¹⁷⁷,
 M.A.L. Leite^{24d}, R. Leitner¹²⁹, D. Lellouch¹⁷³, B. Lemmer⁵⁴, K.J.C. Leney⁷⁸, T. Lenz²¹,
 B. Lenzi³⁰, R. Leone⁷, S. Leone^{124a,124b}, C. Leonidopoulos⁴⁶, S. Leontsinis¹⁰, C. Leroy⁹⁵,
 C.G. Lester²⁸, M. Levchenko¹²³, J. Levêque⁵, D. Levin⁸⁹, L.J. Levinson¹⁷³, M. Levy¹⁸,
 A. Lewis¹²⁰, A.M. Leyko²¹, M. Leyton⁴¹, B. Li^{33b,w}, H. Li¹⁴⁹, H.L. Li³¹, L. Li⁴⁵, L. Li^{33e},
 S. Li⁴⁵, Y. Li^{33c,x}, Z. Liang¹³⁸, H. Liao³⁴, B. Liberti^{134a}, A. Liblong¹⁵⁹, P. Lichard³⁰,
 K. Lie¹⁶⁶, J. Liebal²¹, W. Liebig¹⁴, C. Limbach²¹, A. Limosani¹⁵¹, S.C. Lin^{152,y},
 T.H. Lin⁸³, F. Linde¹⁰⁷, B.E. Lindquist¹⁴⁹, J.T. Linnemann⁹⁰, E. Lipeles¹²²,
 A. Lipniacka¹⁴, M. Lisovyi⁴², T.M. Liss¹⁶⁶, D. Lissauer²⁵, A. Lister¹⁶⁹, A.M. Litke¹³⁸,
 B. Liu¹⁵², D. Liu¹⁵², J. Liu⁸⁵, J.B. Liu^{33b}, K. Liu⁸⁵, L. Liu¹⁶⁶, M. Liu⁴⁵, M. Liu^{33b},
 Y. Liu^{33b}, M. Livan^{121a,121b}, A. Lleres⁵⁵, J. Llorente Merino⁸², S.L. Lloyd⁷⁶,
 F. Lo Sterzo¹⁵², E. Lobodzinska⁴², P. Loch⁷, W.S. Lockman¹³⁸, F.K. Loebinger⁸⁴,
 A.E. Loevschall-Jensen³⁶, A. Loginov¹⁷⁷, T. Lohse¹⁶, K. Lohwasser⁴², M. Lokajicek¹²⁷,
 B.A. Long²², J.D. Long⁸⁹, R.E. Long⁷², K.A. Looper¹¹¹, L. Lopes^{126a}, D. Lopez Mateos⁵⁷,
 B. Lopez Paredes¹⁴⁰, I. Lopez Paz¹², J. Lorenz¹⁰⁰, N. Lorenzo Martinez⁶¹, M. Losada¹⁶³,
 P. Loscutoff¹⁵, P.J. Lösel¹⁰⁰, X. Lou^{33a}, A. Lounis¹¹⁷, J. Love⁶, P.A. Love⁷², N. Lu⁸⁹,
 H.J. Lubatti¹³⁹, C. Luci^{133a,133b}, A. Lucotte⁵⁵, F. Luehring⁶¹, W. Lukas⁶²,
 L. Luminari^{133a}, O. Lundberg^{147a,147b}, B. Lund-Jensen¹⁴⁸, M. Lungwitz⁸³, D. Lynn²⁵,
 R. Lysak¹²⁷, E. Lytken⁸¹, H. Ma²⁵, L.L. Ma^{33d}, G. Maccarrone⁴⁷, A. Macchiolo¹⁰¹,
 C.M. Macdonald¹⁴⁰, J. Machado Miguens^{122,126b}, D. Macina³⁰, D. Madaffari⁸⁵,
 R. Madar³⁴, H.J. Maddocks⁷², W.F. Mader⁴⁴, A. Madsen¹⁶⁷, S. Maeland¹⁴, T. Maeno²⁵,
 A. Maevskiy⁹⁹, E. Magradze⁵⁴, K. Mahboubi⁴⁸, J. Mahlstedt¹⁰⁷, C. Maiani¹³⁷,
 C. Maidantchik^{24a}, A.A. Maier¹⁰¹, T. Maier¹⁰⁰, A. Maio^{126a,126b,126d}, S. Majewski¹¹⁶,
 Y. Makida⁶⁶, N. Makovec¹¹⁷, B. Malaescu⁸⁰, Pa. Malecki³⁹, V.P. Maleev¹²³, F. Malek⁵⁵,
 U. Mallik⁶³, D. Malon⁶, C. Malone¹⁴⁴, S. Maltezos¹⁰, V.M. Malyshev¹⁰⁹, S. Malyukov³⁰,
 J. Mamuzic⁴², G. Mancini⁴⁷, B. Mandelli³⁰, L. Mandelli^{91a}, I. Mandić⁷⁵, R. Mandrysch⁶³,
 J. Maneira^{126a,126b}, A. Manfredini¹⁰¹, L. Manhaes de Andrade Filho^{24b},
 J. Manjarres Ramos^{160b}, A. Mann¹⁰⁰, P.M. Manning¹³⁸, A. Manousakis-Katsikakis⁹,
 B. Mansoulie¹³⁷, R. Mantifel⁸⁷, M. Mantoani⁵⁴, L. Mapelli³⁰, L. March^{146c},

G. Marchiori⁸⁰, M. Marcisovsky¹²⁷, C.P. Marino¹⁷⁰, M. Marjanovic¹³, F. Marroquim^{24a},
 S.P. Marsden⁸⁴, Z. Marshall¹⁵, L.F. Marti¹⁷, S. Marti-Garcia¹⁶⁸, B. Martin⁹⁰,
 T.A. Martin¹⁷¹, V.J. Martin⁴⁶, B. Martin dit Latour¹⁴, M. Martinez^{12,o},
 S. Martin-Haug¹³¹, V.S. Martoiu^{26a}, A.C. Martyniuk⁷⁸, M. Marx¹³⁹, F. Marzano^{133a},
 A. Marzin³⁰, L. Masetti⁸³, T. Mashimo¹⁵⁶, R. Mashinistov⁹⁶, J. Masik⁸⁴,
 A.L. Maslennikov^{109,c}, I. Massa^{20a,20b}, L. Massa^{20a,20b}, N. Massol⁵, P. Mastrandrea¹⁴⁹,
 A. Mastroberardino^{37a,37b}, T. Masubuchi¹⁵⁶, P. Mättig¹⁷⁶, J. Mattmann⁸³, J. Maurer^{26a},
 S.J. Maxfield⁷⁴, D.A. Maximov^{109,c}, R. Mazini¹⁵², S.M. Mazza^{91a,91b},
 L. Mazzaferro^{134a,134b}, G. Mc Goldrick¹⁵⁹, S.P. Mc Kee⁸⁹, A. McCarn⁸⁹,
 R.L. McCarthy¹⁴⁹, T.G. McCarthy²⁹, N.A. McCubbin¹³¹, K.W. McFarlane^{56,*},
 J.A. Mcfayden⁷⁸, G. Mchedlidze⁵⁴, S.J. McMahon¹³¹, R.A. McPherson^{170,k},
 M. Medinnis⁴², S. Meehan^{146a}, S. Mehlhase¹⁰⁰, A. Mehta⁷⁴, K. Meier^{58a}, C. Meineck¹⁰⁰,
 B. Meirose⁴¹, B.R. Mellado Garcia^{146c}, F. Meloni¹⁷, A. Mengarelli^{20a,20b}, S. Menke¹⁰¹,
 E. Meoni¹⁶², K.M. Mercurio⁵⁷, S. Mergelmeyer²¹, P. Mermod⁴⁹, L. Merola^{104a,104b},
 C. Meroni^{91a}, F.S. Merritt³¹, A. Messina^{133a,133b}, J. Metcalfe²⁵, A.S. Mete¹⁶⁴, C. Meyer⁸³,
 C. Meyer¹²², J-P. Meyer¹³⁷, J. Meyer¹⁰⁷, R.P. Middleton¹³¹, S. Miglioranza^{165a,165c},
 L. Mijović²¹, G. Mikenberg¹⁷³, M. Mikestikova¹²⁷, M. Mikuz⁷⁵, M. Milesi⁸⁸, A. Milic³⁰,
 D.W. Miller³¹, C. Mills⁴⁶, A. Milov¹⁷³, D.A. Milstead^{147a,147b}, A.A. Minaenko¹³⁰,
 Y. Minami¹⁵⁶, I.A. Minashvili⁶⁵, A.I. Mincer¹¹⁰, B. Mindur^{38a}, M. Mineev⁶⁵, Y. Ming¹⁷⁴,
 L.M. Mir¹², T. Mitani¹⁷², J. Mitrevski¹⁰⁰, V.A. Mitsou¹⁶⁸, A. Miucci⁴⁹, P.S. Miyagawa¹⁴⁰,
 J.U. Mjörnmark⁸¹, T. Moe^{147a,147b}, K. Mochizuki⁸⁵, S. Mohapatra³⁵, W. Mohr⁴⁸,
 S. Molander^{147a,147b}, R. Moles-Valls¹⁶⁸, K. Mönig⁴², C. Monini⁵⁵, J. Monk³⁶,
 E. Monnier⁸⁵, J. Montejo Berlingen¹², F. Monticelli⁷¹, S. Monzani^{133a,133b}, R.W. Moore³,
 N. Morange¹¹⁷, D. Moreno¹⁶³, M. Moreno Llácer⁵⁴, P. Morettini^{50a}, M. Morgenstern⁴⁴,
 M. Morii⁵⁷, V. Morisbak¹¹⁹, S. Moritz⁸³, A.K. Morley¹⁴⁸, G. Mornacchi³⁰, J.D. Morris⁷⁶,
 S.S. Mortensen³⁶, A. Morton⁵³, L. Morvaj¹⁰³, H.G. Moser¹⁰¹, M. Mosidze^{51b}, J. Moss¹¹¹,
 K. Motohashi¹⁵⁸, R. Mount¹⁴⁴, E. Mountricha²⁵, S.V. Mouraviev^{96,*}, E.J.W. Moyses⁸⁶,
 S. Muanza⁸⁵, R.D. Mudd¹⁸, F. Mueller¹⁰¹, J. Mueller¹²⁵, K. Mueller²¹, R.S.P. Mueller¹⁰⁰,
 T. Mueller²⁸, D. Muenstermann⁴⁹, P. Mullen⁵³, Y. Munwes¹⁵⁴, J.A. Murillo Quijada¹⁸,
 W.J. Murray^{171,131}, H. Musheghyan⁵⁴, E. Musto¹⁵³, A.G. Myagkov^{130,z}, M. Myska¹²⁸,
 O. Nackendorst⁵⁴, J. Nadal⁵⁴, K. Nagai¹²⁰, R. Nagai¹⁵⁸, Y. Nagai⁸⁵, K. Nagano⁶⁶,
 A. Nagarkar¹¹¹, Y. Nagasaka⁵⁹, K. Nagata¹⁶¹, M. Nagel¹⁰¹, E. Nagy⁸⁵, A.M. Nairz³⁰,
 Y. Nakahama³⁰, K. Nakamura⁶⁶, T. Nakamura¹⁵⁶, I. Nakano¹¹², H. Namasivayam⁴¹,
 R.F. Naranjo Garcia⁴², R. Narayan^{58b}, T. Naumann⁴², G. Navarro¹⁶³, R. Nayyar⁷,
 H.A. Neal⁸⁹, P.Yu. Nechaeva⁹⁶, T.J. Neep⁸⁴, P.D. Nef¹⁴⁴, A. Negri^{121a,121b}, M. Negrini^{20a},
 S. Nektarijevic¹⁰⁶, C. Nellist¹¹⁷, A. Nelson¹⁶⁴, S. Nemecek¹²⁷, P. Nemethy¹¹⁰,
 A.A. Nepomuceno^{24a}, M. Nessi^{30,aa}, M.S. Neubauer¹⁶⁶, M. Neumann¹⁷⁶, R.M. Neves¹¹⁰,
 P. Nevski²⁵, P.R. Newman¹⁸, D.H. Nguyen⁶, R.B. Nickerson¹²⁰, R. Nicolaidou¹³⁷,
 B. Nicquevert³⁰, J. Nielsen¹³⁸, N. Nikiforou³⁵, A. Nikiforov¹⁶, V. Nikolaenko^{130,z},
 I. Nikolic-Audit⁸⁰, K. Nikolopoulos¹⁸, J.K. Nilsen¹¹⁹, P. Nilsson²⁵, Y. Ninomiya¹⁵⁶,
 A. Nisati^{133a}, R. Nisius¹⁰¹, T. Nobe¹⁵⁸, M. Nomachi¹¹⁸, I. Nomidis²⁹, T. Nooney⁷⁶,
 S. Norberg¹¹³, M. Nordberg³⁰, O. Novgorodova⁴⁴, S. Nowak¹⁰¹, M. Nozaki⁶⁶, L. Nozka¹¹⁵,
 K. Ntekas¹⁰, G. Nunes Hanninger⁸⁸, T. Nunnemann¹⁰⁰, E. Nurse⁷⁸, F. Nuti⁸⁸,

B.J. O'Brien⁴⁶, F. O'grady⁷, D.C. O'Neil¹⁴³, V. O'Shea⁵³, F.G. Oakham^{29,d},
 H. Oberlack¹⁰¹, T. Obermann²¹, J. Ocariz⁸⁰, A. Ochi⁶⁷, I. Ochoa⁷⁸, S. Oda⁷⁰, S. Odaka⁶⁶,
 H. Ogren⁶¹, A. Oh⁸⁴, S.H. Oh⁴⁵, C.C. Ohm¹⁵, H. Ohman¹⁶⁷, H. Oide³⁰, W. Okamura¹¹⁸,
 H. Okawa¹⁶¹, Y. Okumura³¹, T. Okuyama¹⁵⁶, A. Olariu^{26a}, S.A. Olivares Pino⁴⁶,
 D. Oliveira Damazio²⁵, E. Oliver Garcia¹⁶⁸, A. Olszewski³⁹, J. Olszowska³⁹,
 A. Onofre^{126a,126e}, P.U.E. Onyisi^{31,q}, C.J. Oram^{160a}, M.J. Oreglia³¹, Y. Oren¹⁵⁴,
 D. Orestano^{135a,135b}, N. Orlando¹⁵⁵, C. Oropeza Barrera⁵³, R.S. Orr¹⁵⁹, B. Osculati^{50a,50b},
 R. Ospanov⁸⁴, G. Otero y Garzon²⁷, H. Otono⁷⁰, M. Ouchrif^{136d}, E.A. Ouellette¹⁷⁰,
 F. Ould-Saada¹¹⁹, A. Ouraou¹³⁷, K.P. Oussoren¹⁰⁷, Q. Ouyang^{33a}, A. Ovcharova¹⁵,
 M. Owen⁵³, R.E. Owen¹⁸, V.E. Ozcan^{19a}, N. Ozturk⁸, K. Pachal¹²⁰, A. Pacheco Pages¹²,
 C. Padilla Aranda¹², M. Pagáčová⁴⁸, S. Pagan Griso¹⁵, E. Paganis¹⁴⁰, C. Pahl¹⁰¹,
 F. Paige²⁵, P. Pais⁸⁶, K. Pajchel¹¹⁹, G. Palacino^{160b}, S. Palestini³⁰, M. Palka^{38b},
 D. Pallin³⁴, A. Palma^{126a,126b}, Y.B. Pan¹⁷⁴, E. Panagiotopoulou¹⁰, C.E. Pandini⁸⁰,
 J.G. Panduro Vazquez⁷⁷, P. Pani^{147a,147b}, S. Panitkin²⁵, L. Paolozzi^{134a,134b},
 Th.D. Papadopoulou¹⁰, K. Papageorgiou¹⁵⁵, A. Paramonov⁶, D. Paredes Hernandez¹⁵⁵,
 M.A. Parker²⁸, K.A. Parker¹⁴⁰, F. Parodi^{50a,50b}, J.A. Parsons³⁵, U. Parzefall⁴⁸,
 E. Pasqualucci^{133a}, S. Passaggio^{50a}, F. Pastore^{135a,135b,*}, Fr. Pastore⁷⁷, G. Pásztor²⁹,
 S. Pataraiia¹⁷⁶, N.D. Patel¹⁵¹, J.R. Pater⁸⁴, T. Pauly³⁰, J. Pearce¹⁷⁰, B. Pearson¹¹³,
 L.E. Pedersen³⁶, M. Pedersen¹¹⁹, S. Pedraza Lopez¹⁶⁸, R. Pedro^{126a,126b},
 S.V. Peleganchuk¹⁰⁹, D. Pelikan¹⁶⁷, H. Peng^{33b}, B. Penning³¹, J. Penwell⁶¹,
 D.V. Perepelitsa²⁵, E. Perez Codina^{160a}, M.T. Pérez García-Estañ¹⁶⁸, L. Perini^{91a,91b},
 H. Pernegger³⁰, S. Perrella^{104a,104b}, R. Peschke⁴², V.D. Peshekhonov⁶⁵, K. Peters³⁰,
 R.F.Y. Peters⁸⁴, B.A. Petersen³⁰, T.C. Petersen³⁶, E. Petit⁴², A. Petridis^{147a,147b},
 C. Petridou¹⁵⁵, E. Petrolo^{133a}, F. Petrucci^{135a,135b}, N.E. Pettersson¹⁵⁸, R. Pezoa^{32b},
 P.W. Phillips¹³¹, G. Piacquadio¹⁴⁴, E. Pianori¹⁷¹, A. Picazio⁴⁹, E. Piccaro⁷⁶,
 M. Piccinini^{20a,20b}, M.A. Pickering¹²⁰, R. Piegai²⁷, D.T. Pignotti¹¹¹, J.E. Pilcher³¹,
 A.D. Pilkington⁸⁴, J. Pina^{126a,126b,126d}, M. Pinamonti^{165a,165c,ab}, J.L. Pinfold³,
 A. Pingel³⁶, B. Pinto^{126a}, S. Pires⁸⁰, M. Pitt¹⁷³, C. Pizio^{91a,91b}, L. Plazak^{145a},
 M.-A. Pleier²⁵, V. Pleskot¹²⁹, E. Plotnikova⁶⁵, P. Plucinski^{147a,147b}, D. Pluth⁶⁴,
 R. Poettgen⁸³, L. Poggioli¹¹⁷, D. Pohl²¹, G. Polesello^{121a}, A. Policicchio^{37a,37b},
 R. Polifka¹⁵⁹, A. Polini^{20a}, C.S. Pollard⁵³, V. Polychronakos²⁵, K. Pommès³⁰,
 L. Pontecorvo^{133a}, B.G. Pope⁹⁰, G.A. Popeneciu^{26b}, D.S. Popovic¹³, A. Poppleton³⁰,
 S. Pospisil¹²⁸, K. Potamianos¹⁵, I.N. Potrap⁶⁵, C.J. Potter¹⁵⁰, C.T. Potter¹¹⁶,
 G. Poulard³⁰, J. Poveda³⁰, V. Pozdnyakov⁶⁵, P. Pralavorio⁸⁵, A. Pranko¹⁵, S. Prasad³⁰,
 S. Prell⁶⁴, D. Price⁸⁴, J. Price⁷⁴, L.E. Price⁶, M. Primavera^{73a}, S. Prince⁸⁷, M. Proissl⁴⁶,
 K. Prokofiev^{60c}, F. Prokoshin^{32b}, E. Protopapadaki¹³⁷, S. Protopopescu²⁵, J. Proudfoot⁶,
 M. Przybycien^{38a}, E. Ptacek¹¹⁶, D. Puddu^{135a,135b}, E. Pueschel⁸⁶, D. Pudlon¹⁴⁹,
 M. Purohit^{25,ac}, P. Puzo¹¹⁷, J. Qian⁸⁹, G. Qin⁵³, Y. Qin⁸⁴, A. Quadt⁵⁴, D.R. Quarrie¹⁵,
 W.B. Quayle^{165a,165b}, M. Queitsch-Maitland⁸⁴, D. Quilty⁵³, S. Raddum¹¹⁹, V. Radeka²⁵,
 V. Radescu⁴², S.K. Radhakrishnan¹⁴⁹, P. Radloff¹¹⁶, P. Rados⁸⁸, F. Ragusa^{91a,91b},
 G. Rahal¹⁷⁹, S. Rajagopalan²⁵, M. Rammensee³⁰, C. Rangel-Smith¹⁶⁷, F. Rauscher¹⁰⁰,
 S. Rave⁸³, T. Ravenscroft⁵³, M. Raymond³⁰, A.L. Read¹¹⁹, N.P. Readioff⁷⁴,
 D.M. Rebuffi^{121a,121b}, A. Redelbach¹⁷⁵, G. Redlinger²⁵, R. Reece¹³⁸, K. Reeves⁴¹,

L. Rehnisch¹⁶, H. Reisin²⁷, M. Relich¹⁶⁴, C. Rembser³⁰, H. Ren^{33a}, A. Renaud¹¹⁷,
 M. Rescigno^{133a}, S. Resconi^{91a}, O.L. Rezanova^{109,c}, P. Reznicek¹²⁹, R. Rezvani⁹⁵,
 R. Richter¹⁰¹, S. Richter⁷⁸, E. Richter-Was^{38b}, O. Ricken²¹, M. Ridel⁸⁰, P. Rieck¹⁶,
 C.J. Riegel¹⁷⁶, J. Rieger⁵⁴, M. Rijssenbeek¹⁴⁹, A. Rimoldi^{121a,121b}, L. Rinaldi^{20a},
 B. Ristić⁴⁹, E. Ritsch⁶², I. Riu¹², F. Rizatdinova¹¹⁴, E. Rizvi⁷⁶, S.H. Robertson^{87,k},
 A. Robichaud-Veronneau⁸⁷, D. Robinson²⁸, J.E.M. Robinson⁸⁴, A. Robson⁵³,
 C. Roda^{124a,124b}, S. Roe³⁰, O. Røhne¹¹⁹, S. Rolli¹⁶², A. Romaniouk⁹⁸, M. Romano^{20a,20b},
 S.M. Romano Saez³⁴, E. Romero Adam¹⁶⁸, N. Rompotis¹³⁹, M. Ronzani⁴⁸, L. Roos⁸⁰,
 E. Ros¹⁶⁸, S. Rosati^{133a}, K. Rosbach⁴⁸, P. Rose¹³⁸, P.L. Rosendahl¹⁴, O. Rosenthal¹⁴²,
 V. Rossetti^{147a,147b}, E. Rossi^{104a,104b}, L.P. Rossi^{50a}, R. Rosten¹³⁹, M. Rotaru^{26a},
 I. Roth¹⁷³, J. Rothberg¹³⁹, D. Rousseau¹¹⁷, C.R. Royon¹³⁷, A. Rozanov⁸⁵, Y. Rozen¹⁵³,
 X. Ruan^{146c}, F. Rubbo¹⁴⁴, I. Rubinskiy⁴², V.I. Rud⁹⁹, C. Rudolph⁴⁴, M.S. Rudolph¹⁵⁹,
 F. Rühr⁴⁸, A. Ruiz-Martinez³⁰, Z. Rurikova⁴⁸, N.A. Rusakovich⁶⁵, A. Ruschke¹⁰⁰,
 H.L. Russell¹³⁹, J.P. Rutherford⁷, N. Ruthmann⁴⁸, Y.F. Ryabov¹²³, M. Rybar¹²⁹,
 G. Rybkin¹¹⁷, N.C. Ryder¹²⁰, A.F. Saavedra¹⁵¹, G. Sabato¹⁰⁷, S. Sacerdoti²⁷,
 A. Saddique³, H.F-W. Sadrozinski¹³⁸, R. Sadykov⁶⁵, F. Safai Tehrani^{133a}, M. Saimpert¹³⁷,
 H. Sakamoto¹⁵⁶, Y. Sakurai¹⁷², G. Salamanna^{135a,135b}, A. Salamon^{134a}, M. Saleem¹¹³,
 D. Salek¹⁰⁷, P.H. Sales De Bruin¹³⁹, D. Salihagic¹⁰¹, A. Salnikov¹⁴⁴, J. Salt¹⁶⁸,
 D. Salvatore^{37a,37b}, F. Salvatore¹⁵⁰, A. Salvucci¹⁰⁶, A. Salzburger³⁰, D. Sampsonidis¹⁵⁵,
 A. Sanchez^{104a,104b}, J. Sánchez¹⁶⁸, V. Sanchez Martinez¹⁶⁸, H. Sandaker¹⁴,
 R.L. Sandbach⁷⁶, H.G. Sander⁸³, M.P. Sanders¹⁰⁰, M. Sandhoff¹⁷⁶, C. Sandoval¹⁶³,
 R. Sandstroem¹⁰¹, D.P.C. Sankey¹³¹, M. Sannino^{50a,50b}, A. Sansoni⁴⁷, C. Santoni³⁴,
 R. Santonico^{134a,134b}, H. Santos^{126a}, I. Santoyo Castillo¹⁵⁰, K. Sapp¹²⁵, A. Sapronov⁶⁵,
 J.G. Saraiva^{126a,126d}, B. Sarrazin²¹, O. Sasaki⁶⁶, Y. Sasaki¹⁵⁶, K. Sato¹⁶¹, G. Sauvage^{5,*},
 E. Sauvan⁵, G. Savage⁷⁷, P. Savard^{159,d}, C. Sawyer¹²⁰, L. Sawyer^{79,n}, J. Saxon³¹,
 C. Sbarra^{20a}, A. Sbrizzi^{20a,20b}, T. Scanlon⁷⁸, D.A. Scannicchio¹⁶⁴, M. Scarcella¹⁵¹,
 V. Scarfone^{37a,37b}, J. Schaarschmidt¹⁷³, P. Schacht¹⁰¹, D. Schaefer³⁰, R. Schaefer⁴²,
 J. Schaeffer⁸³, S. Schaepe²¹, S. Schaetzel^{58b}, U. Schäfer⁸³, A.C. Schaffer¹¹⁷, D. Schaile¹⁰⁰,
 R.D. Schamberger¹⁴⁹, V. Scharf^{58a}, V.A. Schegelsky¹²³, D. Scheirich¹²⁹, M. Schernau¹⁶⁴,
 C. Schiavi^{50a,50b}, C. Schillo⁴⁸, M. Schioppa^{37a,37b}, S. Schlenker³⁰, E. Schmidt⁴⁸,
 K. Schmieden³⁰, C. Schmitt⁸³, S. Schmitt^{58b}, S. Schmitt⁴², B. Schneider^{160a},
 Y.J. Schnellbach⁷⁴, U. Schnoor⁴⁴, L. Schoeffel¹³⁷, A. Schoening^{58b}, B.D. Schoenrock⁹⁰,
 E. Schopf²¹, A.L.S. Schorlemmer⁵⁴, M. Schott⁸³, D. Schouten^{160a}, J. Schovancova⁸,
 S. Schramm¹⁵⁹, M. Schreyer¹⁷⁵, C. Schroeder⁸³, N. Schuh⁸³, M.J. Schultens²¹,
 H.-C. Schultz-Coulon^{58a}, H. Schulz¹⁶, M. Schumacher⁴⁸, B.A. Schumm¹³⁸, Ph. Schune¹³⁷,
 C. Schwanenberger⁸⁴, A. Schwartzman¹⁴⁴, T.A. Schwarz⁸⁹, Ph. Schwegler¹⁰¹,
 Ph. Schwemling¹³⁷, R. Schwienhorst⁹⁰, J. Schwindling¹³⁷, T. Schwindt²¹, M. Schwoerer⁵,
 F.G. Sciacca¹⁷, E. Scifo¹¹⁷, G. Sciolla²³, F. Scuri^{124a,124b}, F. Scutti²¹, J. Searcy⁸⁹,
 G. Sedov⁴², E. Sedykh¹²³, P. Seema²¹, S.C. Seidel¹⁰⁵, A. Seiden¹³⁸, F. Seifert¹²⁸,
 J.M. Seixas^{24a}, G. Sekhniaidze^{104a}, S.J. Sekula⁴⁰, K.E. Selbach⁴⁶, D.M. Seliverstov^{123,*},
 N. Semprini-Cesari^{20a,20b}, C. Serfon³⁰, L. Serin¹¹⁷, L. Serkin^{165a,165b}, T. Serre⁸⁵,
 R. Seuster^{160a}, H. Severini¹¹³, T. Sfiligoj⁷⁵, F. Sforza¹⁰¹, A. Sfyrla³⁰, E. Shabalina⁵⁴,
 M. Shamim¹¹⁶, L.Y. Shan^{33a}, R. Shang¹⁶⁶, J.T. Shank²², M. Shapiro¹⁵, P.B. Shatalov⁹⁷,

K. Shaw^{165a,165b}, S.M. Shaw⁸⁴, A. Shcherbakova^{147a,147b}, C.Y. Shehu¹⁵⁰, P. Sherwood⁷⁸,
 L. Shi^{152,ad}, S. Shimizu⁶⁷, C.O. Shimmin¹⁶⁴, M. Shimojima¹⁰², M. Shiyakova⁶⁵,
 A. Shmeleva⁹⁶, D. Shoaleh Saadi⁹⁵, M.J. Shochet³¹, S. Shojaii^{91a,91b}, S. Shrestha¹¹¹,
 E. Shulga⁹⁸, M.A. Shupe⁷, S. Shushkevich⁴², P. Sicho¹²⁷, O. Sidiropoulou¹⁷⁵,
 D. Sidorov¹¹⁴, A. Sidoti^{20a,20b}, F. Siegert⁴⁴, Dj. Sijacki¹³, J. Silva^{126a,126d}, Y. Silver¹⁵⁴,
 S.B. Silverstein^{147a}, V. Simak¹²⁸, O. Simard⁵, Lj. Simic¹³, S. Simion¹¹⁷, E. Simioni⁸³,
 B. Simmons⁷⁸, D. Simon³⁴, R. Simoniello^{91a,91b}, P. Sinervo¹⁵⁹, N.B. Sinev¹¹⁶,
 G. Siragusa¹⁷⁵, A.N. Sisakyan^{65,*}, S.Yu. Sivoklokov⁹⁹, J. Sjölin^{147a,147b}, T.B. Sjørnsen¹⁴,
 M.B. Skinner⁷², H.P. Skottowe⁵⁷, P. Skubic¹¹³, M. Slater¹⁸, T. Slavicek¹²⁸,
 M. Slawinska¹⁰⁷, K. Sliwa¹⁶², V. Smakhtin¹⁷³, B.H. Smart⁴⁶, L. Smestad¹⁴,
 S.Yu. Smirnov⁹⁸, Y. Smirnov⁹⁸, L.N. Smirnova^{99,ae}, O. Smirnova⁸¹, M.N.K. Smith³⁵,
 M. Smizanska⁷², K. Smolek¹²⁸, A.A. Snesarev⁹⁶, G. Snidero⁷⁶, S. Snyder²⁵, R. Sobie^{170,k},
 F. Socher⁴⁴, A. Soffer¹⁵⁴, D.A. Soh^{152,ad}, C.A. Solans³⁰, M. Solar¹²⁸, J. Solc¹²⁸,
 E.Yu. Soldatov⁹⁸, U. Soldevila¹⁶⁸, A.A. Solodkov¹³⁰, A. Soloshenko⁶⁵,
 O.V. Solovyanov¹³⁰, V. Solovyev¹²³, P. Sommer⁴⁸, H.Y. Song^{33b}, N. Soni¹, A. Sood¹⁵,
 A. Sopczak¹²⁸, B. Sopko¹²⁸, V. Sopko¹²⁸, V. Sorin¹², D. Sosa^{58b}, M. Sosebee⁸,
 C.L. Sotiropoulou¹⁵⁵, R. Soualah^{165a,165c}, P. Soueid⁹⁵, A.M. Soukharev^{109,c}, D. South⁴²,
 S. Spagnolo^{73a,73b}, M. Spalla^{124a,124b}, F. Spanò⁷⁷, W.R. Spearman⁵⁷, D. Sperlich¹⁶,
 F. Spettel¹⁰¹, R. Spighi^{20a}, G. Spigo³⁰, L.A. Spiller⁸⁸, M. Spousta¹²⁹, T. Spreitzer¹⁵⁹,
 R.D. St. Denis^{53,*}, S. Staerz⁴⁴, J. Stahlman¹²², R. Stamen^{58a}, S. Stamm¹⁶, E. Stanecka³⁹,
 C. Stanescu^{135a}, M. Stanescu-Bellu⁴², M.M. Stanitzki⁴², S. Stapnes¹¹⁹,
 E.A. Starchenko¹³⁰, J. Stark⁵⁵, P. Staroba¹²⁷, P. Starovoitov⁴², R. Staszewski³⁹,
 P. Stavina^{145a,*}, P. Steinberg²⁵, B. Stelzer¹⁴³, H.J. Stelzer³⁰, O. Stelzer-Chilton^{160a},
 H. Stenzel⁵², S. Stern¹⁰¹, G.A. Stewart⁵³, J.A. Stillings²¹, M.C. Stockton⁸⁷, M. Stoebe⁸⁷,
 G. Stoicea^{26a}, P. Stolte⁵⁴, S. Stonjek¹⁰¹, A.R. Stradling⁸, A. Straessner⁴⁴,
 M.E. Stramaglia¹⁷, J. Strandberg¹⁴⁸, S. Strandberg^{147a,147b}, A. Strandlie¹¹⁹,
 E. Strauss¹⁴⁴, M. Strauss¹¹³, P. Strizenec^{145b}, R. Ströhmer¹⁷⁵, D.M. Strom¹¹⁶,
 R. Stroynowski⁴⁰, A. Strubig¹⁰⁶, S.A. Stucci¹⁷, B. Stugu¹⁴, N.A. Styles⁴², D. Su¹⁴⁴,
 J. Su¹²⁵, R. Subramaniam⁷⁹, A. Succurro¹², Y. Sugaya¹¹⁸, C. Suhr¹⁰⁸, M. Suk¹²⁸,
 V.V. Sulin⁹⁶, S. Sultansoy^{4d}, T. Sumida⁶⁸, S. Sun⁵⁷, X. Sun^{33a}, J.E. Sundermann⁴⁸,
 K. Suruliz¹⁵⁰, G. Susinno^{37a,37b}, M.R. Sutton¹⁵⁰, S. Suzuki⁶⁶, Y. Suzuki⁶⁶, M. Svatos¹²⁷,
 S. Swedish¹⁶⁹, M. Swiatlowski¹⁴⁴, I. Sykora^{145a}, T. Sykora¹²⁹, D. Ta⁹⁰, C. Taccini^{135a,135b},
 K. Tackmann⁴², J. Taenzer¹⁵⁹, A. Taffard¹⁶⁴, R. Tafirout^{160a}, N. Taiblum¹⁵⁴, H. Takai²⁵,
 R. Takashima⁶⁹, H. Takeda⁶⁷, T. Takeshita¹⁴¹, Y. Takubo⁶⁶, M. Talby⁸⁵,
 A.A. Talyshev^{109,c}, J.Y.C. Tam¹⁷⁵, K.G. Tan⁸⁸, J. Tanaka¹⁵⁶, R. Tanaka¹¹⁷, S. Tanaka¹³²,
 S. Tanaka⁶⁶, B.B. Tannenwald¹¹¹, N. Tannoury²¹, S. Tapprogge⁸³, S. Tarem¹⁵³,
 F. Tarrade²⁹, G.F. Tartarelli^{91a}, P. Tas¹²⁹, M. Tasevsky¹²⁷, T. Tashiro⁶⁸, E. Tassi^{37a,37b},
 A. Tavares Delgado^{126a,126b}, Y. Tayalati^{136d}, F.E. Taylor⁹⁴, G.N. Taylor⁸⁸, W. Taylor^{160b},
 F.A. Teischinger³⁰, M. Teixeira Dias Castanheira⁷⁶, P. Teixeira-Dias⁷⁷, K.K. Temming⁴⁸,
 H. Ten Kate³⁰, P.K. Teng¹⁵², J.J. Teoh¹¹⁸, F. Tepel¹⁷⁶, S. Terada⁶⁶, K. Terashi¹⁵⁶,
 J. Terron⁸², S. Terzo¹⁰¹, M. Testa⁴⁷, R.J. Teuscher^{159,k}, J. Therhaag²¹,
 T. Theveneaux-Pelzer³⁴, J.P. Thomas¹⁸, J. Thomas-Wilsker⁷⁷, E.N. Thompson³⁵,
 P.D. Thompson¹⁸, R.J. Thompson⁸⁴, A.S. Thompson⁵³, L.A. Thomsen³⁶, E. Thomson¹²²,

M. Thomson²⁸, R.P. Thun^{89,*}, M.J. Tibbetts¹⁵, R.E. Ticse Torres⁸⁵,
V.O. Tikhomirov^{96,af}, Yu.A. Tikhonov^{109,c}, S. Timoshenko⁹⁸, E. Tiouchichine⁸⁵,
P. Tipton¹⁷⁷, S. Tisserant⁸⁵, T. Todorov^{5,*}, S. Todorova-Nova¹²⁹, J. Tojo⁷⁰, S. Tokár^{145a},
K. Tokushuku⁶⁶, K. Tollefson⁹⁰, E. Tolley⁵⁷, L. Tomlinson⁸⁴, M. Tomoto¹⁰³,
L. Tompkins^{144,ag}, K. Toms¹⁰⁵, E. Torrence¹¹⁶, H. Torres¹⁴³, E. Torró Pastor¹⁶⁸,
J. Toth^{85,ah}, F. Touchard⁸⁵, D.R. Tovey¹⁴⁰, T. Trefzger¹⁷⁵, L. Tremblet³⁰, A. Tricoli³⁰,
I.M. Trigger^{160a}, S. Trincaz-Duvoid⁸⁰, M.F. Tripiana¹², W. Trischuk¹⁵⁹, B. Trocme⁵⁵,
C. Troncon^{91a}, M. Trotter-McDonald¹⁵, M. Trovatelli^{135a,135b}, P. True⁹⁰, M. Trzebinski³⁹,
A. Trzupek³⁹, C. Tsarouchas³⁰, J.C-L. Tseng¹²⁰, P.V. Tsiarehka⁹², D. Tsionou¹⁵⁵,
G. Tsipolitis¹⁰, N. Tsirintanis⁹, S. Tsiskaridze¹², V. Tsiskaridze⁴⁸, E.G. Tskhadadze^{51a},
I.I. Tsukerman⁹⁷, V. Tsulaia¹⁵, S. Tsuno⁶⁶, D. Tsybychev¹⁴⁹, A. Tudorache^{26a},
V. Tudorache^{26a}, A.N. Tuna¹²², S.A. Tupputi^{20a,20b}, S. Turchikhin^{99,ae}, D. Turecek¹²⁸,
R. Turra^{91a,91b}, A.J. Turvey⁴⁰, P.M. Tuts³⁵, A. Tykhonov⁴⁹, M. Tylmad^{147a,147b},
M. Tyndel¹³¹, I. Ueda¹⁵⁶, R. Ueno²⁹, M. Ughetto^{147a,147b}, M. Ugland¹⁴, M. Uhlenbrock²¹,
F. Ukegawa¹⁶¹, G. Unal³⁰, A. Undrus²⁵, G. Unel¹⁶⁴, F.C. Ungaro⁴⁸, Y. Unno⁶⁶,
C. Unverdorben¹⁰⁰, J. Urban^{145b}, P. Urquijo⁸⁸, P. Urrejola⁸³, G. Usai⁸, A. Usanova⁶²,
L. Vacavant⁸⁵, V. Vacek¹²⁸, B. Vachon⁸⁷, C. Valderanis⁸³, N. Valencic¹⁰⁷,
S. Valentineti^{20a,20b}, A. Valero¹⁶⁸, L. Valery¹², S. Valkar¹²⁹, E. Valladolid Gallego¹⁶⁸,
S. Vallecorsa⁴⁹, J.A. Valls Ferrer¹⁶⁸, W. Van Den Wollenberg¹⁰⁷, P.C. Van Der Deijl¹⁰⁷,
R. van der Geer¹⁰⁷, H. van der Graaf¹⁰⁷, R. Van Der Leeuw¹⁰⁷, N. van Eldik¹⁵³,
P. van Gemmeren⁶, J. Van Nieuwkoop¹⁴³, I. van Vulpen¹⁰⁷, M.C. van Woerden³⁰,
M. Vanadia^{133a,133b}, W. Vandelli³⁰, R. Vanguri¹²², A. Vaniachine⁶, F. Vannucci⁸⁰,
G. Vardanyan¹⁷⁸, R. Vari^{133a}, E.W. Varnes⁷, T. Varol⁴⁰, D. Varouchas⁸⁰, A. Vartapetian⁸,
K.E. Varvell¹⁵¹, F. Vazeille³⁴, T. Vazquez Schroeder⁸⁷, J. Veatch⁷, F. Veloso^{126a,126c},
T. Velz²¹, S. Veneziano^{133a}, A. Ventura^{73a,73b}, D. Ventura⁸⁶, M. Venturi¹⁷⁰, N. Venturi¹⁵⁹,
A. Venturini²³, V. Vercesi^{121a}, M. Verducci^{133a,133b}, W. Verkerke¹⁰⁷, J.C. Vermeulen¹⁰⁷,
A. Vest⁴⁴, M.C. Vetterli^{143,d}, O. Viazlo⁸¹, I. Vichou¹⁶⁶, T. Vickey¹⁴⁰,
O.E. Vickey Boeriu¹⁴⁰, G.H.A. Viehhauser¹²⁰, S. Viel¹⁵, R. Vigne³⁰, M. Villa^{20a,20b},
M. Villaplana Perez^{91a,91b}, E. Vilucchi⁴⁷, M.G. Vincter²⁹, V.B. Vinogradov⁶⁵,
I. Vivarelli¹⁵⁰, F. Vives Vaque³, S. Vlachos¹⁰, D. Vladoiu¹⁰⁰, M. Vlasak¹²⁸, M. Vogel^{32a},
P. Vokac¹²⁸, G. Volpi^{124a,124b}, M. Volpi⁸⁸, H. von der Schmitt¹⁰¹, H. von Radziewski⁴⁸,
E. von Toerne²¹, V. Vorobel¹²⁹, K. Vorobev⁹⁸, M. Vos¹⁶⁸, R. Voss³⁰, J.H. Vossebeld⁷⁴,
N. Vranjes¹³, M. Vranjes Milosavljevic¹³, V. Vrba¹²⁷, M. Vreeswijk¹⁰⁷, R. Vuillemet³⁰,
I. Vukotic³¹, Z. Vykydal¹²⁸, P. Wagner²¹, W. Wagner¹⁷⁶, H. Wahlberg⁷¹, S. Wahrmund⁴⁴,
J. Wakabayashi¹⁰³, J. Walder⁷², R. Walker¹⁰⁰, W. Walkowiak¹⁴², C. Wang^{33c},
F. Wang¹⁷⁴, H. Wang¹⁵, H. Wang⁴⁰, J. Wang⁴², J. Wang^{33a}, K. Wang⁸⁷, R. Wang⁶,
S.M. Wang¹⁵², T. Wang²¹, X. Wang¹⁷⁷, C. Wanotayaroj¹¹⁶, A. Warburton⁸⁷,
C.P. Ward²⁸, D.R. Wardrope⁷⁸, M. Warsinsky⁴⁸, A. Washbrook⁴⁶, C. Wasicki⁴²,
P.M. Watkins¹⁸, A.T. Watson¹⁸, I.J. Watson¹⁵¹, M.F. Watson¹⁸, G. Watts¹³⁹, S. Watts⁸⁴,
B.M. Waugh⁷⁸, S. Webb⁸⁴, M.S. Weber¹⁷, S.W. Weber¹⁷⁵, J.S. Webster³¹,
A.R. Weidberg¹²⁰, B. Weinert⁶¹, J. Weingarten⁵⁴, C. Weiser⁴⁸, H. Weits¹⁰⁷, P.S. Wells³⁰,
T. Wenaus²⁵, T. Wengler³⁰, S. Wenig³⁰, N. Vermes²¹, M. Werner⁴⁸, P. Werner³⁰,
M. Wessels^{58a}, J. Wetter¹⁶², K. Whalen²⁹, A.M. Wharton⁷², A. White⁸, M.J. White¹,

R. White^{32b}, S. White^{124a,124b}, D. Whiteson¹⁶⁴, F.J. Wickens¹³¹, W. Wiedenmann¹⁷⁴, M. Wielers¹³¹, P. Wienemann²¹, C. Wiglesworth³⁶, L.A.M. Wiik-Fuchs²¹, A. Wildauer¹⁰¹, H.G. Wilkens³⁰, H.H. Williams¹²², S. Williams¹⁰⁷, C. Willis⁹⁰, S. Willocq⁸⁶, A. Wilson⁸⁹, J.A. Wilson¹⁸, I. Wingerter-Seez⁵, F. Winklmeier¹¹⁶, B.T. Winter²¹, M. Wittgen¹⁴⁴, J. Wittkowski¹⁰⁰, S.J. Wollstadt⁸³, M.W. Wolter³⁹, H. Wolters^{126a,126c}, B.K. Wosiek³⁹, J. Wotschack³⁰, M.J. Woudstra⁸⁴, K.W. Wozniak³⁹, M. Wu⁵⁵, M. Wu³¹, S.L. Wu¹⁷⁴, X. Wu⁴⁹, Y. Wu⁸⁹, T.R. Wyatt⁸⁴, B.M. Wynne⁴⁶, S. Xella³⁶, D. Xu^{33a}, L. Xu^{33b,ai}, B. Yabsley¹⁵¹, S. Yacoob^{146b,aj}, R. Yakabe⁶⁷, M. Yamada⁶⁶, Y. Yamaguchi¹¹⁸, A. Yamamoto⁶⁶, S. Yamamoto¹⁵⁶, T. Yamanaka¹⁵⁶, K. Yamauchi¹⁰³, Y. Yamazaki⁶⁷, Z. Yan²², H. Yang^{33e}, H. Yang¹⁷⁴, Y. Yang¹⁵², L. Yao^{33a}, W-M. Yao¹⁵, Y. Yasu⁶⁶, E. Yatsenko⁴², K.H. Yau Wong²¹, J. Ye⁴⁰, S. Ye²⁵, I. Yeletsikh⁶⁵, A.L. Yen⁵⁷, E. Yildirim⁴², K. Yorita¹⁷², R. Yoshida⁶, K. Yoshihara¹²², C. Young¹⁴⁴, C.J.S. Young³⁰, S. Youssef²², D.R. Yu¹⁵, J. Yu⁸, J.M. Yu⁸⁹, J. Yu¹¹⁴, L. Yuan⁶⁷, A. Yurkewicz¹⁰⁸, I. Yusuff^{28,ak}, B. Zabinski³⁹, R. Zaidan⁶³, A.M. Zaitsev^{130,z}, J. Zalieckas¹⁴, A. Zaman¹⁴⁹, S. Zambito²³, L. Zanello^{133a,133b}, D. Zanzi⁸⁸, C. Zeitnitz¹⁷⁶, M. Zeman¹²⁸, A. Zemla^{38a}, K. Zengel²³, O. Zenin¹³⁰, T. Ženiš^{145a}, D. Zerwas¹¹⁷, D. Zhang⁸⁹, F. Zhang¹⁷⁴, J. Zhang⁶, L. Zhang⁴⁸, R. Zhang^{33b}, X. Zhang^{33d}, Z. Zhang¹¹⁷, X. Zhao⁴⁰, Y. Zhao^{33d,117}, Z. Zhao^{33b}, A. Zhemchugov⁶⁵, J. Zhong¹²⁰, B. Zhou⁸⁹, C. Zhou⁴⁵, L. Zhou³⁵, L. Zhou⁴⁰, N. Zhou¹⁶⁴, C.G. Zhu^{33d}, H. Zhu^{33a}, J. Zhu⁸⁹, Y. Zhu^{33b}, X. Zhuang^{33a}, K. Zhukov⁹⁶, A. Zibell¹⁷⁵, D. Zieminska⁶¹, N.I. Zimine⁶⁵, C. Zimmermann⁸³, R. Zimmermann²¹, S. Zimmermann⁴⁸, Z. Zinonos⁵⁴, M. Zinser⁸³, M. Ziolkowski¹⁴², L. Živković¹³, G. Zobernig¹⁷⁴, A. Zoccoli^{20a,20b}, M. zur Nedden¹⁶, G. Zurzolo^{104a,104b}, L. Zwalinski³⁰.

¹ Department of Physics, University of Adelaide, Adelaide, Australia

² Physics Department, SUNY Albany, Albany NY, United States of America

³ Department of Physics, University of Alberta, Edmonton AB, Canada

⁴ ^(a) Department of Physics, Ankara University, Ankara; ^(c) Istanbul Aydin University, Istanbul; ^(d) Division of Physics, TOBB University of Economics and Technology, Ankara, Turkey

⁵ LAPP, CNRS/IN2P3 and Université Savoie Mont Blanc, Annecy-le-Vieux, France

⁶ High Energy Physics Division, Argonne National Laboratory, Argonne IL, United States of America

⁷ Department of Physics, University of Arizona, Tucson AZ, United States of America

⁸ Department of Physics, The University of Texas at Arlington, Arlington TX, United States of America

⁹ Physics Department, University of Athens, Athens, Greece

¹⁰ Physics Department, National Technical University of Athens, Zografou, Greece

¹¹ Institute of Physics, Azerbaijan Academy of Sciences, Baku, Azerbaijan

¹² Institut de Física d'Altes Energies and Departament de Física de la Universitat Autònoma de Barcelona, Barcelona, Spain

¹³ Institute of Physics, University of Belgrade, Belgrade, Serbia

¹⁴ Department for Physics and Technology, University of Bergen, Bergen, Norway

¹⁵ Physics Division, Lawrence Berkeley National Laboratory and University of California,

Berkeley CA, United States of America

¹⁶ Department of Physics, Humboldt University, Berlin, Germany

¹⁷ Albert Einstein Center for Fundamental Physics and Laboratory for High Energy Physics, University of Bern, Bern, Switzerland

¹⁸ School of Physics and Astronomy, University of Birmingham, Birmingham, United Kingdom

¹⁹ ^(a) Department of Physics, Bogazici University, Istanbul; ^(b) Department of Physics, Dogus University, Istanbul; ^(c) Department of Physics Engineering, Gaziantep University, Gaziantep, Turkey

²⁰ ^(a) INFN Sezione di Bologna; ^(b) Dipartimento di Fisica e Astronomia, Università di Bologna, Bologna, Italy

²¹ Physikalisches Institut, University of Bonn, Bonn, Germany

²² Department of Physics, Boston University, Boston MA, United States of America

²³ Department of Physics, Brandeis University, Waltham MA, United States of America

²⁴ ^(a) Universidade Federal do Rio De Janeiro COPPE/EE/IF, Rio de Janeiro; ^(b) Electrical Circuits Department, Federal University of Juiz de Fora (UFJF), Juiz de Fora; ^(c) Federal University of Sao Joao del Rei (UFSJ), Sao Joao del Rei; ^(d) Instituto de Fisica, Universidade de Sao Paulo, Sao Paulo, Brazil

²⁵ Physics Department, Brookhaven National Laboratory, Upton NY, United States of America

²⁶ ^(a) National Institute of Physics and Nuclear Engineering, Bucharest; ^(b) National Institute for Research and Development of Isotopic and Molecular Technologies, Physics Department, Cluj Napoca; ^(c) University Politehnica Bucharest, Bucharest; ^(d) West University in Timisoara, Timisoara, Romania

²⁷ Departamento de Física, Universidad de Buenos Aires, Buenos Aires, Argentina

²⁸ Cavendish Laboratory, University of Cambridge, Cambridge, United Kingdom

²⁹ Department of Physics, Carleton University, Ottawa ON, Canada

³⁰ CERN, Geneva, Switzerland

³¹ Enrico Fermi Institute, University of Chicago, Chicago IL, United States of America

³² ^(a) Departamento de Física, Pontificia Universidad Católica de Chile, Santiago; ^(b) Departamento de Física, Universidad Técnica Federico Santa María, Valparaíso, Chile

³³ ^(a) Institute of High Energy Physics, Chinese Academy of Sciences, Beijing; ^(b) Department of Modern Physics, University of Science and Technology of China, Anhui; ^(c) Department of Physics, Nanjing University, Jiangsu; ^(d) School of Physics, Shandong University, Shandong; ^(e) Department of Physics and Astronomy, Shanghai Key Laboratory for Particle Physics and Cosmology, Shanghai Jiao Tong University, Shanghai; ^(f) Physics Department, Tsinghua University, Beijing 100084, China

³⁴ Laboratoire de Physique Corpusculaire, Clermont Université and Université Blaise Pascal and CNRS/IN2P3, Clermont-Ferrand, France

³⁵ Nevis Laboratory, Columbia University, Irvington NY, United States of America

³⁶ Niels Bohr Institute, University of Copenhagen, Kobenhavn, Denmark

³⁷ ^(a) INFN Gruppo Collegato di Cosenza, Laboratori Nazionali di Frascati; ^(b) Dipartimento di Fisica, Università della Calabria, Rende, Italy

- ³⁸ (a) AGH University of Science and Technology, Faculty of Physics and Applied Computer Science, Krakow; (b) Marian Smoluchowski Institute of Physics, Jagiellonian University, Krakow, Poland
- ³⁹ Institute of Nuclear Physics Polish Academy of Sciences, Krakow, Poland
- ⁴⁰ Physics Department, Southern Methodist University, Dallas TX, United States of America
- ⁴¹ Physics Department, University of Texas at Dallas, Richardson TX, United States of America
- ⁴² DESY, Hamburg and Zeuthen, Germany
- ⁴³ Institut für Experimentelle Physik IV, Technische Universität Dortmund, Dortmund, Germany
- ⁴⁴ Institut für Kern- und Teilchenphysik, Technische Universität Dresden, Dresden, Germany
- ⁴⁵ Department of Physics, Duke University, Durham NC, United States of America
- ⁴⁶ SUPA - School of Physics and Astronomy, University of Edinburgh, Edinburgh, United Kingdom
- ⁴⁷ INFN Laboratori Nazionali di Frascati, Frascati, Italy
- ⁴⁸ Fakultät für Mathematik und Physik, Albert-Ludwigs-Universität, Freiburg, Germany
- ⁴⁹ Section de Physique, Université de Genève, Geneva, Switzerland
- ⁵⁰ (a) INFN Sezione di Genova; (b) Dipartimento di Fisica, Università di Genova, Genova, Italy
- ⁵¹ (a) E. Andronikashvili Institute of Physics, Iv. Javakhishvili Tbilisi State University, Tbilisi; (b) High Energy Physics Institute, Tbilisi State University, Tbilisi, Georgia
- ⁵² II Physikalisches Institut, Justus-Liebig-Universität Giessen, Giessen, Germany
- ⁵³ SUPA - School of Physics and Astronomy, University of Glasgow, Glasgow, United Kingdom
- ⁵⁴ II Physikalisches Institut, Georg-August-Universität, Göttingen, Germany
- ⁵⁵ Laboratoire de Physique Subatomique et de Cosmologie, Université Grenoble-Alpes, CNRS/IN2P3, Grenoble, France
- ⁵⁶ Department of Physics, Hampton University, Hampton VA, United States of America
- ⁵⁷ Laboratory for Particle Physics and Cosmology, Harvard University, Cambridge MA, United States of America
- ⁵⁸ (a) Kirchhoff-Institut für Physik, Ruprecht-Karls-Universität Heidelberg, Heidelberg; (b) Physikalisches Institut, Ruprecht-Karls-Universität Heidelberg, Heidelberg; (c) ZITI Institut für technische Informatik, Ruprecht-Karls-Universität Heidelberg, Mannheim, Germany
- ⁵⁹ Faculty of Applied Information Science, Hiroshima Institute of Technology, Hiroshima, Japan
- ⁶⁰ (a) Department of Physics, The Chinese University of Hong Kong, Shatin, N.T., Hong Kong; (b) Department of Physics, The University of Hong Kong, Hong Kong; (c) Department of Physics, The Hong Kong University of Science and Technology, Clear Water Bay, Kowloon, Hong Kong, China
- ⁶¹ Department of Physics, Indiana University, Bloomington IN, United States of America

- ⁶² Institut für Astro- und Teilchenphysik, Leopold-Franzens-Universität, Innsbruck, Austria
- ⁶³ University of Iowa, Iowa City IA, United States of America
- ⁶⁴ Department of Physics and Astronomy, Iowa State University, Ames IA, United States of America
- ⁶⁵ Joint Institute for Nuclear Research, JINR Dubna, Dubna, Russia
- ⁶⁶ KEK, High Energy Accelerator Research Organization, Tsukuba, Japan
- ⁶⁷ Graduate School of Science, Kobe University, Kobe, Japan
- ⁶⁸ Faculty of Science, Kyoto University, Kyoto, Japan
- ⁶⁹ Kyoto University of Education, Kyoto, Japan
- ⁷⁰ Department of Physics, Kyushu University, Fukuoka, Japan
- ⁷¹ Instituto de Física La Plata, Universidad Nacional de La Plata and CONICET, La Plata, Argentina
- ⁷² Physics Department, Lancaster University, Lancaster, United Kingdom
- ⁷³ ^(a) INFN Sezione di Lecce; ^(b) Dipartimento di Matematica e Fisica, Università del Salento, Lecce, Italy
- ⁷⁴ Oliver Lodge Laboratory, University of Liverpool, Liverpool, United Kingdom
- ⁷⁵ Department of Physics, Jožef Stefan Institute and University of Ljubljana, Ljubljana, Slovenia
- ⁷⁶ School of Physics and Astronomy, Queen Mary University of London, London, United Kingdom
- ⁷⁷ Department of Physics, Royal Holloway University of London, Surrey, United Kingdom
- ⁷⁸ Department of Physics and Astronomy, University College London, London, United Kingdom
- ⁷⁹ Louisiana Tech University, Ruston LA, United States of America
- ⁸⁰ Laboratoire de Physique Nucléaire et de Hautes Energies, UPMC and Université Paris-Diderot and CNRS/IN2P3, Paris, France
- ⁸¹ Fysiska institutionen, Lunds universitet, Lund, Sweden
- ⁸² Departamento de Física Teórica C-15, Universidad Autónoma de Madrid, Madrid, Spain
- ⁸³ Institut für Physik, Universität Mainz, Mainz, Germany
- ⁸⁴ School of Physics and Astronomy, University of Manchester, Manchester, United Kingdom
- ⁸⁵ CPPM, Aix-Marseille Université and CNRS/IN2P3, Marseille, France
- ⁸⁶ Department of Physics, University of Massachusetts, Amherst MA, United States of America
- ⁸⁷ Department of Physics, McGill University, Montreal QC, Canada
- ⁸⁸ School of Physics, University of Melbourne, Victoria, Australia
- ⁸⁹ Department of Physics, The University of Michigan, Ann Arbor MI, United States of America
- ⁹⁰ Department of Physics and Astronomy, Michigan State University, East Lansing MI, United States of America
- ⁹¹ ^(a) INFN Sezione di Milano; ^(b) Dipartimento di Fisica, Università di Milano, Milano,

Italy

⁹² B.I. Stepanov Institute of Physics, National Academy of Sciences of Belarus, Minsk, Republic of Belarus

⁹³ National Scientific and Educational Centre for Particle and High Energy Physics, Minsk, Republic of Belarus

⁹⁴ Department of Physics, Massachusetts Institute of Technology, Cambridge MA, United States of America

⁹⁵ Group of Particle Physics, University of Montreal, Montreal QC, Canada

⁹⁶ P.N. Lebedev Institute of Physics, Academy of Sciences, Moscow, Russia

⁹⁷ Institute for Theoretical and Experimental Physics (ITEP), Moscow, Russia

⁹⁸ National Research Nuclear University MEPhI, Moscow, Russia

⁹⁹ D.V. Skobeltsyn Institute of Nuclear Physics, M.V. Lomonosov Moscow State University, Moscow, Russia

¹⁰⁰ Fakultät für Physik, Ludwig-Maximilians-Universität München, München, Germany

¹⁰¹ Max-Planck-Institut für Physik (Werner-Heisenberg-Institut), München, Germany

¹⁰² Nagasaki Institute of Applied Science, Nagasaki, Japan

¹⁰³ Graduate School of Science and Kobayashi-Maskawa Institute, Nagoya University, Nagoya, Japan

¹⁰⁴ ^(a) INFN Sezione di Napoli; ^(b) Dipartimento di Fisica, Università di Napoli, Napoli, Italy

¹⁰⁵ Department of Physics and Astronomy, University of New Mexico, Albuquerque NM, United States of America

¹⁰⁶ Institute for Mathematics, Astrophysics and Particle Physics, Radboud University Nijmegen/Nikhef, Nijmegen, Netherlands

¹⁰⁷ Nikhef National Institute for Subatomic Physics and University of Amsterdam, Amsterdam, Netherlands

¹⁰⁸ Department of Physics, Northern Illinois University, DeKalb IL, United States of America

¹⁰⁹ Budker Institute of Nuclear Physics, SB RAS, Novosibirsk, Russia

¹¹⁰ Department of Physics, New York University, New York NY, United States of America

¹¹¹ Ohio State University, Columbus OH, United States of America

¹¹² Faculty of Science, Okayama University, Okayama, Japan

¹¹³ Homer L. Dodge Department of Physics and Astronomy, University of Oklahoma, Norman OK, United States of America

¹¹⁴ Department of Physics, Oklahoma State University, Stillwater OK, United States of America

¹¹⁵ Palacký University, RCPTM, Olomouc, Czech Republic

¹¹⁶ Center for High Energy Physics, University of Oregon, Eugene OR, United States of America

¹¹⁷ LAL, Université Paris-Sud and CNRS/IN2P3, Orsay, France

¹¹⁸ Graduate School of Science, Osaka University, Osaka, Japan

¹¹⁹ Department of Physics, University of Oslo, Oslo, Norway

¹²⁰ Department of Physics, Oxford University, Oxford, United Kingdom

- 121 (a) INFN Sezione di Pavia; (b) Dipartimento di Fisica, Università di Pavia, Pavia, Italy
- 122 Department of Physics, University of Pennsylvania, Philadelphia PA, United States of America
- 123 Petersburg Nuclear Physics Institute, Gatchina, Russia
- 124 (a) INFN Sezione di Pisa; (b) Dipartimento di Fisica E. Fermi, Università di Pisa, Pisa, Italy
- 125 Department of Physics and Astronomy, University of Pittsburgh, Pittsburgh PA, United States of America
- 126 (a) Laboratório de Instrumentação e Física Experimental de Partículas - LIP, Lisboa; (b) Faculdade de Ciências, Universidade de Lisboa, Lisboa; (c) Department of Physics, University of Coimbra, Coimbra; (d) Centro de Física Nuclear da Universidade de Lisboa, Lisboa; (e) Departamento de Física, Universidade do Minho, Braga; (f) Departamento de Física Teórica y del Cosmos and CAFPE, Universidad de Granada, Granada (Spain); (g) Dep Física and CEFITEC of Faculdade de Ciências e Tecnologia, Universidade Nova de Lisboa, Caparica, Portugal
- 127 Institute of Physics, Academy of Sciences of the Czech Republic, Praha, Czech Republic
- 128 Czech Technical University in Prague, Praha, Czech Republic
- 129 Faculty of Mathematics and Physics, Charles University in Prague, Praha, Czech Republic
- 130 State Research Center Institute for High Energy Physics, Protvino, Russia
- 131 Particle Physics Department, Rutherford Appleton Laboratory, Didcot, United Kingdom
- 132 Ritsumeikan University, Kusatsu, Shiga, Japan
- 133 (a) INFN Sezione di Roma; (b) Dipartimento di Fisica, Sapienza Università di Roma, Roma, Italy
- 134 (a) INFN Sezione di Roma Tor Vergata; (b) Dipartimento di Fisica, Università di Roma Tor Vergata, Roma, Italy
- 135 (a) INFN Sezione di Roma Tre; (b) Dipartimento di Matematica e Fisica, Università Roma Tre, Roma, Italy
- 136 (a) Faculté des Sciences Ain Chock, Réseau Universitaire de Physique des Hautes Energies - Université Hassan II, Casablanca; (b) Centre National de l'Énergie des Sciences Techniques Nucleaires, Rabat; (c) Faculté des Sciences Semlalia, Université Cadi Ayyad, LPHEA-Marrakech; (d) Faculté des Sciences, Université Mohamed Premier and LPTPM, Oujda; (e) Faculté des sciences, Université Mohammed V-Agdal, Rabat, Morocco
- 137 DSM/IRFU (Institut de Recherches sur les Lois Fondamentales de l'Univers), CEA Saclay (Commissariat à l'Énergie Atomique et aux Énergies Alternatives), Gif-sur-Yvette, France
- 138 Santa Cruz Institute for Particle Physics, University of California Santa Cruz, Santa Cruz CA, United States of America
- 139 Department of Physics, University of Washington, Seattle WA, United States of America
- 140 Department of Physics and Astronomy, University of Sheffield, Sheffield, United

Kingdom

¹⁴¹ Department of Physics, Shinshu University, Nagano, Japan

¹⁴² Fachbereich Physik, Universität Siegen, Siegen, Germany

¹⁴³ Department of Physics, Simon Fraser University, Burnaby BC, Canada

¹⁴⁴ SLAC National Accelerator Laboratory, Stanford CA, United States of America

¹⁴⁵ ^(a) Faculty of Mathematics, Physics & Informatics, Comenius University, Bratislava;

^(b) Department of Subnuclear Physics, Institute of Experimental Physics of the Slovak Academy of Sciences, Kosice, Slovak Republic

¹⁴⁶ ^(a) Department of Physics, University of Cape Town, Cape Town; ^(b) Department of Physics, University of Johannesburg, Johannesburg; ^(c) School of Physics, University of the Witwatersrand, Johannesburg, South Africa

¹⁴⁷ ^(a) Department of Physics, Stockholm University; ^(b) The Oskar Klein Centre, Stockholm, Sweden

¹⁴⁸ Physics Department, Royal Institute of Technology, Stockholm, Sweden

¹⁴⁹ Departments of Physics & Astronomy and Chemistry, Stony Brook University, Stony Brook NY, United States of America

¹⁵⁰ Department of Physics and Astronomy, University of Sussex, Brighton, United

Kingdom

¹⁵¹ School of Physics, University of Sydney, Sydney, Australia

¹⁵² Institute of Physics, Academia Sinica, Taipei, Taiwan

¹⁵³ Department of Physics, Technion: Israel Institute of Technology, Haifa, Israel

¹⁵⁴ Raymond and Beverly Sackler School of Physics and Astronomy, Tel Aviv University, Tel Aviv, Israel

¹⁵⁵ Department of Physics, Aristotle University of Thessaloniki, Thessaloniki, Greece

¹⁵⁶ International Center for Elementary Particle Physics and Department of Physics, The University of Tokyo, Tokyo, Japan

¹⁵⁷ Graduate School of Science and Technology, Tokyo Metropolitan University, Tokyo, Japan

¹⁵⁸ Department of Physics, Tokyo Institute of Technology, Tokyo, Japan

¹⁵⁹ Department of Physics, University of Toronto, Toronto ON, Canada

¹⁶⁰ ^(a) TRIUMF, Vancouver BC; ^(b) Department of Physics and Astronomy, York University, Toronto ON, Canada

¹⁶¹ Faculty of Pure and Applied Sciences, University of Tsukuba, Tsukuba, Japan

¹⁶² Department of Physics and Astronomy, Tufts University, Medford MA, United States of America

¹⁶³ Centro de Investigaciones, Universidad Antonio Narino, Bogota, Colombia

¹⁶⁴ Department of Physics and Astronomy, University of California Irvine, Irvine CA, United States of America

¹⁶⁵ ^(a) INFN Gruppo Collegato di Udine, Sezione di Trieste, Udine; ^(b) ICTP, Trieste; ^(c) Dipartimento di Chimica, Fisica e Ambiente, Università di Udine, Udine, Italy

¹⁶⁶ Department of Physics, University of Illinois, Urbana IL, United States of America

¹⁶⁷ Department of Physics and Astronomy, University of Uppsala, Uppsala, Sweden

¹⁶⁸ Instituto de Física Corpuscular (IFIC) and Departamento de Física Atómica,

Molecular y Nuclear and Departamento de Ingeniería Electrónica and Instituto de Microelectrónica de Barcelona (IMB-CNM), University of Valencia and CSIC, Valencia, Spain

¹⁶⁹ Department of Physics, University of British Columbia, Vancouver BC, Canada

¹⁷⁰ Department of Physics and Astronomy, University of Victoria, Victoria BC, Canada

¹⁷¹ Department of Physics, University of Warwick, Coventry, United Kingdom

¹⁷² Waseda University, Tokyo, Japan

¹⁷³ Department of Particle Physics, The Weizmann Institute of Science, Rehovot, Israel

¹⁷⁴ Department of Physics, University of Wisconsin, Madison WI, United States of America

¹⁷⁵ Fakultät für Physik und Astronomie, Julius-Maximilians-Universität, Würzburg, Germany

¹⁷⁶ Fachbereich C Physik, Bergische Universität Wuppertal, Wuppertal, Germany

¹⁷⁷ Department of Physics, Yale University, New Haven CT, United States of America

¹⁷⁸ Yerevan Physics Institute, Yerevan, Armenia

¹⁷⁹ Centre de Calcul de l'Institut National de Physique Nucléaire et de Physique des Particules (IN2P3), Villeurbanne, France

^a Also at Department of Physics, King's College London, London, United Kingdom

^b Also at Institute of Physics, Azerbaijan Academy of Sciences, Baku, Azerbaijan

^c Also at Novosibirsk State University, Novosibirsk, Russia

^d Also at TRIUMF, Vancouver BC, Canada

^e Also at Department of Physics, California State University, Fresno CA, United States of America

^f Also at Department of Physics, University of Fribourg, Fribourg, Switzerland

^g Also at Departamento de Física e Astronomia, Faculdade de Ciências, Universidade do Porto, Portugal

^h Also at Tomsk State University, Tomsk, Russia

ⁱ Also at CPPM, Aix-Marseille Université and CNRS/IN2P3, Marseille, France

^j Also at Università di Napoli Parthenope, Napoli, Italy

^k Also at Institute of Particle Physics (IPP), Canada

^l Also at Particle Physics Department, Rutherford Appleton Laboratory, Didcot, United Kingdom

^m Also at Department of Physics, St. Petersburg State Polytechnical University, St. Petersburg, Russia

ⁿ Also at Louisiana Tech University, Ruston LA, United States of America

^o Also at Institutio Catalana de Recerca i Estudis Avancats, ICREA, Barcelona, Spain

^p Also at Department of Physics, National Tsing Hua University, Taiwan

^q Also at Department of Physics, The University of Texas at Austin, Austin TX, United States of America

^r Also at Institute of Theoretical Physics, Ilia State University, Tbilisi, Georgia

^s Also at CERN, Geneva, Switzerland

^t Also at Georgian Technical University (GTU), Tbilisi, Georgia

^u Also at O Chadai Academic Production, Ochanomizu University, Tokyo, Japan

- v* Also at Manhattan College, New York NY, United States of America
- w* Also at Institute of Physics, Academia Sinica, Taipei, Taiwan
- x* Also at LAL, Université Paris-Sud and CNRS/IN2P3, Orsay, France
- y* Also at Academia Sinica Grid Computing, Institute of Physics, Academia Sinica, Taipei, Taiwan
- z* Also at Moscow Institute of Physics and Technology State University, Dolgoprudny, Russia
- aa* Also at Section de Physique, Université de Genève, Geneva, Switzerland
- ab* Also at International School for Advanced Studies (SISSA), Trieste, Italy
- ac* Also at Department of Physics and Astronomy, University of South Carolina, Columbia SC, United States of America
- ad* Also at School of Physics and Engineering, Sun Yat-sen University, Guangzhou, China
- ae* Also at Faculty of Physics, M.V.Lomonosov Moscow State University, Moscow, Russia
- af* Also at National Research Nuclear University MEPhI, Moscow, Russia
- ag* Also at Department of Physics, Stanford University, Stanford CA, United States of America
- ah* Also at Institute for Particle and Nuclear Physics, Wigner Research Centre for Physics, Budapest, Hungary
- ai* Also at Department of Physics, The University of Michigan, Ann Arbor MI, United States of America
- aj* Also at Discipline of Physics, University of KwaZulu-Natal, Durban, South Africa
- ak* Also at University of Malaya, Department of Physics, Kuala Lumpur, Malaysia
- * Deceased